Project No. 10-105

VERIFICATION OF TRAFFIC SPEED DEFLECTION DEVICES' (TSDDS) MEASUREMENTS

FINAL REPORT

Prepared for

NCHRP
Transportation Research Board
of
The National Academies of Sciences, Engineering, and Medicine

Prepared by

Gonzalo Rada, Ph.D., P.E.
WSP USA Environment & Infrastructure Inc.
Hanover, MD

Soheil Nazarian, Ph.D., P.E., Cesar Tirado, Ph.D. and Mahsa Beizaei, Ph.D. candidate
The University of Texas at El Paso
El Paso, TX

Gerardo Flintsch, Ph.D., P.E. and Samer Katicha, Ph.D.
Virginia Tech Transportation Institute
Blacksburg, VA

May 2023

ACKNOWLEDGEMENT OF SPONSORSHIP

This work was sponsored by one or more of the following as noted:

☒ American Association of State Highway and Transportation Officials, in cooperation with the Federal Highway Administration, and was conducted in the **National Cooperative Highway Research Program**,

☐ Federal Transit Administration and was conducted in the **Transit Cooperative Research Program**,

☐ Federal Aviation Administration and was conducted in the **Airport Cooperative Research Program**,

☐ The National Highway Safety Administration and was conducted in the **Behavioral Traffic Safety Cooperative Research Program**,

which is administered by the Transportation Research Board of the National Academies of Sciences, Engineering, and Medicine.

DISCLAIMER

Project No. 10-105

VERIFICATION OF TRAFFIC SPEED DEFLECTION DEVICES' (TSDDS) MEASUREMENTS

FINAL REPORT

Prepared for

NCHRP
Transportation Research Board
of
The National Academies of Sciences, Engineering, and Medicine

Prepared by

Gonzalo Rada, Ph.D., P.E.
WSP USA Environment & Infrastructure Inc.
Hanover, MD

Soheil Nazarian, Ph.D., P.E., Cesar Tirado, Ph.D. and Mahsa Beizaei, Ph.D. candidate
The University of Texas at El Paso
El Paso, TX

Gerardo Flintsch, Ph.D., P.E. and Samer Katicha, Ph.D.
Virginia Tech Transportation Institute
Blacksburg, VA

May 2023

TABLE OF CONTENTS

LIST OF FIGURES

LIST OF TABLES

LIST OF ABBREVIATIONS, ACRONYMS, INITIALISMS, AND SYMBOLS

AASHTO	American Association of State Highway Transportation Officials
AC	asphalt concrete
ANN	artificial neural network
ARA	Applied Research Associates
ASTM	American Society for Testing and Materials (now ASTM International)
BDI	base-damage index
CDD	continuous deflection device
COV	coefficient of variation
CTB	cement-treated base
DMI	distance measuring instrument
DOT	Department of Transportation
FHWA	Federal Highway Administration
FWD	falling weight deflectometer
GPR	ground penetrating radar
HMA	hot mix asphalt
IRI	International Roughness Index
LTB	lime-treated base
LTPP	Long-Term Pavement Performance
LVR	MnROAD low-volume road
ML	MnROAD mainline
MMP	moving measurement platform
NCHRP	National Cooperative Highway Research Program
PCC	Portland cement concrete
RAPTOR	Rapid Pavement Tester
RDT	road deflection tester
RWD	rolling weight deflectometer
SCI	surface curvature index
SEE	standard error of estimate
SHA	State Highway Administration
SHRP 2	Second Strategic Highway Research Program
TPF	Transportation Pooled Fund

TRB	Transportation Research Board
TSD	traffic speed deflectometer
TSDD	traffic speed deflection device
UGB	unbound granular base
VTI	Swedish National Road and Transport Research Institute

AUTHOR ACKNOWLEDGMENT

The preparation of this report was performed under NCHRP Project 10-105 by WSP USA Environment & Infrastructure Inc. (E&I). Dr. Gonzalo R. Rada of E&I served as the principal investigator. The other authors of this report included Dr. Soheil Nazarian, Dr. Cesar Tirado and Ms. Mahsa Beizaei (Ph.D. candidate), with The University of Texas at El Paso, and Dr. Gerardo Flintsch and Dr. Samer Katicha with the Virginia Tech Transportation Institute. The work was done under the general supervision of Dr. Rada.

ABSTRACT

Recent research studies have shown the usefulness and applicability of traffic-speed deflection devices (TSDDs) in support of network-level pavement management processes. There is, however, no accepted procedure for verification of the TSDD measurements, and consequently, some State highway agencies have reservations about implementing them in their network-level pavement management efforts. To address this need, NCHRP Project 10-105 was undertaken to develop a proposed TSDD verification procedure for consideration by the American Association of Highway Transportation Officials. A two-phase approach was executed to accomplish the stated objective. The project commenced with an information-gathering effort, and the results were used to develop a list of relevant deflection measurement characteristics and factors affecting them. Field experiments were then carried out in Minnesota, and the resulting data were used to develop the falling weight deflectometer-TSDD relationships—to estimate TSDD deflection velocities from measured FWD deflections—required by the TSDD verification procedure. A draft of the proposed practice was prepared around these relationships, and it was revised based on the outcomes from field tests in Texas and Virginia. The findings of the research are documented in this report and the proposed practice is included as an attachment. These findings are based on measurements by one device and may not apply to other devices; however, the general approach should be applicable in verifying other devices.

CHAPTER 1. INTRODUCTION

PROBLEM STATEMENT

State highway agencies (SHAs) have traditionally relied on surface conditions, such as ride quality and distresses, to characterize the condition of their pavement network and to assess their maintenance and rehabilitation needs. However, surface conditions do not adequately reflect the structural condition of the pavements, which is an important driver of deterioration. Ignoring structural condition can result in less-than-optimal treatment selection at the network level. Moreover, the correlation between surface conditions and structural measurements is weak (Flora 2009, Bryce et al. 2012), while the rate of pavement deterioration is affected by the structural condition (Katicha et al. 2016). Incorporating structural conditions, along with surface conditions, into the pavement management decision-making process can lead to better-informed and more cost-effective decisions (Ferne et al. 2013, Zaghloul et al. 1998, Steele 2015).

Several SHAs have used falling weight deflectometer (FWD) measurements to enhance their network-level pavement management processes (Flintsch and McGhee 2009, Katicha et al. 2013), but FWDs are not practical devices for network-level testing. The limitations of the FWD and the desire to characterize the network-level structural condition have led to research efforts to investigate, validate, and demonstrate traffic-speed deflection devices (TSDDs). These include the Second Strategic Highway Research Program 2 (SHRP 2) R06(F) (Flintsch et al. 2013), two Federal Highway Administration (FHWA)-sponsored research projects (Rada and Nazarian 2011, Rada et al. 2016), two national Transportation Pooled Fund (TPF) studies TPF-5(282) (Katicha et al. 2017) and TPF-5(385), and State-sponsored projects in Louisiana (Elseifi et al. 2012), Texas (Stokoe et al. 2011), and Virginia (Katicha et al. 2020).

These research efforts have shown the usefulness and applicability of TSDDs, but no widely accepted practices for verifying the TSDD measurements are currently available. Consequently, there was an urgent need for developing a TSDD verification procedure. The purpose of the verification procedure is to check that TSDD-measured data reflects the actual pavement deflections.

PROJECT OBJECTIVE

The objective of the research carried out under National Cooperative Highway Research Program (NCHRP) Project 10-105 was to develop a proposed practice for verification of the measurements obtained by TSDDs on highway pavements for consideration by the American Association of Highway Transportation Officials (AASHTO).

RESEARCH APPROACH

NCHRP Project 10-105 commenced with a literature review to identify relevant deflection measurement characteristics and the factors that affect them. The literature review results confirmed that loading characteristics and pavement structure and properties are critical and that deflections are affected by temperature, moisture, and aging. Moreover, it was determined that the development of the TSDD measurements verification procedure would benefit from the instrumentation of pavement test sections. Consequently, field experiments were conducted at the MnROAD facility in Minnesota, and they produced the instrumentation, FWD, and TSDD data needed to develop the FWD-TSDD relationships—to estimate TSDD deflection velocities from measured FWD deflections—required by the proposed practice.

The resulting FWD-TSDD relationships were field tested at pavement sections in Virginia and Texas, which offered varying pavement structure, subgrade soil, traffic, and environmental conditions. The field test results were first used to validate and calibrate the FWD-TSDD relationships that resulted from the MnROAD field experiments. They were then used to prepare the draft of the proposed practice. Finally, a report documenting the entire research effort was prepared, which includes the proposed practice as an attachment.

When formulating this research approach, it was anticipated that multiple TSDDs would be included in the field experiments and testing, but only one device could be used. Therefore, the findings of this research are based on measurements by one device and those findings may not apply to other devices. However, the general approach should be applicable in verifying other TSDDs.

REPORT ORGANIZATION

This final report is organized into seven chapters. Chapter 1 provides the problem statement and project objective, summarizes the research approach, and describes the report's organization. Chapter 2 details the literature review as well as the resulting list of relevant deflection measurement characteristics and factors that affect them. The field-testing experiments carried out at the MnROAD facility and the validation of the resulting TSDD measurements are detailed in Chapter 3. The development of the FWD-TSDD relationships required to estimate TSDD deflection velocities from FWD deflections are detailed in Chapter 4. The validation and calibration of the FWD-TSDD relationships based on the Texas and Virginia field testing results are detailed in Chapter 5, while the development of the recommended proposed practice is addressed in Chapter 6. The most salient findings, conclusions, and recommendations from the research effort are detailed in Chapter 7. The references used throughout the report are included after Chapter 7.

In addition to the referenced chapters, this report includes three appendices: Appendix A documents the effects of spatial averaging on the TSDD measurements, Appendix B documents the evaluation of the 3D-Move models, and Appendix C documents the evaluation of the FWD-TSDD relationships. The report also includes one attachment containing the proposed practice for verification of TSDD measurements.

CHAPTER 2. LITERATURE REVIEW

The objective of the literature review was to gather information related to TSDD measurements, with a focus on available technologies, deflection measurement characteristics, and verifications. The literature defines continuous deflection devices (CDDs) (Flintsch et al. 2013) or moving measurement platforms (MMPs) (Andersen et al. 2017, Madsen and Pedersen 2019) as a group of devices that measure the surface deflections produced by the device's weight as it travels over the pavement. TSDDs are a sub-group of these devices, which measure pavement deflections at or near traffic speeds (35 mph [55 km/h] or higher, as defined by Flintsch et al. 2013, or 25 mph [40 km/h] or higher as defined by Elseifi et al. 2011).

The development of TSDDs began in the 1990s, with the initial working prototypes released in the late 1990s and early 2000s (Arora et al. 2006, Hildebrand and Rasmussen 2002). After those early prototypes, numerous studies have been performed to assess their performance and how to best use them for pavement structural evaluations. A few example studies include Rada and Nazarian 2011, Rada et al. 2016, Flintsch et al. 2013, Elseifi and Elbagalati 2017, Arora et al. 2006, Rada and Nazarian 2011, and Flintsch et al. 2013 in the United States and Andrén 2006 and Brezina and Stryk 2015 abroad.

AVAILABLE TECHNOLOGY

The road deflection tester (RDT), rolling wheel deflectometer (RWD), rapid pavement tester (RAPTOR) and traffic speed deflectometer (TSD) were identified in the literature and considered for use in the project.

RDT

The RDT was developed by the Swedish National Road and Transport Research Institute (VTI) during the 1990s for network-level pavement structural evaluations (Andrén 1999, 2006). Andrén (2006) provides the RDT development history, from its early prototype stage to the first trial runs on in-service pavements. The RDT used a modified single-unit truck with the engine at the back to redistribute the weight towards the rear axle, and the dual wheels in the rear axle were substituted by super-wide single tires. During testing, a load of 25,117 lb. (112 kN) was applied via the rear axle (Andrén 2006).

The RDT deflection measurements were taken using two arrays of 20 laser sensors symmetrically distributed and mounted on an 8.2-ft (2.5-m) aluminum bar perpendicular to the direction of travel; i.e., the deflection bowl was measured perpendicular to traffic unlike other TSDDs that measure the deflection bowl in the travel direction. One array was located 1.6 ft (0.50 m) behind the rear axle and the other 8.2 ft (2.5 m) in front of the rear axle. The first array collected data from the deflection basin caused by the rear axle load, while the other array collected measurements from a non-deflected area (Andrén 2006). RDT deflections were sampled at a 1-kHz frequency, which at a travel speed of 44 mph (70 km/h) yielded deflection basins at 19.4-mm (0.76-in.) intervals (Andrén 1999). However, to account for road roughness that resulted in the truck bouncing, the deflection measurements were spatially averaged at about 164-ft (50-m) intervals (Andrén 1999). The 164 ft (50 m) averaging was considered adequate because the top speed of the truck was 56 mph (90 km/h = 25 m/s) and the bouncing frequency was lower than 2 Hz. The resulting data were used to compute various deflection parameters, including the "deflection area" (area of deflection profile) and "wire deflection area" (area

between deflection profile and line drawn between left-most and right-most points) (Andrén and Lenngren 2002, Andrén 2006).

In 1997, the RDT became the property of the Swedish VTI (Andrén 2006), while Rada and Nazarian (2011) reported that further RDT development had stopped.

RWD

The RWD was developed by Applied Research Associates (ARA) in collaboration with the FHWA. Development commenced in the 1990s, and a first-generation unit was launched in 2003 for demonstration projects throughout the United States (Arora et al. 2006, Rada and Nazarian 2011, Wilke 2014, Steele et al. 2015, Flintsch et al. 2013, Rada et al. 2016). This device measured the deflection basin produced by the load applied by its rear axle—a dual-wheel single axle with a total load of 18 kips (80 kN). The RWD instrumentation was mounted on a 53-feet-long (16.2-m) trailer to isolate the rear axle basin from the deflections produced by the tractor unit axles. The trailer was climate-controlled to maintain the sensing equipment at a constant temperature (Rada and Nazarian 2011, Steele et al. 2015).

In the first-generation RWD, the deflection measuring system consisted of four triangulation lasers mounted on a longitudinal beam ahead of the trailer's rear axle. The lasers had a resolution of 0.7 mils (18 μm) with an accuracy of 0.2% of the measuring range (Steele et al. 2002). The pavement deflection was calculated using the spatially coincident methodology first proposed by Dickerson and Mace (1976) and developed by Harr and Ng-A-Qui (1977). The data sampling frequency was 2 kHz (which at 55 mph [88 km/h] returns a measurement every 0.5 in. [12.7 mm]), but measurements were spatially averaged at 100 ft (33 m) (Arora et al. 2006, Flintsch et al. 2013, Rada et al. 2016) or 0.1-mile (0.16-km) intervals (Steele et al. 2015, Rada et al. 2016). Although the lasers themselves had a resolution of 0.7 mils (18 μm) and an accuracy of 0.2 percent of the measuring range, the random measurement errors were affected by factors such as pavement surface texture and roughness. These errors were larger than 4 mils (102 μm) for the data averaged over 1 m, which is larger than the laser resolution (Elseifi et al. 2012).

After the Rada et al. (2016) evaluation, the RWD underwent a redesign of the deflection measuring system. This redesign is documented in Steele (2020) and some of the more significant changes, as detailed in Steele (2020), are summarized over the remainder of this paragraph. The laser measuring system was replaced with a camera light combination called RWD-Vision. The new system allowed for measurement of the full deflection basin as opposed to specific spot deflections obtained from the lasers. The determination of pavement deflections still relied on the spatially coincident methodology, but with two images—one of the undeflected pavement and another of the deflected pavement. Light-emitting diodes (LEDs) were used to light the areas captured by the cameras to reduce the changes in lighting conditions between the deflected and undeflected images. Customized image-processing software was used to determine pavement deflections based on the two captured images. The imaging system captured the pictures of the pavement every 25 ft (7.62 m), and the deflection basins were reported as the average deflection over 500-ft (152.4-m) intervals.

RAPTOR

The RAPTOR was jointly developed by Dynatest and the Technical University of Denmark. The truck's trailer unit encases the deflection measurement instrumentation, the independent wheels with their corresponding suspension system, and additional weight units to adjust the load

to 11.2 kips (50 kN) on each rear wheel (Andersen et al. 2017, Athanasiadis and Zoulis 2019, Skar et al. 2020). The device uses an array of 12-line lasers—located ahead and behind the vehicle's rear wheels and mounted onto a beam—to scan a strip of the pavement (Andersen et al. 2017, Deep et al. 2020). Each line laser sweeps an 8-in. (200-mm) long transverse line. All lasers measure the distance to the pavement surface and the pavement texture at a frequency of 4 kHz. Proprietary image correlation software detects specific features in the pavement texture and uses those to match the imagery from all sources and different timestamps. A gyroscope and accelerometer are mounted on the support beam to measure the changes in its horizontal and vertical alignments. Unlike other TSDDs, the pavement response is measured by the RAPTOR at an offset from the wheel load travel path.

Andersen et al. (2017), Madsen and Pedersen (2019), Athanasiadis and Zoulis (2019), and Skar et al. (2020) report that pavement deflections are determined from RAPTOR measurements by the spatially coincident methodology, based on a principle like the one used by the ARA RWD. Unlike the ARA RWD, where the three reference laser sensors are placed far from the wheel load to measure the undeflected pavement, the RAPTOR sensors are more closely spaced so that two spatially coincident measurements occur in the deflected pavement.

The measurement obtained from the RAPTOR consists of the curvature, which is a second-order differential equation of the deflections (Andersen et al., 2017). Another important factor considered by the RAPTOR that is not considered by the RWD is the horizontal rotational movement of the beam on which the sensors are mounted. This rotation results in a variable angle between the laser sensors and a vertical plane, which influences the measured deflection. The gyroscope and accelerometer mounted on the beam are used to determine that angle and make appropriate corrections (Andersen et al. 2017, Athanasiadis and Zoulis 2019).

TSD

Information about the TSD is found in the reports by Hildebrand et al. (1999), Hildebrand and Rasmussen (2002), Flintsch et al. (2013), and Rada et al. (2016). The TSD was developed by Greenwood Engineering in collaboration with the Danish Road Institute. It is an articulated truck with a rear-axle load that can be varied from 13 kips to 29 kips (60 kN to 130 kN). The device has lasers mounted on a servo-hydraulic beam to measure the deflection velocity of a loaded pavement. The TSD operating in the United States prior to this study used six lasers, positioned at nominal distances of 4, 8, 12, 24, 36 and 60 in. (100, 200, 300, 600, 900 and 1,500 mm) in front of the loading axle. A seventh sensor was positioned 11.5 ft (3.5 m) in front of the rear axle to act as a reference laser. The beam on which the lasers was mounted moved up and down opposite to the trailer movement to keep the lasers at a constant height from the pavement's surface. To prevent thermal distortion of the beam, a climate control system maintained the trailer temperature at 68°F (20°C). Data were collected at speeds up to 60 mph (100 km/h) with sampling rates between 250 and 1,000 Hz.

The TSD measurements are deflection velocities rather than deflections. These measurements are collected by lasers that rely on the Doppler effect (Hildebrand et al. 1999, Hildebrand and Rasmussen 2002). Each laser sends a wave that is reflected from the pavement surface to a receiver within the laser. If an object is moving toward the laser, each successive wave peak reaches the object in a shorter time than the original time interval between the two peaks. In the case in which an object is moving away from the laser, the effect is reversed, and

the reflected wave will exhibit a decreased frequency. Moreover, since the wave speed is known, the change in frequency is used to determine the velocity at which the object is moving.

The TSD lasers are mounted at an angle of about 2 degrees (to the vertical) to measure the vertical pavement deflection velocity together with components of the horizontal vehicle speed and the vertical and horizontal vehicle suspension velocities (Hildebrand et al. 1999, Hildebrand and Rasmussen 2002). The reference laser, located midway between the loaded trailer axle and rear axle of the tractor unit, takes measurements outside the load influence zone, and can be used to remove unwanted signals from other lasers (Hildebrand et al. 1999, Hildebrand and Rasmussen 2002).

The measured deflection velocity depends on the driving speed. To remove this dependence, the deflection velocity is divided by the instantaneous vehicle speed to obtain the deflection slope. Typically, deflection velocity is measured in in./s (mm/s) and vehicle speed is measured in mph (km/h), so deflection slope measurements are output in units of in./ft (mm/m) and typically reported at 33-ft (10-m) intervals (Flintsch et al. 2013). At a speed of 50 mph (80 km/h) and a data collection frequency of 1 kHz, an average of 446 measurements over a 33 ft (10 m) length are made. Newer versions of the Doppler laser operate at a sampling rate of 250 kHz, which results in more than 10,000 measurements per 3.3 ft (1 m).

DEFLECTION CHARACTERISTICS AND FACTORS AFFECTING MEASUREMENTS

TSDD versus FWD Measurements

TSDDs and FWDs are different in terms of the loading type, load contact area, measurement technology, and the way pavement deflections are estimated. Most TSDDs are full-sized trucks that house the measuring equipment. The load is imparted via the trailer's rear axle while the device is in motion. Since the load is transmitted via tire-pavement interaction, the contact area is elliptical with non-uniform contact pressure (Elseifi et al. 2019). FWDs, on the other hand, use stationary impulse loading dropped onto the pavement surface through a circular steel load plate.

Another difference is the pavement response recorded by each device. TSDDs measure the instantaneous pavement response experienced by the sensors. This response occurs at the same time the maximum load is applied. Because of the time needed for the stress wave caused by wheel load to propagate and the viscoelastic nature of hot-mix asphalt (HMA) pavements, the instantaneous response does not correspond to the maximum deflection response. In the case of FWDs, the recorded deflection measurements correspond to the maximum deflection experienced by the sensors (Shrestha et al. 2018). Consequently, it is difficult to obtain a direct relationship between TSD and FWD measurements (Saremi 2018). The difference becomes more pronounced for sensors further from the load (Chatti et al. 2017).

Factors Affecting TSDD Measurements

Pavement Factors

Characteristics such as pavement type, layer materials, pavement smoothness, gradient, and curvature affect TSDD measurements. While several studies were found in the literature on the effect of these parameters, they were limited in scope. Elseifi and Zihan (2018) evaluated TSD measurements on sections having different roughness and found that rougher pavements resulted in a higher coefficient of variation (COV). Flintsch et al. (2013) looked at the effect of pavement surface on the laser capabilities and found that new binder-rich surfaces—which does not imply all new asphalt pavements—cause faulty operation of the TSD Doppler lasers. Therefore, it is

not recommended to use TSDs in these conditions; however, as the surface becomes less reflective due to traffic, the TSD can provide reliable measurements regardless of surface type.

Rada et al. (2016) pursued the effect of pavement characteristics and found that the accuracy of the TSD and RWD measurements is affected by pavement stiffness but not the International Roughness Index (IRI). Diefenderfer 2010 evaluated the RWD in Virginia and found surface mixture type influenced the standard deviation of the measurements. Elseifi et al. (2012) compared RWD and FWD on sections with varying structural condition and found the agreement improved for sections in structurally sound condition and speculated that for roads not structurally in sound conditions, the increase in road roughness may cause greater truck bouncing and vibrations, which may explain the differences between FWD and RWD measurements.

Saremi (2018) conducted a numerical analysis using 3D-Move to simulate the responses of TSD at different speeds for 10,000 different pavement sections with different layer thicknesses and moduli to relate TSD deflection parameters to FWD. The study showed that for pavements with an HMA thickness of less than 4 in. (100 mm), varying the modulus of the HMA between 200 ksi and 700 ksi to account for viscoelasticity, resulted in less than 5% variation in the deflection velocity of the TSD measurements. Thus, the impact of viscoelasticity was found to be much less than the uncertainty of the TSD measurements, which is often greater than 20%. Moreover, the study indicated that the TSD deflection parameters at speeds varying from 30 mph to 60 mph were similar; however, the TSD pavement response under stationary conditions was somewhat different from those obtained under moving conditions. The difference in the deflection basins was mostly evident in the farther sensors.

Environmental Factors

Surface and subsurface moisture and temperature conditions influence TSDD measurements. In addition, temperature has a significant effect on the beams on which the TSD and RWD lasers are mounted. As a result, both devices incorporate a climate control system that maintains a trailer temperature of 68°F (20°C) (Flintsch et al. 2013). Rada et al. (2016) analyzed the impact of temperature on TSD and RWD precision and found that TSD measurements precision decreased with increases in temperature but increased for the RWD. The precision was measured in terms of the COV of the measurements and the authors found that for the RWD, the tests performed in the afternoon were more precise (COV decreased by 7%) than the tests performed in the morning. On the other hand, for the TSD, afternoon tests had COV values that were 32% greater than the tests performed in the morning.

Rain also affects TSDD measurements as they are based on laser technology, which cannot report accurate measurements on wet pavement surfaces. Elseifi et al. (2011) reported that the presence of rain on the pavement surface can lead to erroneous data. Flintsch et al. (2013) reported that the TSD failed to measure deflection parameters correctly when the road was damp or wet. Rada et al. (2016) recommended testing not be performed if the pavement surface is wet or during precipitation, as the TSD and RWD sensors are affected by moisture.

In addition, a crosswind perpendicular to the trailer can cause asymmetric loads between the two sides of the TSDD. Zofka et al. (2015) performed a theoretical evaluation of the effect of wind on the load distribution between the two sides, while Rada et al. (2016) recommended that testing not be performed under strong crosswind conditions, especially if the applied load on each side of the trailer was not being measured. If the load is measured, then the measured

response can be normalized by the applied load, which will account for the asymmetric loading caused by the crosswind (Katicha, 2017).

Operating Conditions

TSDD measurements can be affected by operating conditions. A theoretical investigation by Elseifi and Zihan (2018) suggested speed had a limited impact on surface deflections, although increasing speed slightly reduced deflections. Rada et al. (2016) reported on the impact of vehicle speed on the accuracy and precision of the TSD and RWD. They calculated the COV of the RWD and TSD on different pavement sections at the MnROAD testing facility. The authors found that the COV increased by a factor of 5 to 10% as the testing speed increased from 30 mph (48 km/h) to 60 mph (96 km/h).

Horizontal and vertical curves may also affect TSDD measurements. Flintsch et al. (2013) looked at the effect of road geometry based on data collected in the United Kingdom in 2010 and 2011 and concluded there was no obvious relationship between longitudinal profile, gradient, transverse slope, or curvature on TSD measurements. Rada et al. (2016) analyzed the impact of vertical gradient and horizontal curves on the precision of the TSD and RWD on an 18-mile (29-km) loop using 33-ft (10-m) interval data. The authors did not observe a clear correlation between a vertical gradient and COV. For the case of horizontal curves, the study reported that most of the high COVs corresponded to sharp turns or stop sign locations, but quantitatively there was no clear correlation between horizontal curvature and COV.

TSDD EVALUATIONS

TSD Evaluations

Numerous studies have been performed throughout the world to assess the accuracy and precision of TSD measurements. Some of the more relevant studies to the project at hand are detailed here in chronological order. Hildebrand et al. (1999) determined the precision of the Doppler lasers' to be 5.5 mils/s (0.14 mm/s). For measurements averaged over 33-ft (10-m) intervals and collected at 45 mph (72 km/h), this corresponds to a deflection slope precision of 0.084 mils/ft (7 μm/m). The authors also estimated the deflection slope precision to be about 0.2 mils (5 μm).

Ferne et al. (2009) looked at short- and long-term TSD repeatability. For the short-term repeatability evaluation, six TSD runs were conducted at a test track on the same day and the results were plotted. For long-term repeatability, an investigation was conducted of possible causes linking temperature variations to variations in the TSD data. Detailed temperature measurements at various points on the beam were collected during the surveys. The authors described that the short-term repeatability of the TSD was acceptable based on visual inspection of repeated measurements; however, according to Ferne et al. (2009), a comparison of the temperature measurements with the survey results showed that the repeatability at beam temperatures below 59°F (15°C) was poor.

Bryce et al. (2012) and Flintsch et al. (2013) assessed the repeatability of TSD measurements at 45 mph (72 km/h) and found that the repeatability was relatively constant over a range of measurements, and the bias was generally not significant. In both publications, the repeatability was defined as the standard deviation of the difference between repeated measurements. For 3.3-ft (1-m) averaged TSD measurements, the average repeatability standard deviation for deflection slope measurements was 1.68 mils/ft (0.14 mm/m) and the standard deviation was reduced by a

factor of 3.3 for measurements averaged over 33 ft (10 m) and by a factor of 10 for measurements averaged over 330 ft (100 m). Similarly, Katicha and Flintsch (2015) presented the results of TSD testing in New York and concluded that the measurements agreed well, suggesting the TSD is repeatable, and that the measurement variations were due to the pavement structural conditions.

Muller and Wix (2014) conducted a series of field trials at three locations to evaluate the repeatability of the maximum TSDD deflection measurements. Five or six runs were made at each location and the authors found the TSD maximum deflections to be repeatable ($R^2 = 0.88$).

Ferne et al. (2015) compared two first-generation TSDs and one second-generation TSD. The resulting measurements followed similar trends, but they were sensitive to the laser angle calibration. The authors observed a maximum variation of 0.003 degrees in the angle of the calibrated second-generation TSD using two concrete pavement sections. For the first-generation TSDs, the maximum observed angle difference was 0.007 degrees. These differences were large enough to produce different measurements, which equal to 60% and 140% of the range used by Highways England to define the pavement structural condition categories.

GeoSolve (2016) carried out TSD repeatability studies at different vehicle speeds. They found the measurements varied slightly at speeds over 19 to 25 mph (30 to 40 km/h). At lower speeds, the measurements tended to be higher, sometimes by a factor of 2 or more, as speeds diminished toward 0 mph (0 kph).

Rada et al. (2016) performed field tests in Minnesota to evaluate the TSD at different speeds and times of the day (hence different temperatures). The authors found that the TSD could provide reasonably accurate and precise measurements. The overall comparison of deflection velocities measured with the TSD and by geophones embedded in the pavement resulted in a correlation coefficient of $R^2 = 0.97$ and a standard error 49.2 mils/s (1.25 mm/s). The analyses were used to recommend the optimum operational conditions and device limitations. More specifically, the researchers recommended the optimal placing of the lasers. For example, sensors at distances of 4, 8, 12, and 18 in. (101.6, 203.2, 304.8, and 457.2 mm) from the center of the wheel load were recommended to evaluate fatigue cracking and 24 and 48 in. (609.6 and 1,219.2 mm) were recommended to evaluate subgrade rutting. In terms of testing speed, Rada et al. (2016) recommended testing at the lowest possible speed as lower speeds reduce the measurement error. The authors also recommended a conservative operational temperature range of 45°F to 85°F (7.22°C to 29.44°C). In terms of limitations, testing is not recommended during precipitation; the effect of temperature and seasonal variation on the interpretation of the measurement has not been thoroughly investigated, and the calibration procedure of the TSD should still be improved.

Katicha et al. (2017) conducted TSD field demonstrations in nine states to demonstrate how TSD results could be implemented within network-level pavement management and to evaluate the TSD's short- and long-term repeatability. Based on subjective visual inspection of the plots, they found the short- and long-term repeatability to be good; repeated measurements on consecutive days or two years apart followed similar trends.

Other studies have attempted to evaluate the TSD accuracy and precision by comparing their measurements with other deflection-based testing devices, such as the FWD. Some of the more significant studies in the United States are listed next in chronological order. Flintsch et al. (2013) performed TSD and FWD measurements on asphalt- and concrete-surfaced pavements to

assess the comparability of the device measurements using two surface indices: surface curvature index (SCI) and base damage index (BDI). The authors concluded that the TSD-derived indices were comparable to those from the FWD. For the SCI index, the authors found that the standard deviation of the difference between TSD and FWD measurements depended on the average SCI value. The standard deviation changed linearly from 0.4 mils (10 μm) for average SCI values of 0.4 mils (10 μm) to about 4 mils (100 μm) for average SCI values of 20 mils (500 μm).

Jansen (2017) reported on TSD measurements made on 188 mi (300 km) of German roads with different structural conditions. The measurements were supplemented with FWD, Deflectograph, and Curviameter measurements. The author concluded that the TSD results were similar to those from other devices and, while a correlation between TSD and FWD measurements was not reported by the author, the same deflection levels were observed via plots of the TSD and FWD measurements along the roads tested.

Elbagalati et al. (2018) used TSD and FWD measurements to train and validate an artificial neural network (ANN) model that converted TSD deflection measurements to FWD measurements. The authors found acceptable accuracy (coefficient of determination of 0.90) and good agreement between the back-calculated moduli from the FWD and TSD measurements.

Saremi (2018) used numerical analyses to relate FWD and TSD deflection measurements. A total of 10,000 asphalt pavement sections with randomly distributed layer thickness and moduli were considered. The software 3D-Move was used to simulate the responses under TSD and FWD loads. The authors found strong relationships between the deflection measurements from the two devices and developed relationships using symbolic regression for estimating FWD deflections from TSD measurements. Their best model had a correlation greater than 0.98 and consisted of the following equation, which converts TSD deflection to FWD deflection:

$$d_{FWD}(x) = 0.85 d_{TSD}(x) + \beta(x) \frac{d_{TSD}(x)}{H_{AC}}$$

where $d_{FWD}(x)$ is the FWD deflection at location x measured from the center of the applied load, $d_{TSD}(x)$ is the TSD deflection at location x, H_{AC} is the asphalt layer thickness, and $\beta(x)$ is given by the following equation.

$$\beta(x) = \begin{cases} 0.0017x^2 - 0.078x + 0.92 & for\ 0 \le x \le 0.24 \\ 0.02 & for\ 0.24 < x \le 0.48 \end{cases}$$

Unlike the TSD-FWD studies in the United States, some international studies observed no direct correlation between the TSD and FWD (Kannemeyer et al. 2014, Muller and Wix 2014, Jansen 2017). However, other studies have shown that a strong correlation exists when curvature indices are used (Muller and Robert 2013, Chai et al. 2016, Lee et al. 2019). For example, Muller and Roberts (2013) observed a correlation between the TSD and FWD of 0.89 for the maximum deflection and 0.85 for the surface curvature index 12 (SCI12) [SCI 300], which was defined as the difference between the deflections measured at 0 in. (0 mm) and 12 in. (300 mm) (0 mm) from the center of the applied load.

Muller (2015) explored the combined use of TSD and ground penetrating radar (GPR) technology for assessing the potential for rapid pavement nondestructive investigations. Approximately 6,250 mi (10,000 km) of TSD data were collected for comparison with FWD and GPR data. The authors found that the overall patterns of the TSD appeared similar in shape and magnitude to those from the FWD when normalized to 11 kips (50 kN).

A couple of international studies have also verified TSD measurements using instrumented pavement test sections. Kannemeyer et al. (2014) conducted a verification of the TSD measurements by instrumenting—with eMU coils, strain gauges, pressure cells, multi-depth deflectometers, thermocouples, and time-domain reflectometers— eight asphalt test sections in South Africa. They found the TSD measurements to be repeatable. They also concluded that the stiffer pavements were more sensitive to changes in speed.

Lee et al. (2019) documented the results of testing performed on two deflection validation sites established in Australia. The ground response for different deflection equipment was measured using embedded arrays of geophones and accelerometers to demonstrate that in-ground sensors can validate the TSD measurement. The authors found that the geophones were less susceptible to integration errors than the accelerometers. Moreover, they suggested that a system was needed to assist the driver of the TSD to travel as close as possible to the instrumentation array and minimize wander.

RWD Evaluations

Various studies have been carried out in the United States to assess the accuracy and precision of the RWD measurements. Elseifi et al. (2012) describe a field evaluation of the RWD at 16 different test sites in Louisiana representing a wide range of pavement conditions. The measurements were used to assess RWD repeatability, evaluated in terms of the COV, and the effect of speed. The authors found the RWD repeatability was acceptable, with an average COV at all test speeds of 15%. Flintsch et al. (2013) evaluated the repeatability, evaluated in terms of the standard deviation of the difference between two measurements of the RWD with data collected from three runs over 20 mi (32 km) on I-64 (both directions) in Virginia. The runs were averaged at 0.1-mi (160-m) intervals and the repeatability was found to be 2 mils (51 μm). The repeated runs had, on average, a statistically significant bias of 0.43 mils (10.9 μm).

Rada et al. (2016) evaluated the RWD at the MnROAD facility to quantify the precision and accuracy of the surface deflections. They concluded that the RWD could provide reasonably accurate and precise pavement response measurements for network-level analyses. The authors characterized accuracy in terms of the calculated regression slope between repeated measurements and the standard error of the regression. The slope varied between 0.84 and 1.68 and the average standard error was 1.45 mils (36.83 μm). The precision was characterized in terms of the regression slope and standard error between RWD measurements and embedded geophones sensors in the pavement sections. The average regression slope was 0.95 and the average standard error was 4 mils (101.6 μm). Similarly, Briggs et al. (2000) conducted a study for the Washington Department of Transportation to compare the RWD and FWD results along a stretch of SR-18. They found, based on the visual inspection of plots, that the RWD and FWD trends were similar; however, various anomalies were identified.

CHAPTER 3. TSDD MEASUREMENTS VALIDATION

This chapter contains the results of the process that led to the development of the TSDD validation procedure. The process was probabilistic in nature—the variability in the FWD and TSDD deflection measurements, being due to variability in the pavement structure or the uncertainty in the device measurements, was considered in the analysis. After addressing the variability, the accuracy of measurements was ascertained at six accuracy test sections, and the validity of the measurements was determined.

Field experiments were conducted at the MnROAD facility in Albertville, Minnesota, to establish the variability and accuracy of the TSDD measurements and to support development of the TSDD verification procedure. Information collected as part of the experiments included TSDD, FWD, and geophone data. It was anticipated that multiple TSDDs would be included in the experiments. However, only one device could be included and consequently, the findings of this research are based on measurements by one device and may not apply to other devices.

FIELD EXPERIMENTS

The MnROAD facility was selected as the site for the field experiments, since it provided a multitude of test cells in one location. The facility consists of a 3.5-mi (5.6-km) mainline (ML) roadway comprising 45 cells. In addition, a 2.5-mi (4-km) closed-loop low-volume road (LVR) containing 28 cells is also available. The cell lengths were typically about 500-ft (150-m) long.

Experiment Test Cells

Six accuracy test cells, covering a range of factors affecting the deflection measurement characteristics, were selected for instrumentation and for conducting TSDD and FWD tests. Information for the six test cells is provided in Table 1, including pavement and surface type, surface layer and total pavement thicknesses, length, SCI12 ([SCI300], and ride quality as measured by the IRI. Three test cells were selected along the ML, while the other three were selected along the LVR. This allowed for the accuracy testing of the three cells in each facility to take place on the same day.

Five other test cells were selected for conducting FWD and TSDD tests (without instrumentation) to verify the repeatability of the devices on a wider variety of surfaces, pavement types, and stiffnesses. The information for these test cells is also presented in Table 1.

In addition to the test cells listed in Table 1, TSDD measurements were performed on the remaining ML and LVR test cells and transition areas to assess the macro- and micro-variability of the TSDD device. Macro-variability refers to the variability of the TSDD measurements as determined from the data collected over the length of the MnROAD facility. Micro-variability, on the other hand, refers to the variability associated with the measurements collected at the individual accuracy test cells—i.e., measurements over shorter, more uniform pavement lengths. Both the macro- and micro-variability are discussed in more depth later in this chapter. These variability analyses were limited to the TSDD as they are well-documented for the FWD (Irwin et al. 2011, Rocha et al. 2014).

Table 1. MnROAD accuracy and precision test cells.

Facility	Test Cell	Cell	Surface Type	HMA/PCC* Thickness (in.)	Pavement Thickness (in.)	Length (ft)	SCI12 (mils)	IRI (in/mi)
ML	Accuracy	215	HMA	14.8	14.8	283	4.1	92
		12	PCC	9.5	13.5	499	1.7	141
		70	HMA/PCC	3.0 HMA/ 6.0 PCC	17.0	480	1.4	63
LVR	Accuracy	186	HMA	3.5	19.0	201	4.2	90
		728	HMA	3.5	18.5	131	13.0	177
		31	HMA	4.0	20.0	500	23.7	307
	Precision	135	HMA	1.5	17.5	425	20.5	119
		233	Chip Seal	0	16.0	425	43.0	169
		139	PCC	3.0	13.0	275.5	9.4	193
		238	PCC	8.0	13.0	270	1.7	91
		124-624	PCC	6.0	12.0	568	2.4	78

*PCC: Portland Cement Concrete

Instrumentation

Three geophones were embedded in the outer wheel path of each MnROAD accuracy test cell to measure the velocity-time histories from the FWD impulse loading and the TSDD transient loading. The geophones were encased in metallic holders to protect them. The top of the geophone assemblies was flush with the pavement surface, and the bottom was at a depth of about 2 in. (50 mm). Since the geophones were embedded in rigid casing, the differential movements between the top of the pavement and base of the geophone were minimal.

As shown in Figure 1, the geophones were spaced 3 ft (1 m) apart along the center of the wheel path. The deflections measured with the three geophones were averaged and compared with the average deflection measurements from the consecutive TSDD passes—averaged over 2 in. (50 mm) or 3.3 ft (1 m)—and the average of the FWD deflection measurements at the location of the geophones.

The performance of the geophones was verified using FWD test data. For that purpose, one of the FWD sensors was placed directly on top of one of the geophones. The deflections reported by the FWD were then compared with the corresponding deflections reported by the geophones. The results from the comparison are presented in Figure 2. The deflections from the FWD sensors and the geophones were quite similar. Based on the reported statistics in Figure 2, the deflections of the FWD and geophones were within about 0.2 mils (0.005 mm) of one another.

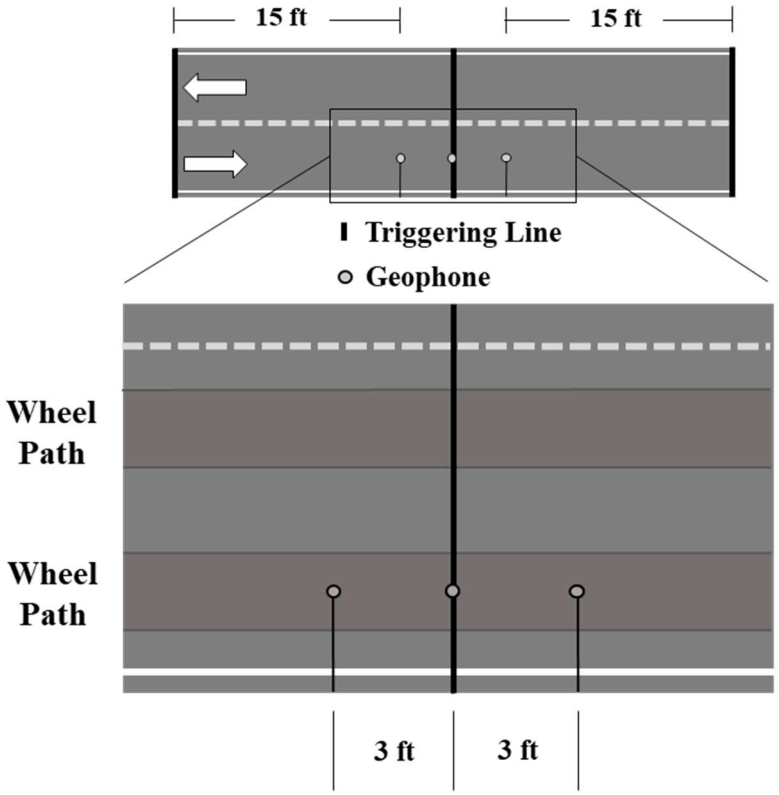

Figure 1. Typical test cell instrumentation.

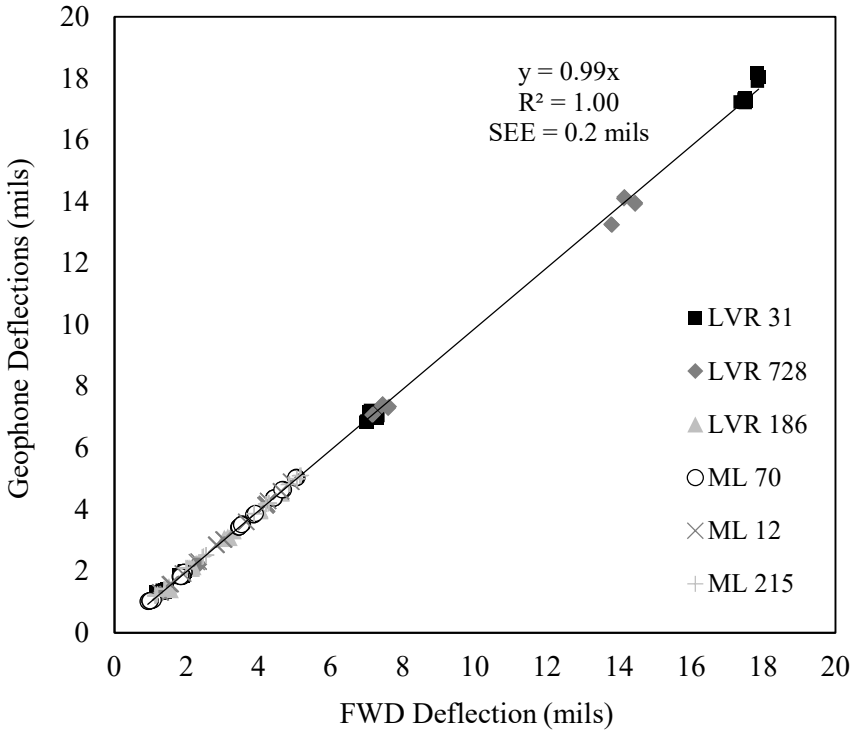

Figure 2. Comparison of field geophones and FWD deflections.

TSDD Pressures and Weights

The TSDD tire pressures and axle weights are important parameters that were measured at the MnROAD facility. The TSDD tire pressure and axle load measurements are listed in Table 2. The axle loads were measured one axle at a time using portable truck scales.

Table 2. TSDD tire pressures and axle loads.

Tire Type	Tire Pressures (psi [kPa])				Axle Loads (lbs. [kg])	
	Left Outer	Left Inner	Right Inner	Right Outer	Left	Right
Tractor Front (Steer)	N/A	110 (759)	110 (759)	N/A	5,200 (2,360)	5,247 (2,380)
Tractor Rear (Drive)	105 (724)	105 (724)	105 (724)	110 (759)	8,465 (3,840)	9,127 (4,140)
Trailer	110 (759)	Could not access	Could not access	120 (827)	9,260 (4,200)	10,780 (4,890)

Temperature Data

The ambient temperature during the MnROAD field experiments ranged from 64°F (18°C) in the morning to 80°F (27°C) in the afternoon. The subsurface temperatures for the accuracy and precision test cells were taken every 15 minutes with thermocouples located at various depths. Figure 3 illustrates the temperatures at three depths for test cell 31; 0, 4, and 48 in. (0, 100, and 1,200 mm) from the surface. The subsurface temperatures for the accuracy and precision test cells had similar ranges to the ambient temperatures illustrated in Figure 3.

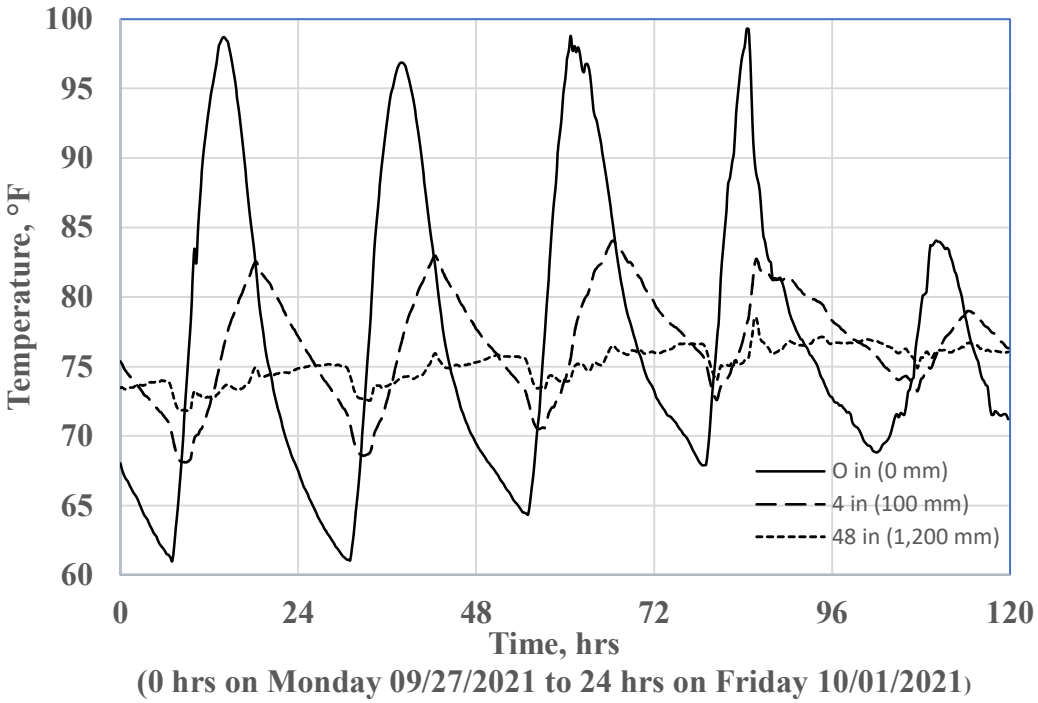

Figure 3. Subsurface pavement temperatures during field experiments – test cell 31.

The temperatures shown in Figure 3 are for the period of 0 hours on Monday September 27 to 24 hours on Friday October 1, 2021, which corresponds to the field experiments period. Little

change was observed at the 48 in. (1,200 mm) depth, with values ranging between 72°F and 78°F (22°C and 26°C), but the changes at or near the surface were significant, ranging from 61°F to 99°F (16 and 37°C). However, since FWD and TSDD measurements at each test cell were performed roughly at the same time of the day, temperature adjustments were not deemed necessary.

Moreover, it was originally envisioned that environmental factors such as temperature and moisture condition would be incorporated into the project analyses and model development efforts. After further consideration, however, the research team concluded that this was not necessary. The objective of the project was not to develop temperature or moisture correction procedures to estimate deflections under different temperature and moisture regimes, but rather to develop a procedure for verifying the TSDD measurements based on FWD measurements. Accordingly, the research team opted for a proposed practice that requires TSDD and FWD testing to be carried out on the same day, under similar conditions. By doing this, temperature becomes a non-issue, which in turn, results in a simpler verification procedure.

Distress Data

The surface condition of the six accuracy test cells was mapped using the TSDD-mounted camera. Besides surface distresses, the camera captured the location of the geophones at each test cell as well as the FWD locations. The resulting images were used to identify valid TSDD runs based on the location of the load relative to the geophones.

DEFLECTION-BASED DEVICES

A series of FWD drops were conducted at the test cells listed in Table 1, at a nominal 10 kips (45 kN) load on a 5.91-in. (150-mm) radius plate that nominally exerted a 90-psi (550-kPa) pressure. The FWD was configured with a modified Long-Term Pavement Performance (LTPP) sensor configuration, with sensors located at the distances shown in Figure 4. At each test cell, FWD tests were conducted every 3.3 ft (1 m) at up to 13 locations. Each FWD test consisted of collecting deflection data for three consecutive drops after applying three seating drops.

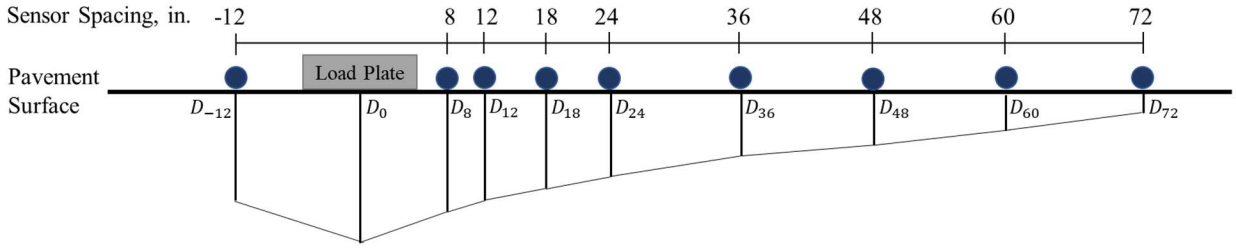

Figure 4. Modified SHRP FWD sensor configuration.

The available TSDD had the axle, load and Doppler laser configurations shown in Figure 5. A tire pressure of 120 psi (827 kPa) and a nominal load of 5,200 lbs. (2,350 kg) per tire were measured. Three Doppler laser sensors were mounted behind the tire at distances of 18, 12, and 8 in. (450, 300, and 200 mm) from the load center. Eight more sensors were located ahead of the tire at 5, 8, 12, 18, 24, 36, 48, and 60 in. (130, 200, 300, 450, 600, 900, 1,200, and 1,500 mm) from the center of the two tires.

At each accuracy test cell, the TSDD data were recorded at 2-in. (50-mm) intervals over a distance of 46 ft (14 m), starting 23 ft (7 m) before the middle geophone and ending 23 ft (7 m)

ahead of it. For the LVR cells, five runs were conducted at 30 mph (48 km/h) and six runs at 45 mph (72 km/h) mph. For the ML cells, six, five, and six passes were conducted at operating speeds of 30, 45, and 60 mph (48, 72, and 96 km/h), respectively. The raw deflection velocities collected at a speed of 30 mph (48 km/h) at cell 31 are illustrated in Figure 6 for the TSDD sensors located at 8, 24, and 60 in. (200, 600, and 1,500 mm).

MACRO-VARIABILITY OF DEVICE MEASUREMENTS

Before moving on to the validation of the TSDD measurements, the TSDD macro-variability was determined using the complete set of measurements collected at the MnROAD facility. Figure 7 shows an example of the measured deflection velocity of two runs collected over the entire LVR loop (28 test sections and transitions) at a resolution of 2 in. (50 mm) and at a speed of 30 mph (18 km/h). Matching of the two runs was performed in two steps: (1) runs were aligned using GPS coordinates and (2) cross-correlation was used to further match the two runs. Although the two runs look similar, a plot of the difference in the measured deflection velocities between the two runs highlights the discrepancies.

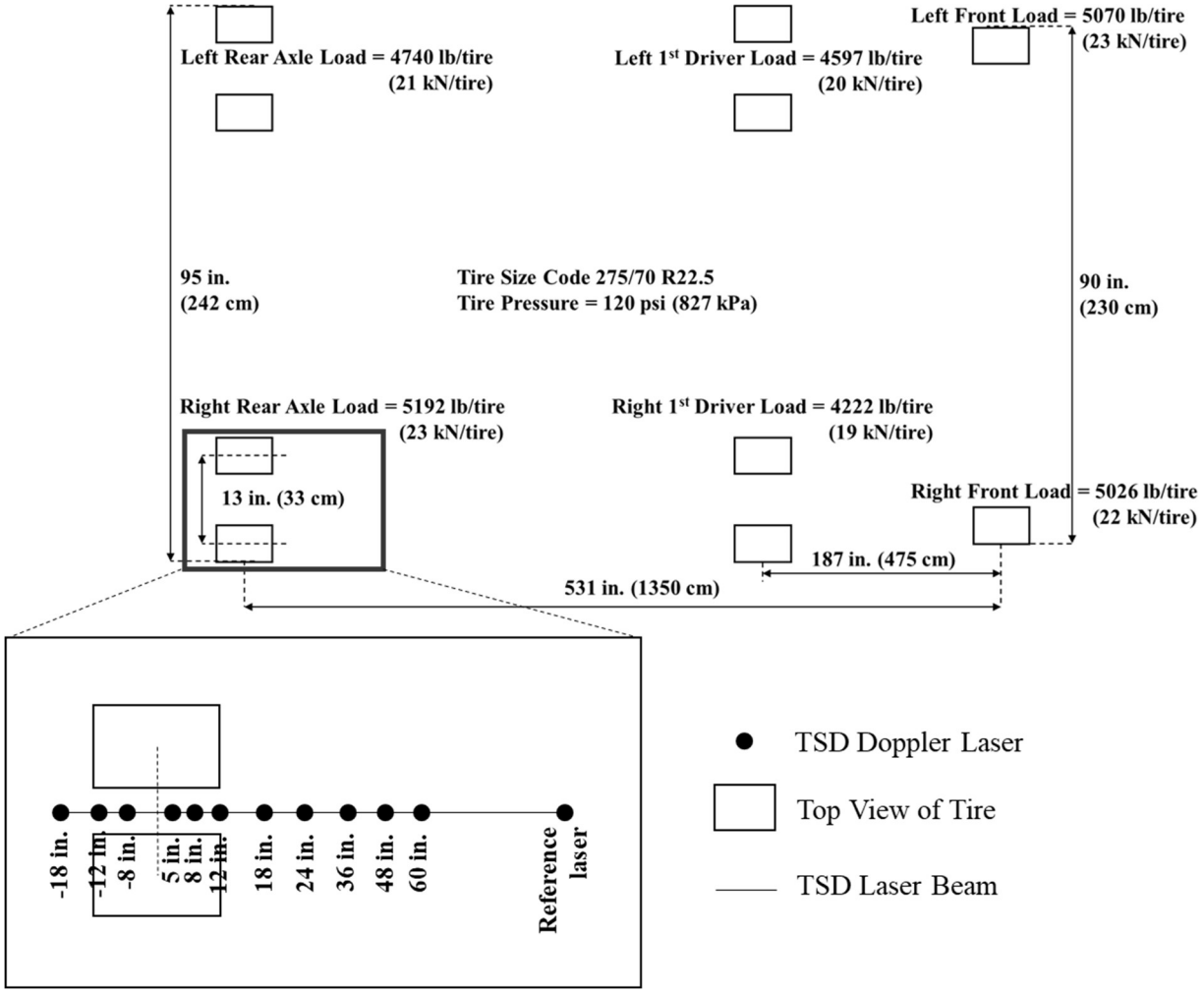

Figure 5. TSDD axle configuration, loads, and instrumented rear axle.

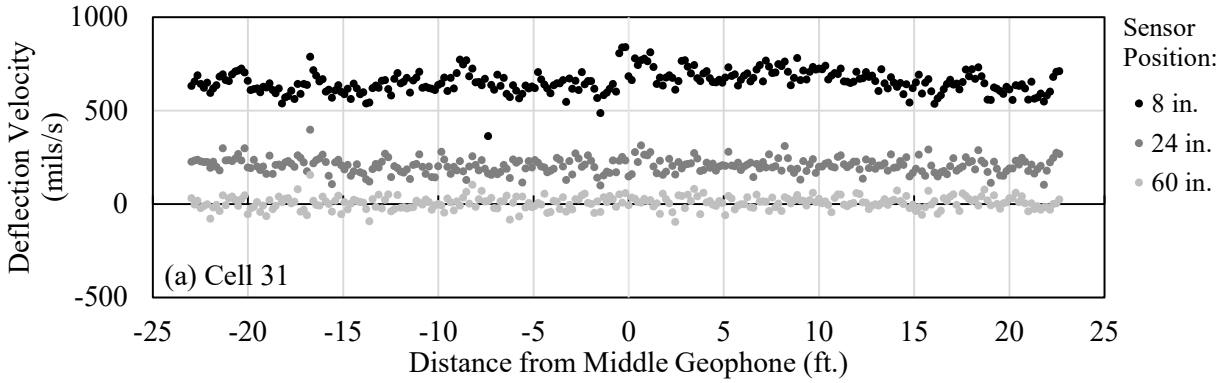

Figure 6. TSDD deflection measurements in LVR test cell 31.

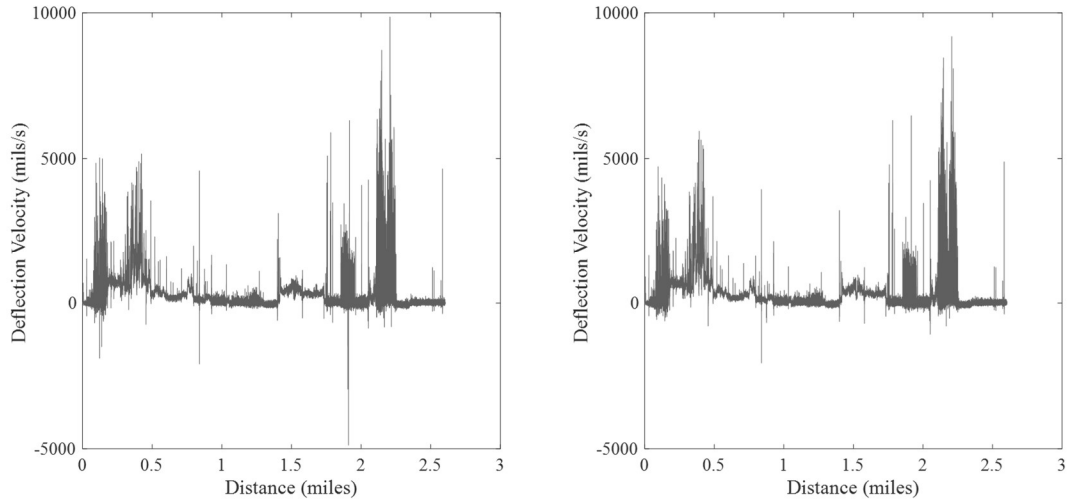

Figure 7. Two TSDD runs collected at 30 mph on LVR.

Figure 8 shows the difference along the LVR and the absolute value of the difference as a function of the average of the two runs. For the latter, a moving average estimate of the error difference standard deviation as a function of the measurement is plotted. This was calculated by first squaring the differences, applying the moving average at a specific window size (number of points in the moving average), and taking the square root of the result (Fan and Yao 1998, Ruppert et al. 1997). The best window size was selected by minimizing the Generalized Cross Validation (GCV) criterion (Wahba 1990). The resulting estimate divided by the square root of two gives an estimate of the TSD error standard deviation as a function of the measurement. Finally, dividing that estimate by the measurement value gives the COV.

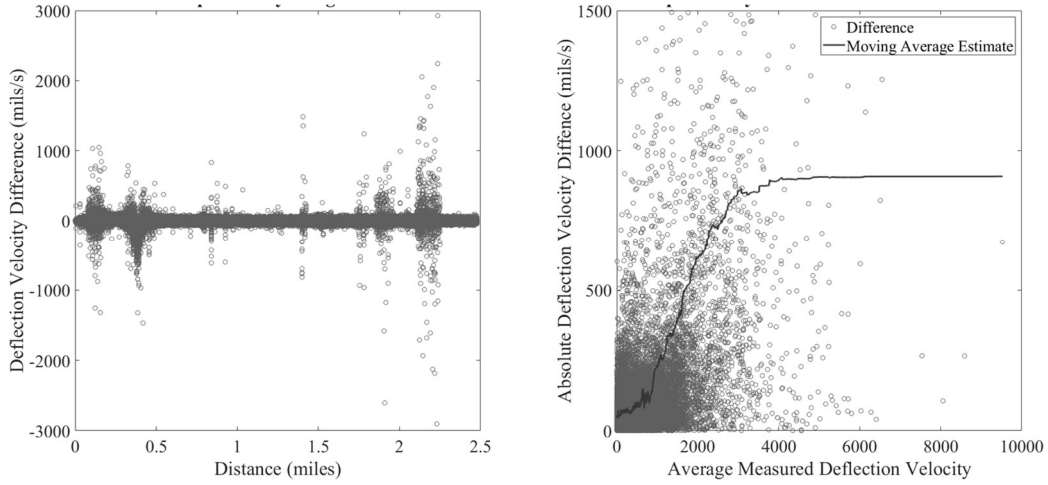

Figure 8. Difference between repeated TSDD measurements at 30 mph on the LVR.

The COVs as a function of the measured deflection velocity for the tests performed at speeds of 30 and 45 mph (48 and 72 km/h) are shown in Figure 9. Because the macro-analysis results were the same for the two speeds, the measurements were combined and only one COV value for each averaging length is included in the figure. As shown, the COV is initially high for low measurements—the error standard deviation is never zero and dividing that quantity by a measurement close to zero yields a high COV. The COV then drops rapidly and levels out around 25% for the 2-in. (50-mm) measurement interval, and between 5% and 10% for the 3.3-ft (1-m) and 33-ft (10-m) measurement intervals; see Table 3.

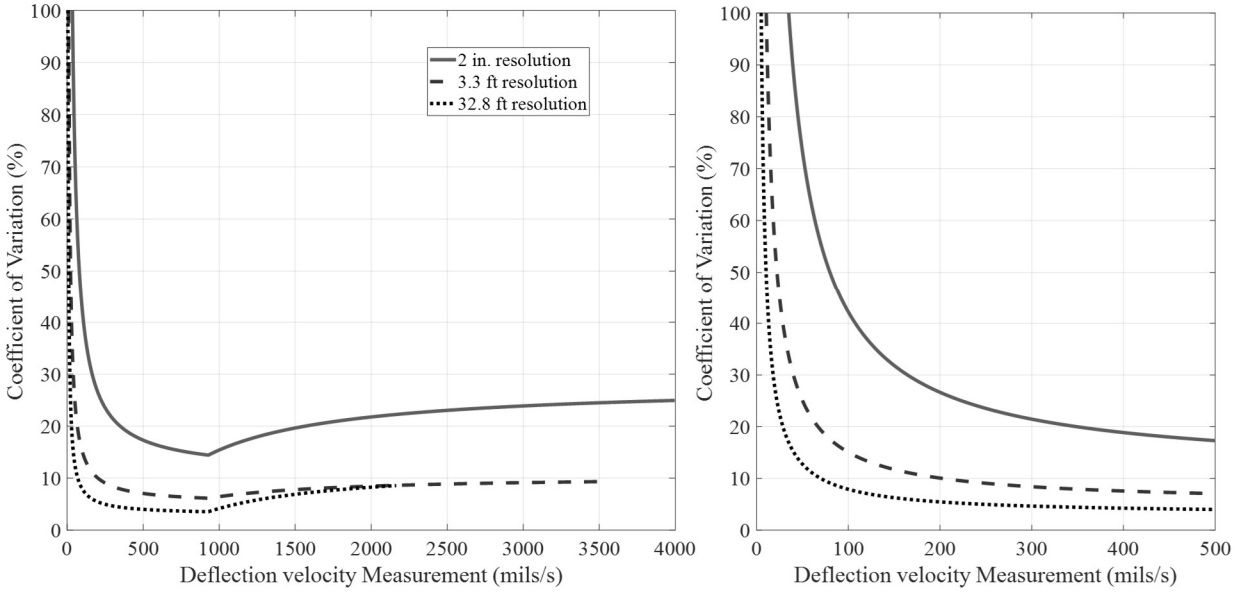

Figure 9. COV versus TSDD deflection velocity at combined 30 mph and 45 mph.

Table 3. COV as a function of speed and averaging distance.

Test Speed	COV (%) for different data averaging distances		
	2 in. (5 cm)	3.3 ft (1 m)	32.8 ft (10 m)
30 mph (48 km/h)	25	10	10
45 mph (72 km/h	25	10	10
60 mph (96 km/h)	35	15	10

The results for measurements collected at 60 mph (96 km/h) are presented in Figure 10. For measurement intervals of 3.3 ft (1 m) and 32.8 ft (10 m), the COV decreases to values less than 10%, but at a slower rate than for those at 30 mph and 45 mph (48 km/h and 72 km/h). For the 2-in. (50-mm) measurement interval, the COV decreases to less than 15% at deflection velocities close to 1,000 mils/s (25.4 mm/s), but then increases to more than 30%. The tests at 60 mph (100 km/h) were only performed on the ML (due to safety concerns at the LVR), which had fewer measurements of 1,000 mils/s (25.4 mm/s) or more, and most of these measurements were obtained at the joints of concrete pavements, which are less homogeneous and therefore less reliable—e.g., small deviations in the path between two runs can result in large differences in the measurements, which increases the COV.

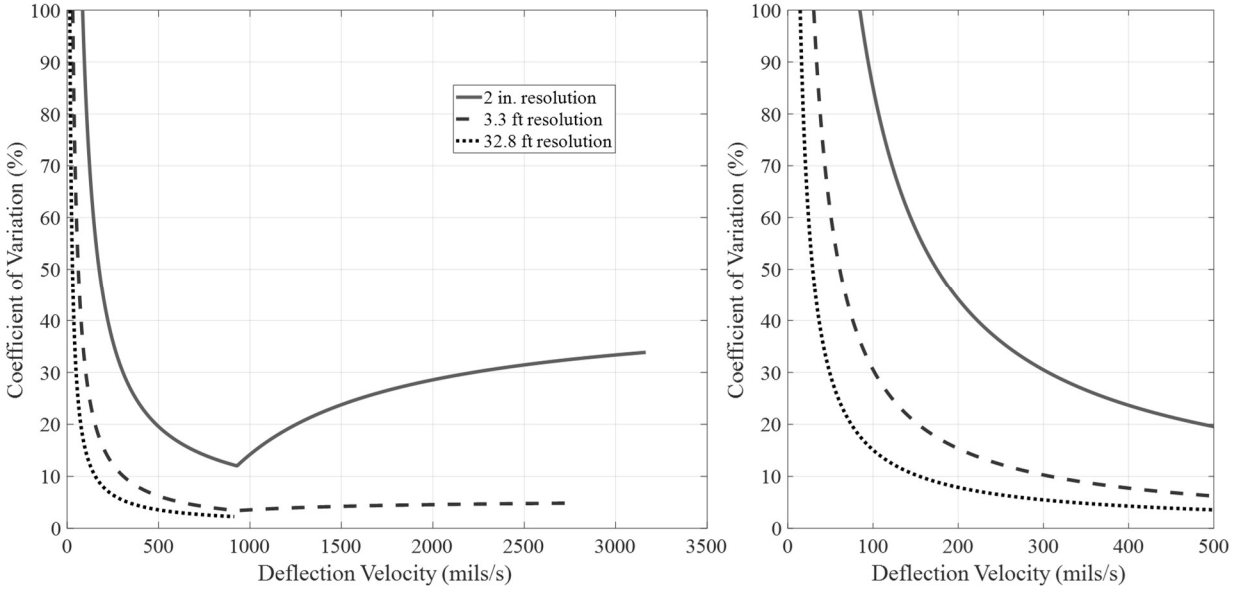

Figure 10. COV versus TSDD deflection velocity at 60 mph.

MICRO-VARIABILITY OF DEVICE MEASUREMENTS

The macro-variability presented in the previous section was considered appropriate for defining the TSDD operational limits but too general for validation of the TSDD measurements. While the available TSDD can record deflection velocities at 2-in. (50-mm) intervals, the results are averaged over 3.3-ft (1-m) or 33-ft (10-m) intervals in consideration of data variability. For a rational validation, however, the measurement uncertainty needs to be understood and considered. Figure 11 shows the average FWD deflection from the 39 drops (three drops at 13 locations) for each sensor at each test cell. Error bars represent the ±1 standard deviation for the

deflections. The corresponding COVs are shown on top of each bar. FWD deflections exhibited a maximum COV of 25% for the ML and a maximum COV of 10% for the LVR.

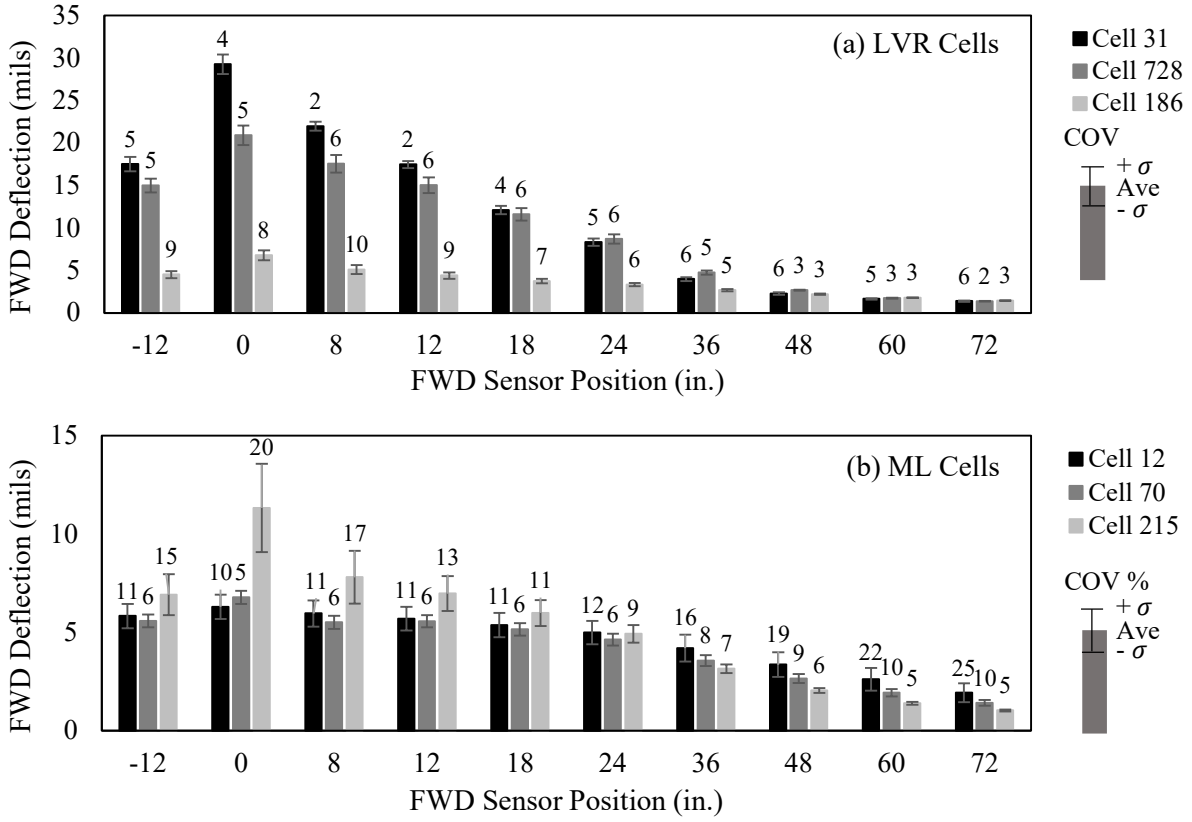

σ = standard deviation, Ave = average

Figure 11. FWD deflection measurements at LVR and ML test cells.

Statistical information about the 2-in. (50-mm) TSDD measurements at different speeds is shown in Figure 12 and Figure 13 for the LVR and ML test cells, respectively. To eliminate outliers, only measurements between the 10th and 90th percentiles were used in the analysis. As shown in the two figures, the data variability is significantly different between sensor locations and test cells. The COVs for the two farthest sensors exceeded 100% for almost all cells, but the COVs decreased as the sensors got closer to the tire load.

The COVs are also notably higher for the ML cells compared to the LVR ones. They exceeded 100% for most sensors, even those close to the load. This is attributed to the stiffer concrete pavements in the ML. To study the effect of spatial averaging, measurements at 3.3-ft (1-m) intervals were averaged for each sensor. The analysis outcomes are presented in Appendix A; they show the deflection velocity COVs decrease significantly for averaged data when compared to the 2-in. (50-mm) data. The COV decreases for sensors with larger deflection velocities are more pronounced, but the variability at the ML cells for many sensors is still significant, as the COVs still exceed 50%.

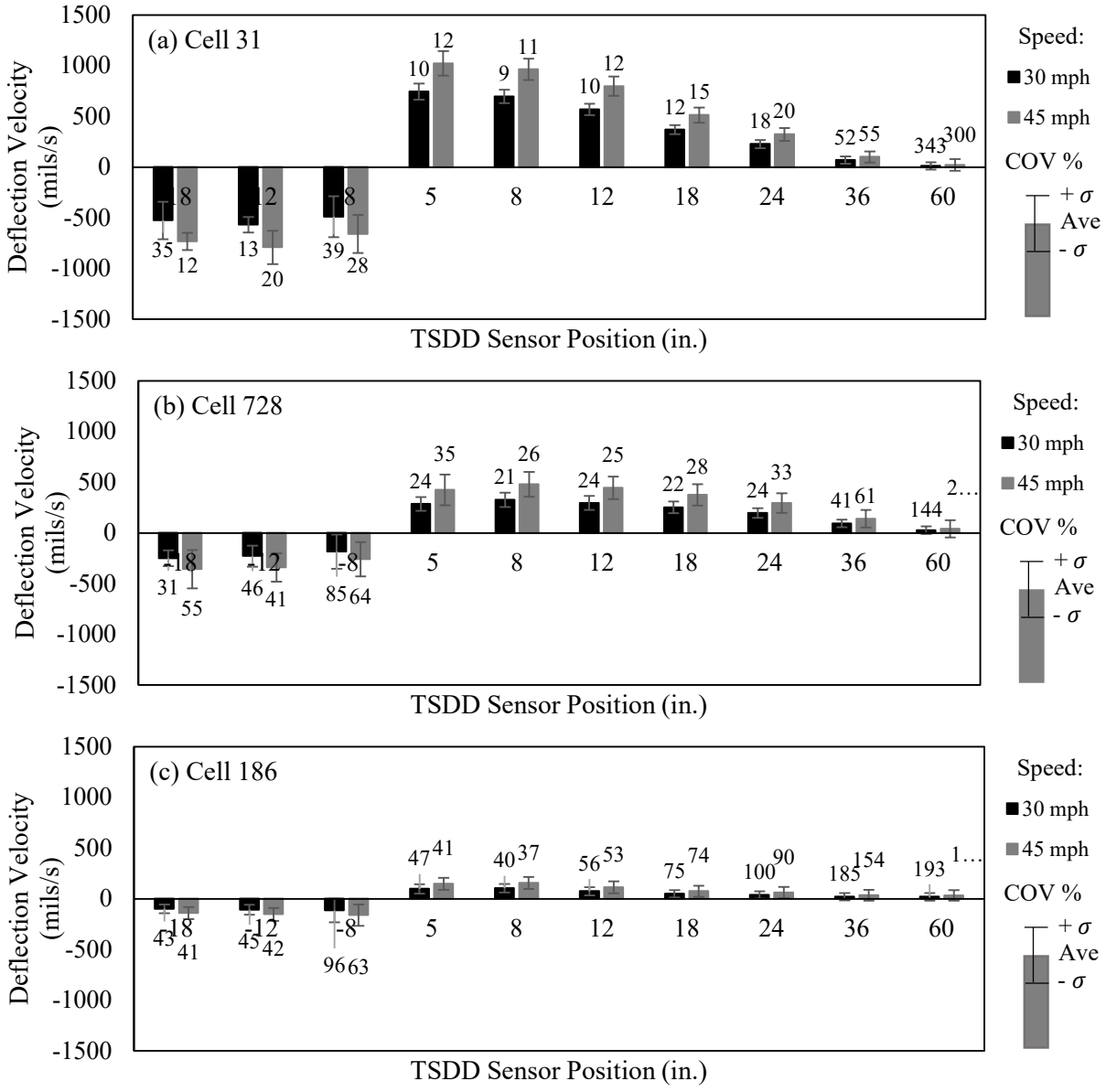

σ = standard deviation, Ave = average

Figure 12. Variability of TSDD measurements at LVR test cells for 2-in. data interval.

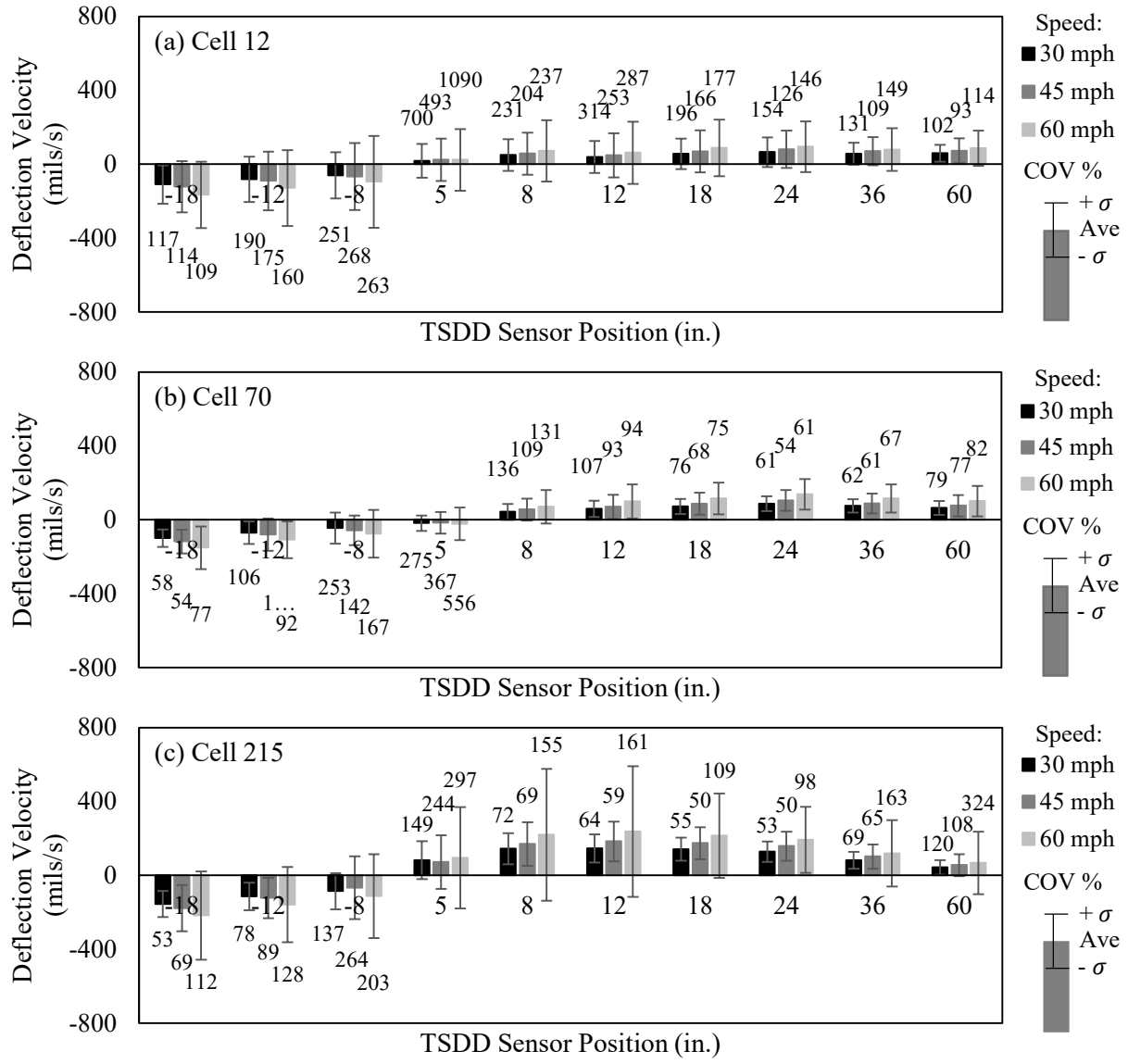

σ = standard deviation, Ave = average

Figure 13. Variability of TSDD measurements at ML test cells for 2-in. data interval.

The TSDD deflection velocity variability for all sensors, speeds and test cells is plotted against the corresponding average deflection velocities in Figure 14. An inverse relationship is observed between the average deflection velocity COVs and average deflection velocities. The variability seems to increase with speed. Also, lower deflection velocities correspond to measurements made with sensors located farther away from the load or measured at stiffer pavements. The COV of less than 20% corresponds to measurements greater than 200 mils/s (5 mm/s).

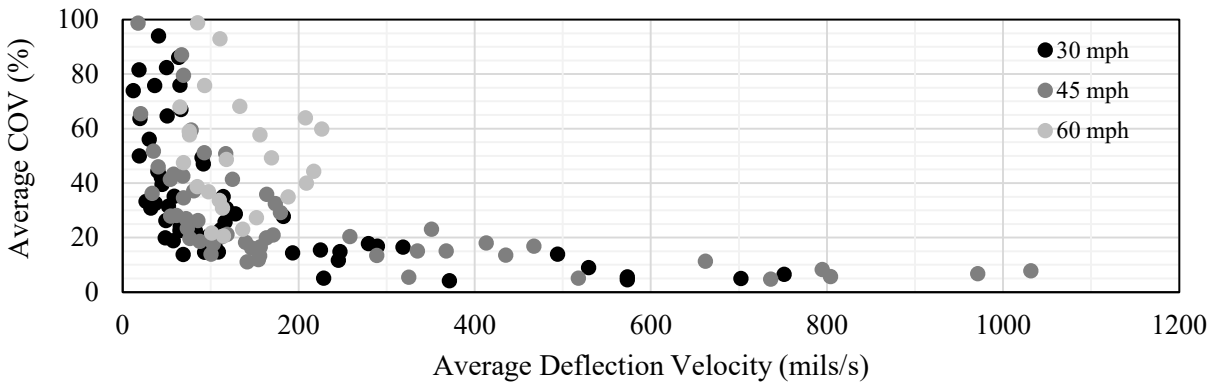

Figure 14. Deflection velocity COVs for 3.3-ft data interval.

To minimize the effects of vehicle speed, the deflection velocities were converted to deflection slopes by dividing the velocities by the corresponding TSDD vehicle speed. As shown in Figure 15, the variability increases as the slope decreases. To maintain measurements within a 20% COV, the deflection slopes should be greater than 4 mils/ft (0.33 mm/m).

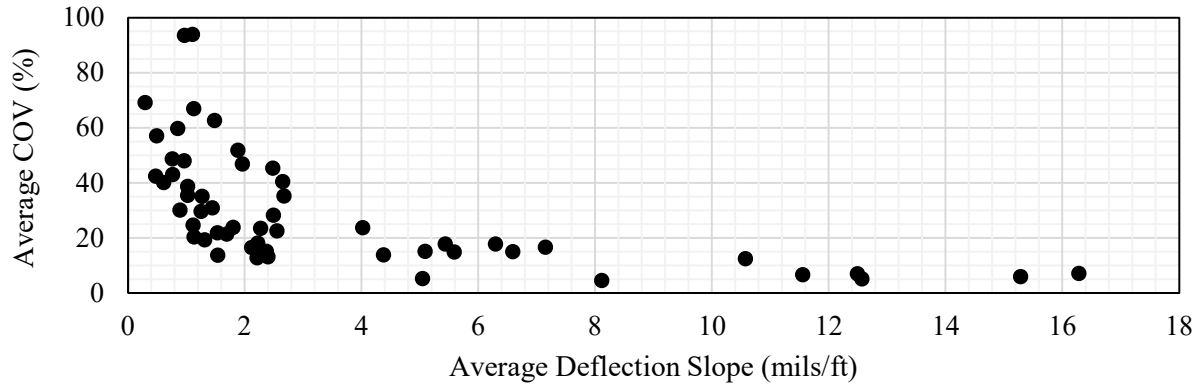

Figure 15. Deflection slope COVs for 3.3-ft data interval.

ACCURACY OF DEVICE MEASUREMENTS

To evaluate the accuracy of the TSDD measurements, the deflection velocities were compared with the corresponding geophone measurements. To properly perform this comparison, the three TSDD passes with the best alignments at each test cell were identified by review of the TSDD camera video recordings. Plots of deflection velocities from the geophones and best aligned TSDD passes were then compared, as illustrated in Figure 16 for test cell 31, at a speed of 30 mph (48 km/h). TSDD deflection velocities were selected within a range spanning 120 in. (3 m), starting 60 in. (1.5 m) before the first geophone to 60 in. (1.5 m) ahead of the third geophone. Measurements within ±2 in. (±50 mm) were averaged for each sensor position. For passes 3 and 4, one of the rear-axle tires passed directly on top of the geophone, causing a geophone peak that is not present for pass 2. Despite the alignment complication, the TSDD deflection velocities matched the geophone ones.

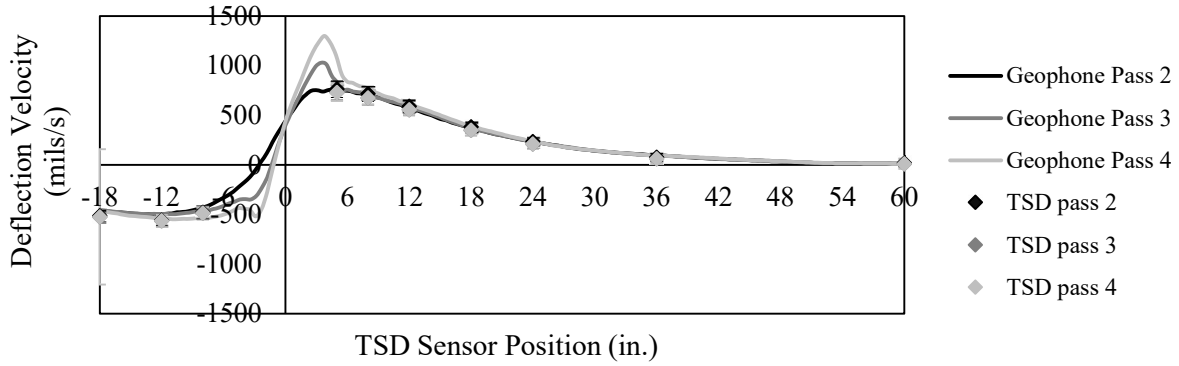

Figure 16. Comparison of geophone and TSDD measurements for test cell 31 at 30 mph.

A finite element simulation using ABAQUS was done to corroborate the reason for the geophone peaks. A 3-D dynamic model of the pavement was developed with the rear tires of the instrumented trailing axle simulated passing on top of a response point, representative of a geophone. Two scenarios were considered: (1) laser sensors pass directly on top of the geophone, and (2) a tire passes directly on top of geophone. The deflection velocities generated by a TSDD pass are shown in Figure 17 for test cell 31 and a speed of 30 mph (48 km/h). As shown, a peak develops as the tire passes directly on top of the geophone, while the sensor between the tires sees no peak. Past 6 in. (150 mm), the TSDD and geophones exhibit similar responses.

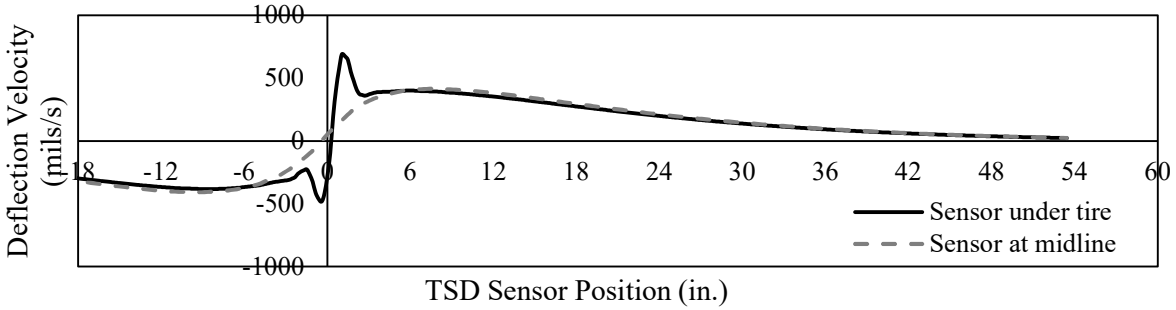

Figure 17. Deflection velocity finite element simulation for test cell 31 at 30 mph.

The geophone and TSDD deflection velocities are plotted in Figure 18; the standard deviation of each averaged parameter is presented as an error bar. TSDD deflection velocities were selected within the earlier referenced 120-in. (3-m) range. As shown, the TSDD measurements are closer to the geophone ones for the LVR cells—a significant number of data points fall within the ±20% uncertainty bounds, which were selected as a reasonable measure of variability given the TSDD micro- and macro-variability. The deflection velocities tend to deviate from the line of equality for those sensors closest to the load. As illustrated in Figure 17, this may be due to the interaction of the vehicle and TSDD sensors, the lateral distance between the tires, or the geophones.

The TSD deflection velocities for the ML cells exhibited higher variability than the LVR cells. This is due to the stiffer ML pavements, leading to smaller magnitude measurements. Speed also seems to affect the accuracy of the measurements. Other factors (e.g., IRI) may also impact on the measurement deviations, but these parameters were not considered. Most of the plots exhibit a greater overall deviation of the TSDD measurements from the corresponding geophone deflection velocities at higher speeds compared to the 30 mph (45 kph) speed.

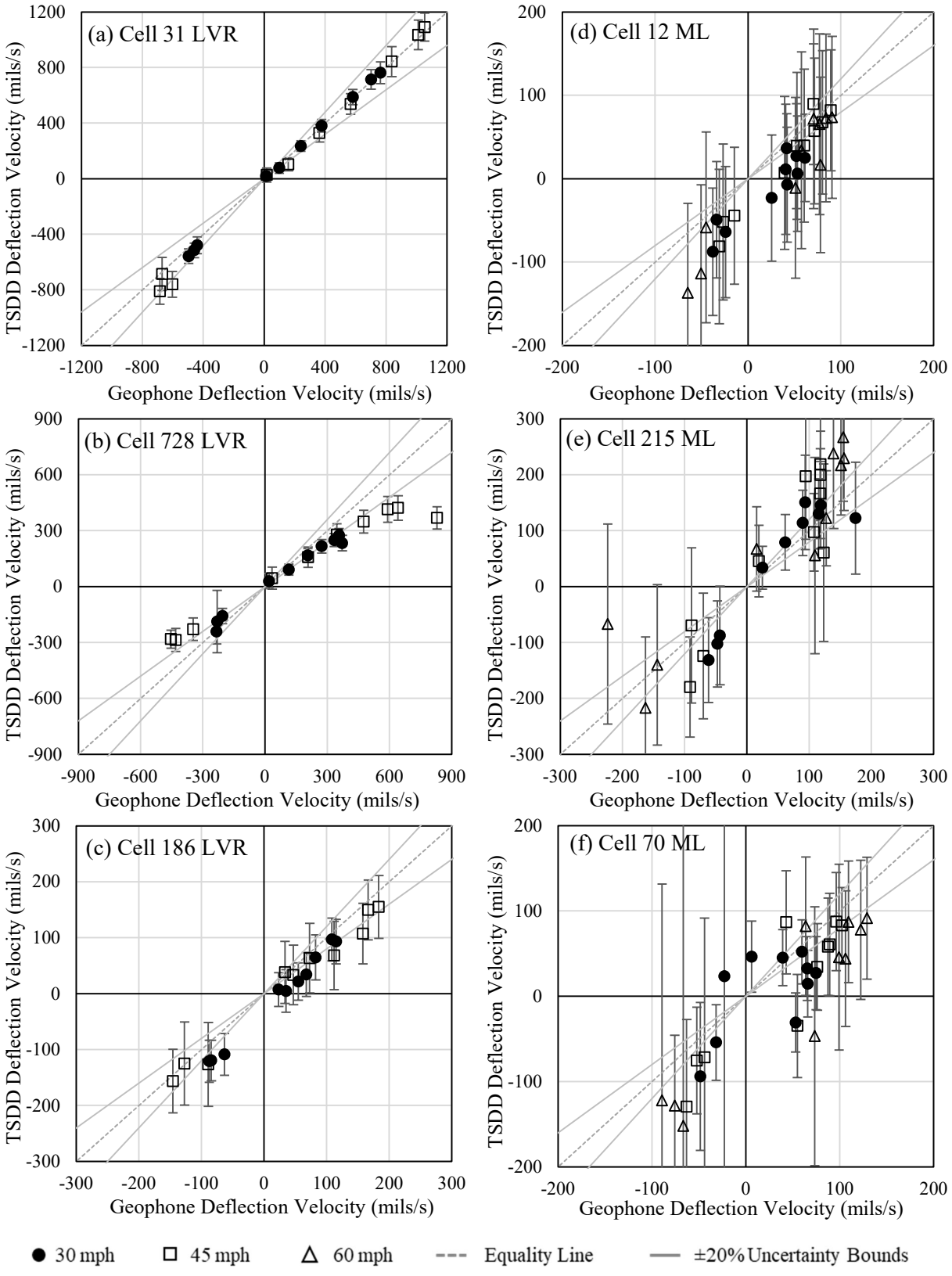

Figure 18. Comparison of TSDD and geophone deflection velocities.

CHAPTER 4. TSDD VERIFICATION PROCEDURE

The proposed TSDD verification procedure consists of the review of TSDD-generated data to check that the equipment is producing reasonable results. The reference data for this verification are FWD deflection measurements. However, a direct verification is not possible because (1) FWDs record vertical deflections due to stationary, impact loading, while TSDDs record deflections or deflection velocities as they move over the pavement; and (2) due to the stationary and discrete nature of the FWD measurements versus the dynamic nature of the TSDD ones, the number of measurement points and their locations are different. Since measurements from the two devices cannot be directly compared, FWD-TSDD relationships were developed to estimate TSDD deflection velocities from FWD deflections.

To establish the relationships, a database of pavement responses for different structures subjected to FWD and TSDD loadings was assembled. It was not practical to assemble such a database based on field measurements, so numerical techniques were used to simulate the responses. The 3D-Move program was used to simulate the FWD and TSDD responses and, in turn, to populate the database. This program predicts the response of pavement structures subjected to moving loads. It is based on a continuum-based, finite-layer model that uses a Fourier transform method, which enables users to simulate multiple loads, different tire print shapes, and non-uniform tire contact stress distribution, with a constant speed. In addition to a linear elastic response, 3D-Move allows rate-dependent material properties to accommodate the viscoelastic behavior of asphalt. Frequency-domain solutions are also incorporated, which enable direct use of HMA frequency sweep test data (Siddharthan et al. 2000).

To build confidence in the simulations, the results were validated and calibrated with data from the MnROAD field experiments. In addition, to reduce execution time, the database was used to train and validate ANN models to convert measured FWD deflections to estimated TSDD deflection velocities. It is emphasized that the findings presented in this chapter are based on measurements by one TSDD device and those findings may not apply to other TSDD devices.

DEVELOPMENT OF FWD-TSDD RELATIONSHIPS

A comprehensive database of linear elastic responses for three-layered asphalt pavements and two-layered concrete pavements subjected to stationary FWD and dynamic TSDD loads was assembled. Use of the stationary FWD loading was justified by the work of Chang et al (1992), which noted that in the absence of a shallow stiff layer, the peak deflections from static and dynamic analysis are virtually the same. The viscoelasticity of HMA layers was also not considered for two reasons: (1) Saremi et al. (2018) demonstrated (as indicated in Chapter 2) the viscoelastic impact to be negligible relative to the TSDD measurements' uncertainties if the HMA thickness is less than 4 in. (100 mm) thick; and (2) incorporation of viscoelasticity in the ANN models requires other parameters that may be impractical for highway agencies to obtain. Also, while most of the impact of the change in the deflection velocities due to the consideration of viscoelasticity would be close to the TSD tires, the first TSD sensor is 8 in. (200 mm) away from the center of the tire.

The resulting database was used to evaluate the sensitivity of the TSDD and FWD responses to different input parameters. The database contained the following data:

1. Type of device: FWD or TSDD, and TSDD operating speed.

2. Pavement structure and material properties: layer thicknesses and elastic moduli.
3. Pavement responses for structure and material properties subjected to FWD and TSDD loadings: FWD deflections and TSDD deflection velocities.

The process used to assemble the database is illustrated in Figure 19. To consider different pavement conditions, a Monte Carlo simulation was conducted using a range of structures, with randomly selected layer thicknesses and moduli, to generate the 3D-Move inputs. Table 4 shows the parameters considered for flexible pavements on unbound aggregate base courses—a total of 10,000 structures subjected to TSDD loadings and another 10,000 subjected to FWD loadings were simulated. Increments of 0.1 in. for layer thicknesses and 1 psi for moduli were used. TSDD speed was also incorporated as deflection velocities are speed dependent. Ultimately, ANN models for speeds of 30, 45, and 60 mph (48, 72, and 96 km/h) were developed.

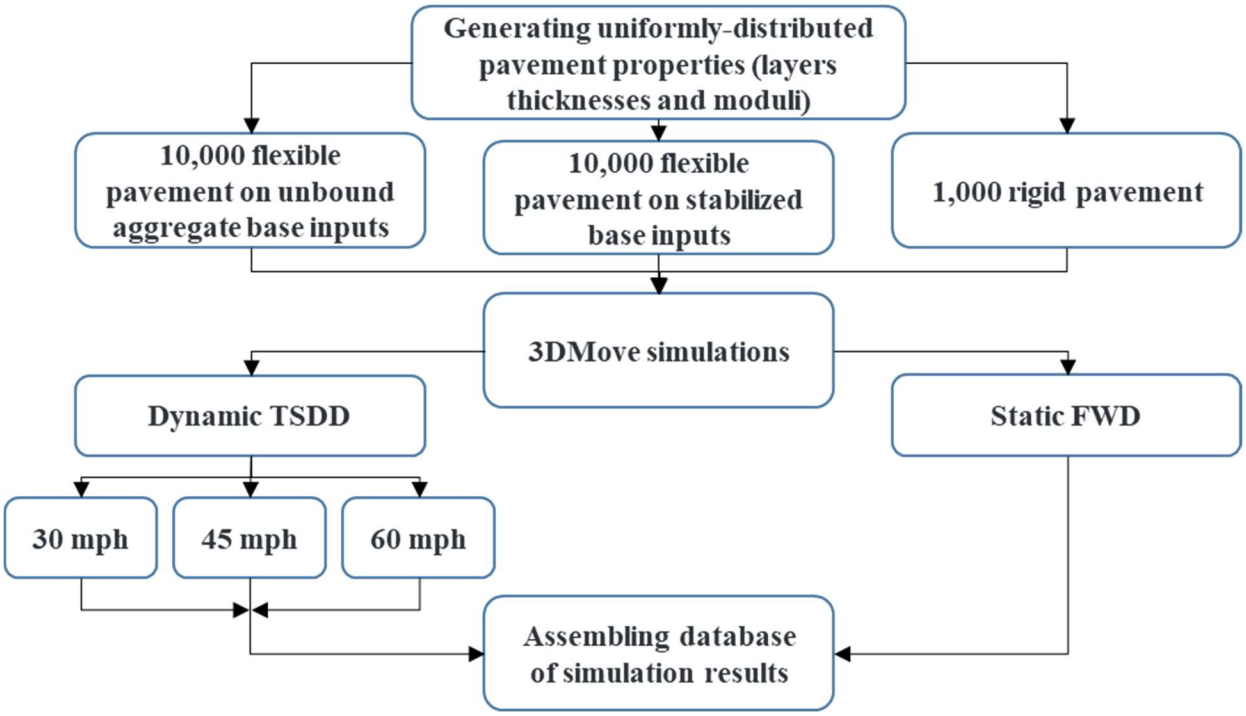

Figure 19. Database assembling process.

Table 4. Layer thicknesses and material properties for numerical modeling.

Pavement Type	Values	HMA/Slab Thickness (in.)	Base Thickness (in.)	HMA/Slab Modulus (ksi)	Base Modulus (ksi)	Subgrade Modulus (ksi)
Flexible on Unbound Base	Minimum	1	6	300	5	4
	Maximum	12	18	700	85	45
Flexible on Stabilized Base	Minimum	1	6	300	85	4
	Maximum	12	18	700	2,000	45
Rigid Pavement	Minimum	5	-	2,000	-	4
	Maximum	15	-	8,000	-	45

The procedure was repeated for 10,000 flexible pavements on stabilized base layers to consider the stiffer base moduli. The range of layer thicknesses and asphalt and subgrade moduli

were identical to those for the flexible pavements on unbound aggregate base, but the stabilized base moduli were randomly selected within the ranges shown in Table 4.

In terms of rigid pavements, the use of TSDDs to date has focused on joint load transfer and, to a much lesser degree, structural evaluations. Consequently, the rigid pavement simulations were limited to linear elastic analyses of a two-layer structure. The slab thickness varied between 5 and 15 in. (125 and 375 mm), while the PCC and subgrade moduli varied within the limits shown in Table 4. In all, 1,000 cases were simulated using 3D-Move at three TSDD speeds and the stationary condition for the FWD.

VALIDATION OF NUMERICAL MODEL

To assess the reliability of the models for use in development of the FWD-TSDD relationships, the 3D-Move numerical responses were validated with data from the field experiments as detailed in Figure 20. The FWD and TSDD data from the LVR cells were considered as the reference for comparison. Given the uncertainties in the data collected at the MnROAD ML cells, the research team could not justify considering them in the model validation. Layer elastic moduli were back-calculated using the measured FWD deflection basins. The resulting moduli, together with the layer thicknesses for the three LVR cells, were used as inputs to obtain the FWD surface deflections and the TSDD deflection velocities. A summary of the results for each cell and device is contained in Appendix B. As shown, the numerical and experimental responses from the FWD agreed with an uncertainty better than ±10% for all cells and sensor locations, indicating the backcalculated layer moduli were reasonable. The mean measured TSDD deflection velocities were also within ±10% of the estimated ones in most cases; however, as indicated by the error bars, the uncertainty of the measured values was high, especially for the stiffer sections.

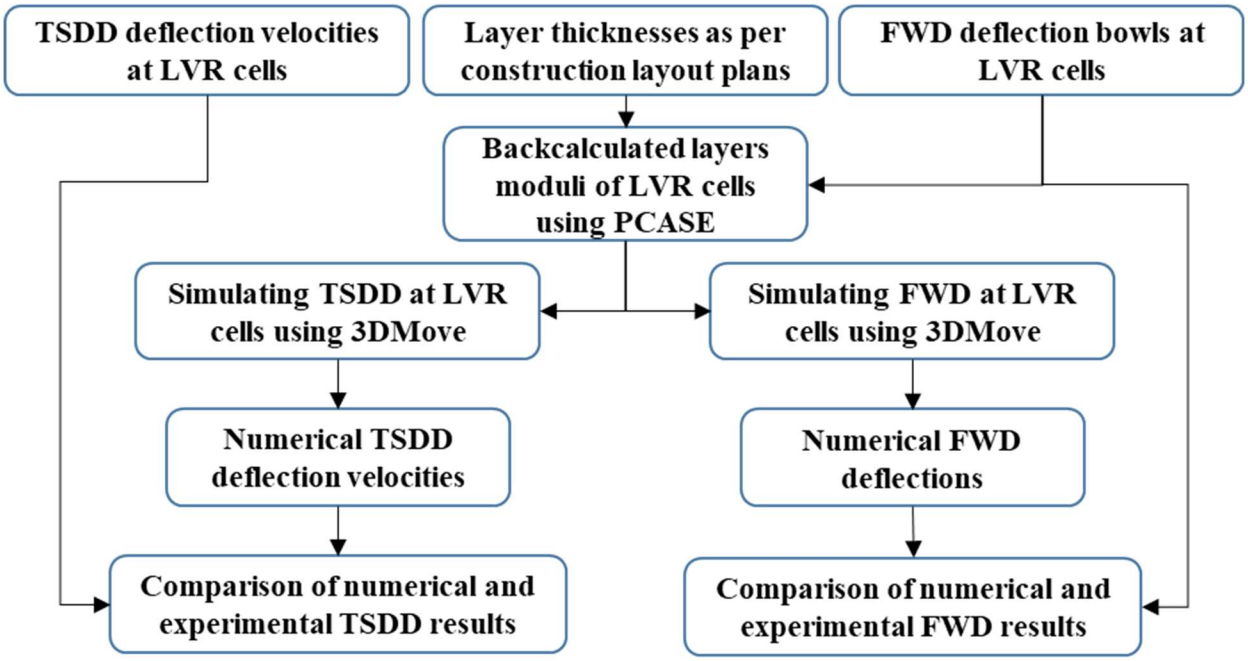

Figure 20. Procedure for validation of 3D-Move models.

Developing ANN Models

For purposes of the TSDD verification procedure, ANN numerical models were developed using the 3D-Move software to predict the equivalent TSDD pavement responses from FWD measurements. An ANN approach was selected because of its predictive analytics and machine learning components, which provide powerful material behavior predictive capabilities while lowering computing effort and time. The ANN model development procedure is shown in Figure 21. FWD and TSDD pavement responses were recorded at several sensor locations. The inputs included the thicknesses of the asphalt and concrete pavement layers, as well as the FWD deflections at sensor locations of 8, 12, 18, 24, 36, and 60 in. (200, 300, 450, 600, 900, and 1500 mm). Pavement layer moduli were not used as input to eliminate the need for back-calculation. The outputs consisted of the TSDD deflection velocities at the same sensor locations as the FWD.

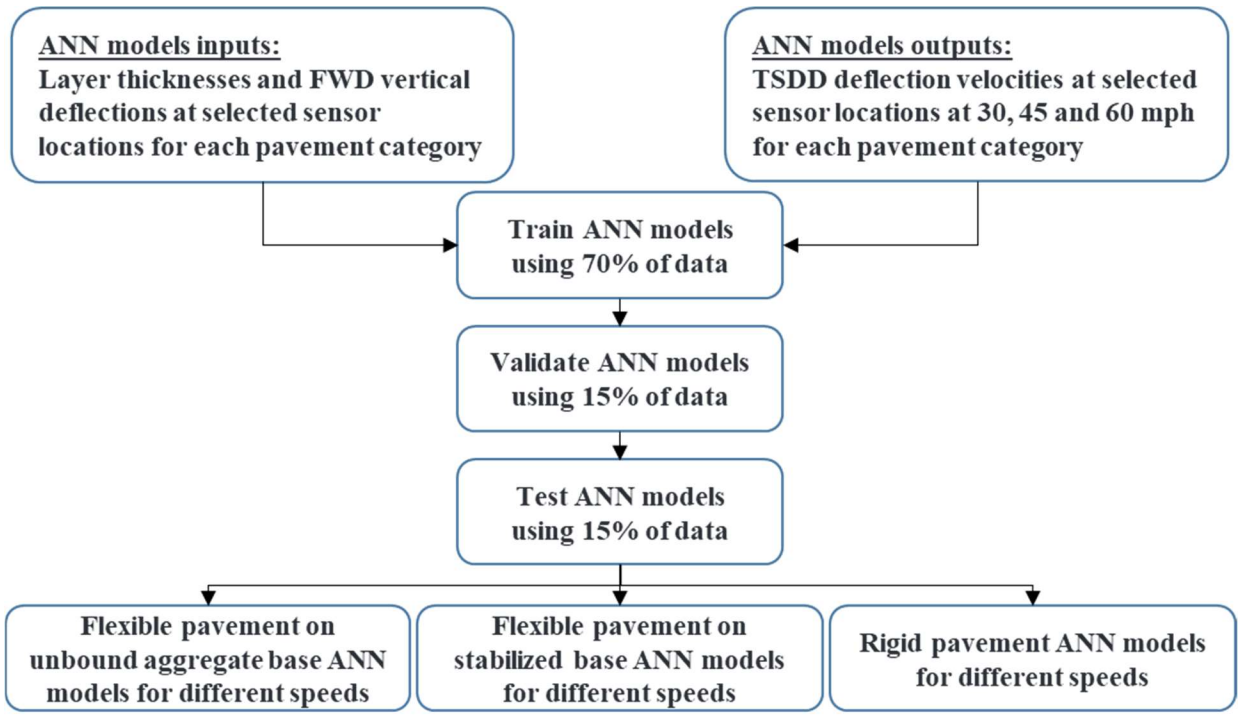

Figure 21. ANN model development procedure.

A multilayered feed-forward ANN with a Levenberg-Marquardt algorithm was used (Ilonen et al. 2003, Hastie et al. 2009). For HMA pavements, the input layer consisted of nine neurons, while the output layer consisted of seven neurons. The input and output layers for rigid pavements consisted of eight and seven neurons, respectively. All models included two hidden layers with 10 and seven neurons each.

The ANN models were formulated using 10,000 and 1,000 deflection velocity basins for the flexible and rigid pavements, respectively. The data were divided into three subsets: 70%, 15%, and 15% for training, validation, and testing, respectively, as this resulted in the best model performance. The pavement structures in the subsets were randomly selected. To avoid overfitting, the training was terminated when the validation error leveled. For each pavement type, separate ANN models were developed for speeds of 30, 45, and 60 mph (48, 72, and 96 km/h). Using the testing dataset, the ANN models predicted the theoretical TSDD surface

deflection velocities for the various combinations of pavement type and speed with correlation of determination values close to unity and maximum standard error estimate of about 1 mil/s (0.0254 mm/s). Appendix C summarizes the results of the validation of the ANN models.

VERIFICATION OF TSDD MEASUREMENTS

The ANN validation showed that the models can estimate TSDD deflection velocities well based on pavement layer thicknesses and FWD deflections. To further evaluate the performance of the ANN models, MnROAD field data were used to verify the models. The LVR cells were selected for this evaluation as the variability of the ML measurements was significant. Since the FWD tests were conducted at 3.3-ft (1-m) intervals, while TSDD measurements were recorded at 2-in. (50-mm) intervals, both the ANN-predicted and field TSDD data were averaged over a length of 3.3 ft (1 m). The cross plots of the ANN-predicted and field-measured TSDD parameters at 30 and 45 mph (48 and 72 km/h) are shown in Figure 22 for the three LVR test cells; the standard deviations are presented as error bars. As shown, TSDD deflection velocities were predicted using the ANN models within an uncertainty level of less than 20% for all TSDD sensors except the one at 8 in. (200 mm) and, for test cells 31and 186, at 12 in. (300 mm).

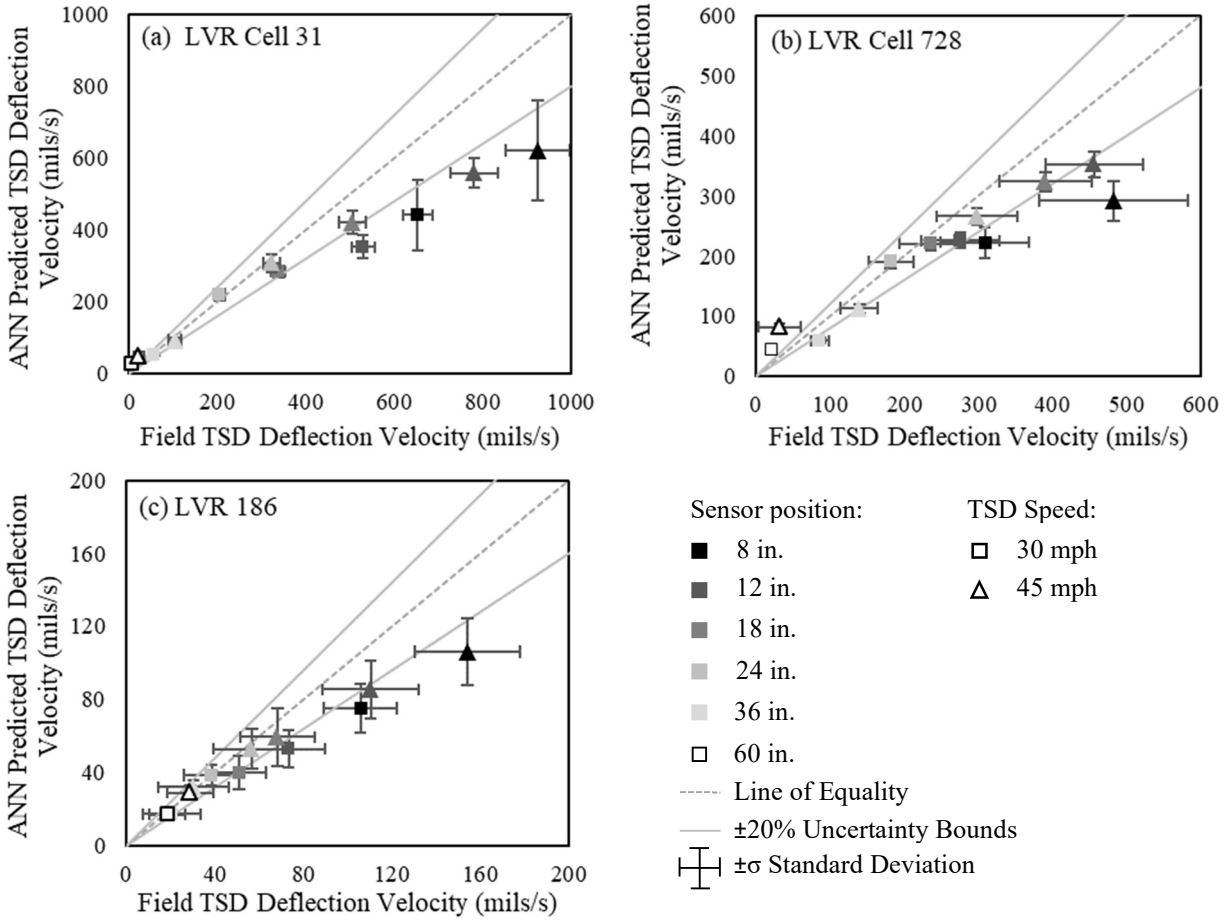

Figure 22. ANN-predicted versus experimental TSDD measurements for LVR.

Ideally, the uncertainty bounds associated with any device would be much tighter than the 20% selected in this study. However, a careful review of the macro- and micro-variability of the raw data collected by the TSD in Minnesota, Texas, and Virginia led the research team to set the

uncertainty bound at 20%. As shown in Figure 14 (and later in Figure 28), a COV of 20% would allow deflection velocity measurements of greater than 200 mils/sec (HMA on unbound granular base [UGB] pavements) to be considered reasonable. If the limit is reduced to 10%, the deflection velocities will be limited to values greater than 500 mils/sec, corresponding to very thin HMA over UGB pavements.

CHAPTER 5. VALIDATION OF ANN MODELS

This chapter summarizes the field testing carried out in Virginia (August 2022) and Texas (October 2022) to validate the appropriateness of the ANN models discussed in the previous chapter for conditions different than those at MnROAD. Three test sections were selected in each State based on the following criteria: (1) closeness of test sections to each other; (2) HMA or HMA over PCC pavement structures only; (3) range of structural conditions; and (4) sites with relatively low traffic volumes to help mitigate traffic and safety concerns. Geophones were installed at each test section in support of the field-testing objective. Like the field experiments, the Virginia and Texas field testing findings are based on measurements by one device and may not apply to other devices.

FIELD TESTING

The three Virginia test sections were located on US 460 between Appomattox and Farmville. The pavement structure information is summarized in Table 5. The HMA surface layer varied between 8.1 in. and 9.9 in. (202 mm and 248 mm), while the underlying macadam layer varied between 2.1 in. and 4.5 in. (52 mm and 112 mm). These two layers were constructed on top of 6.6 in. (165 mm) of granular base (based on ground penetrating radar [GPR] testing) and the subgrade layer. (Note: macadam is not a common base layer material. Its presence was not established until coring performed well after the FWD and TSDD field testing activities had been completed. It is hypothesized the presence of the macadam may have contributed to the TSDD measurement variability, and hence the reason GPR or coring to confirm the pavement layer thicknesses and material types was incorporated into the proposed practice).

Table 5. Layer thicknesses and material for Virginia validation test sections.

Test Section	Core No.	Layer Thicknesses, in. (mm)	
		Asphalt	Macadam
VA-1	1	8.7 (217)	not recovered
	2	8.1 (202)	not recovered
	3	9.0 (226)	2.1 (52)
VA-2	1	7.4 (184)	not recovered
	2	9.2 (229)	4.5 (112)
	3	7.7 (193)	not recovered
VA-3	1	8.9 (222)	2.2 (56)
	2	9.9 (248)	not recovered
	3	9.2 (229)	3.2 (80)

After establishing the center of each test section, markings were painted along the outer wheel path at 3.3-ft (1-m) intervals up to 16.5 ft (5 m) on each side of the center as well as at the center. These marks established the 11 FWD testing locations. In addition, two geophones were installed 1.7 ft (0.5 m) on each side of the section center, along the outer wheel path. In addition to the 11 FWD testing locations, FWD tests were also conducted directly on top of the geophones to confirm that the geophones were properly functioning.

The Texas field testing followed the process used in Virginia, but marking of the test sections was achieved by first conducting FWD tests at 10-ft (3-m) intervals along 100 ft (30 m) to

identify a length of pavement that was reasonably uniform. The test sections were located approximately 7 miles outside of College Station, Texas on State Highway (SH 47). The pavement structure information, as determined from coring, is summarized in Table 6. The HMA surface layer varied between 2.5 in. and 5.5 in. (64 mm and 140 mm). At the first section, the HMA layer was constructed on top of 9 in. (229 mm) of cement-treated base (CTB), 6 in. of UGB, 6 in. of lime-treated base (LTB), and a clay subgrade layer. The asphalt layer in the other two sections was constructed on 14 in. (356 mm) of UGB and a clay subgrade layer.

Table 6. Layer thicknesses and material for Texas validation test sections.

Test Section	Layer Thicknesses, in. (mm)			
	HMA	CTB	UGB	LTB
TX-1	2.5 (63.5)	9 (229)	6 (152)	6 (152)
TX-2	5.5 (140)	-	14 (356)	-
TX-3	5 (127)	-	14 (356)	-

ANALYSIS RESULTS

To verify the installation of the geophones, the deflections measured by the third FWD sensor and the two geophones at each test section were compared. The third FWD sensor was used to avoid damaging the embedded geophones by directly impacting on them with the load plate. Figure 23 shows the comparison results; the geophone and FWD deflections compare well, as evidenced by the 1.01 slope of the best fit line and a coefficient of determination of approximately 1.00. The trend in Figure 23 does not necessarily follow the one that would be observed if using the FWD sensor directly under the load center, so it cannot be used to confirm if the Texas test sections were stiffer or not compared to the Virginia test sections.

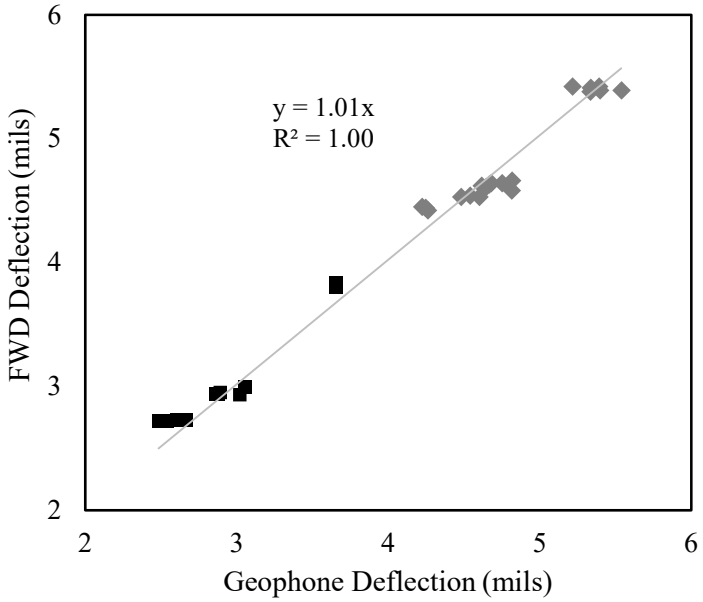

Figure 23. Comparison of field geophones and FWD deflections.

TSDD data at the Virginia and Texas test sections were nominally recorded at 2-in. (50-mm) intervals over a distance of 45 ft (14 m). The raw deflection velocity measurements, collected at 45 mph (72 km/h) along a length of about 45 ft (14 m) at one of the Texas sections, are illustrated in Figure 24.

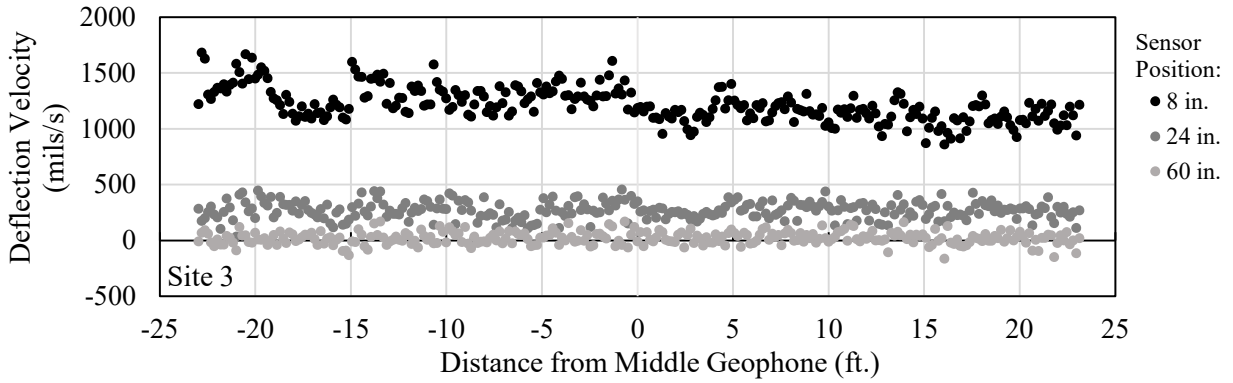

Figure 24. Example TSDD deflection measurements at Texas test section.

Figure 25 shows the average FWD deflections from the 22 drops (two drops at 11 locations). Error bars represent the one standard deviation range. The corresponding COVs are shown on top of each bar. FWD measurements exhibited a maximum COV of 49% for the Virginia test sections and a maximum COV of 20% for the Texas test sections.

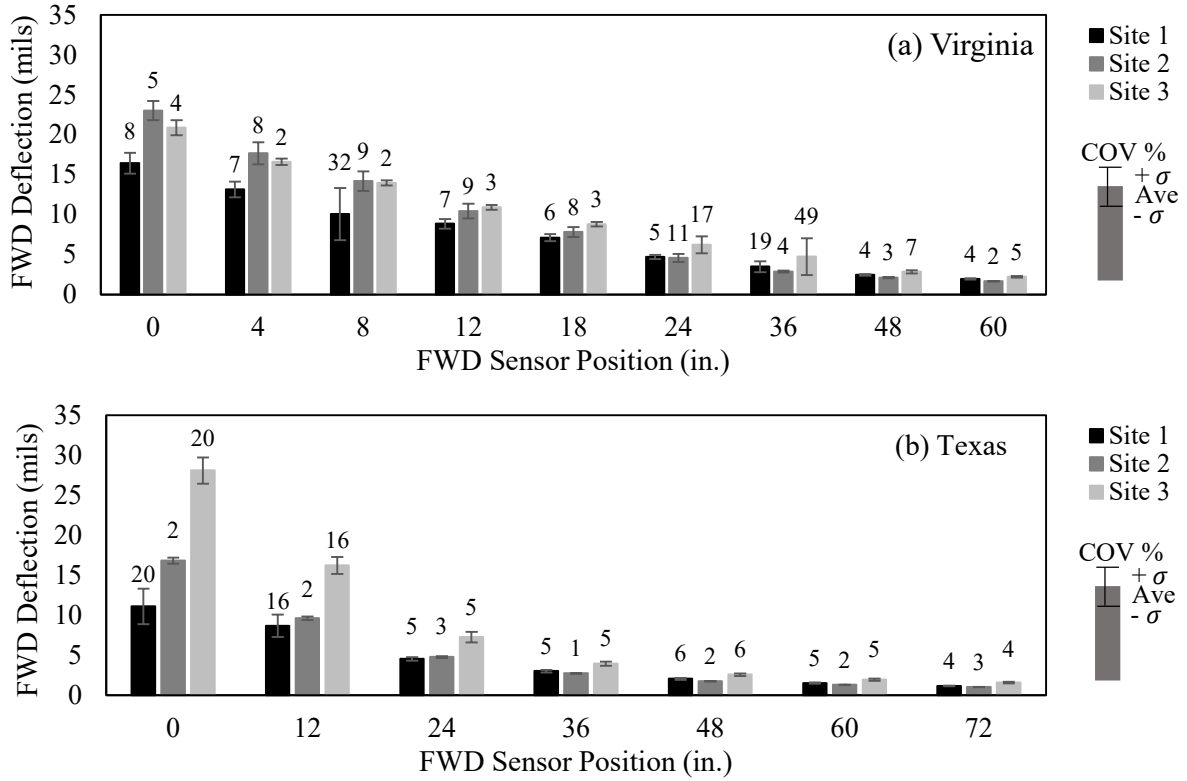

σ = standard deviation, Ave = average

Figure 25. FWD deflection measurements at Virginia and Texas test sections.

Statistical information about the 2-in. (50-mm) TSDD measurements at different speeds is presented in Figure 26 and Figure 27 for the Virginia and Texas test sections, respectively. Both figures show that the average deflection velocities seem to increase as the pavement sections become less stiff when compared to the deflections shown in Figure 23. However, other factors may affect the TSDD responses. The TSDD data variability is significantly different between

sensor locations and test sections. For the Virginia test sections, most sensors exhibited COVs of more than 100%. The farther sensors generally showed higher COVs compared to those closer to the load. Although the COVs for the Texas test sections were notably lower, the two farthest sensors still show COVs of more than 100%.

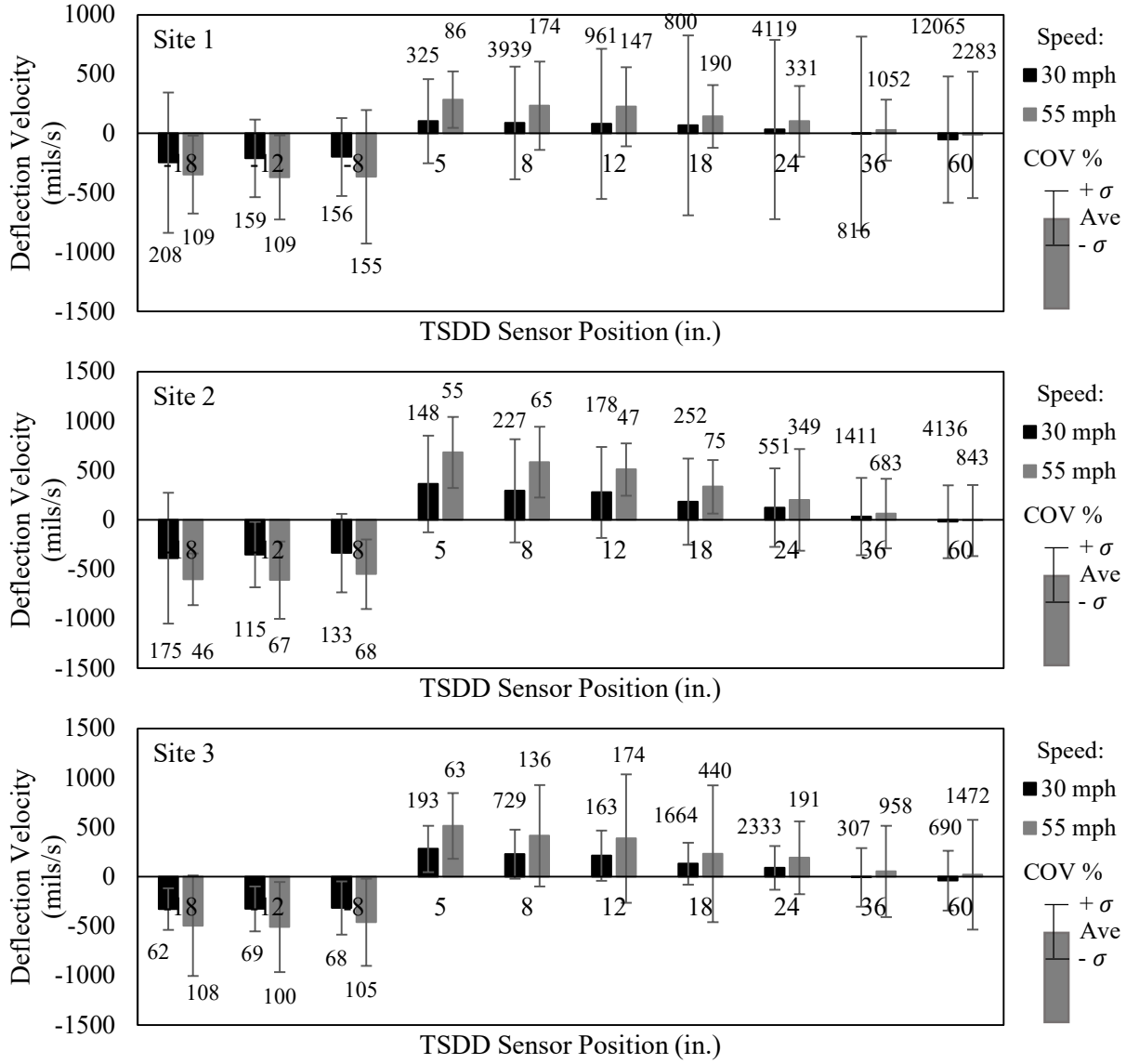

σ = standard deviation, Ave = average

Figure 26. Variability of Virginia TSDD deflection measurements for 2-in. data interval.

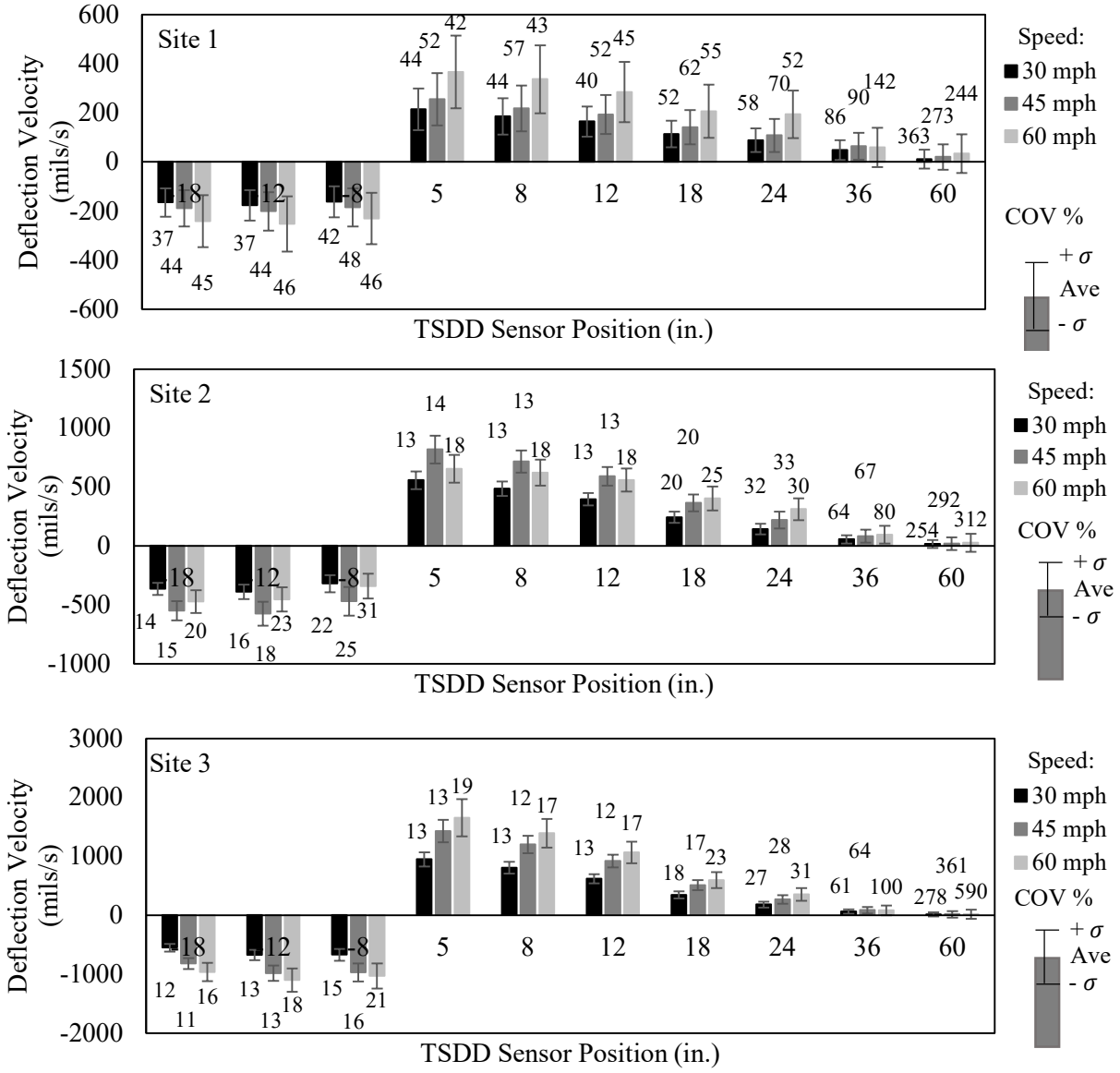

σ = standard deviation, Ave = average

Figure 27. Variability of Texas TSDD deflection measurements for 2-in. data interval.

As with the MnROAD field experiments data, the Virginia and Texas TSDD deflection velocities were averaged at 3.3-ft (1-m) intervals for each sensor to study the effect of spatial averaging on the deflection. Like the MnROAD findings (see Appendix A), the outcome of this analysis showed that decreases in the COVs of the sensors with larger deflection velocities were more pronounced. However, the variability of the data for the Virginia test sections for many sensors was still significant, as the COVs exceeded 100%.

The variability of the TSDD deflection velocities at the Virginia and Texas test sections is plotted against their corresponding average deflection velocities in Figure 28. Like the MnROAD results, an inverse relationship is observed between the average deflection velocity COVs and average deflection velocities. Unlike the MnROAD results, the measurement variability does not seem to have a specific relationship with speed. Lower deflection velocities

correspond to measurements made with sensors located farther away from the loading or measured at sites with stiffer pavements. Also, while in many cases COVs less than 20% corresponded to deflection velocities greater than about 200 mils/s (5 mm/s), in some cases the COVs were greater than 20%. For deflection velocities greater than about 600 mils/s (15 mm/s), the COVs were always less than 20%.

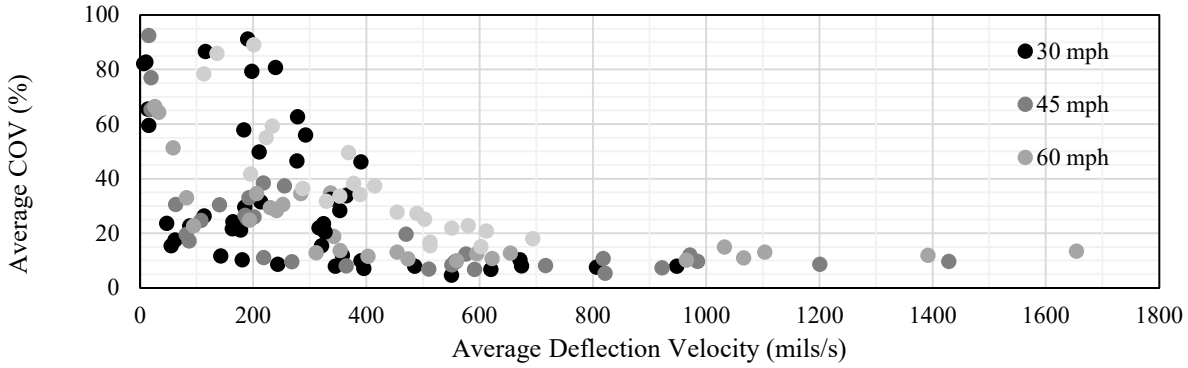

Figure 28. Average COV as a function of average deflection velocity for 3.3 ft interval.

The effects of vehicle speed were minimized by converting the deflection velocities to deflection slopes by dividing the velocities by the corresponding vehicle speed. As shown in Figure 29, the variability increases as the deflection slope decreases. The COV of less than 20% corresponded to deflection slopes greater than about 8 mils/ft (0.7 mm/m).

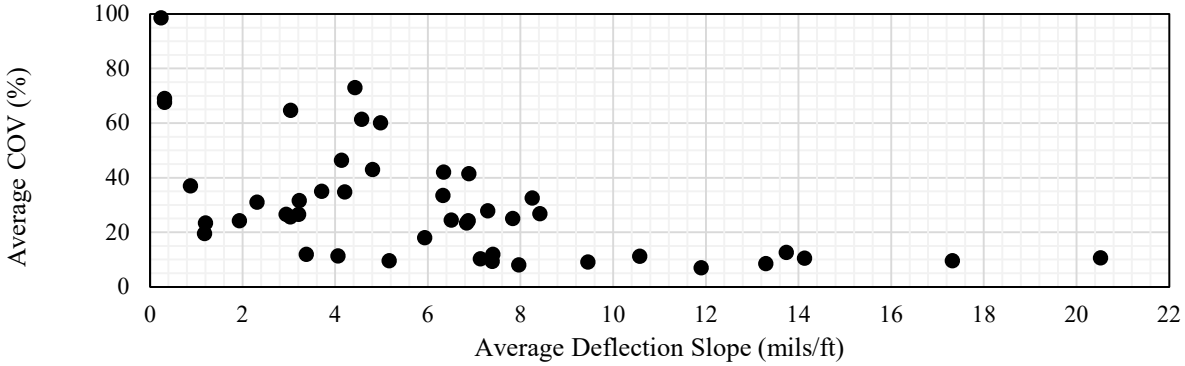

Figure 29. Average COV as a function of average deflection slope for 3.3 ft interval.

To evaluate the accuracy of the TSDD measurements, the deflection velocities for each test section were compared with the corresponding geophone measurements. The TSDD passes with the best alignments were determined based on the TSDD camera video recordings or the absence of geophone peaks. The geophone deflection velocities are plotted against those of the TSDD sensors for the Virginia and Texas test sections in Figure 30 and Figure 31, respectively. Only two of the three Virginia test sections are shown due to a hard disk failure associated with the data acquisition system computer.

For the Virginia test sections, the TSDD results are outside the ±20% uncertainty bounds at some of the TSDD sensors, and the deviation seems to increase with higher vehicle speed. The Texas test sections, on the other hand, generally exhibited less deviation, as most of the TSDD sensors' deflection velocities fall within the ±20% uncertainty bounds.

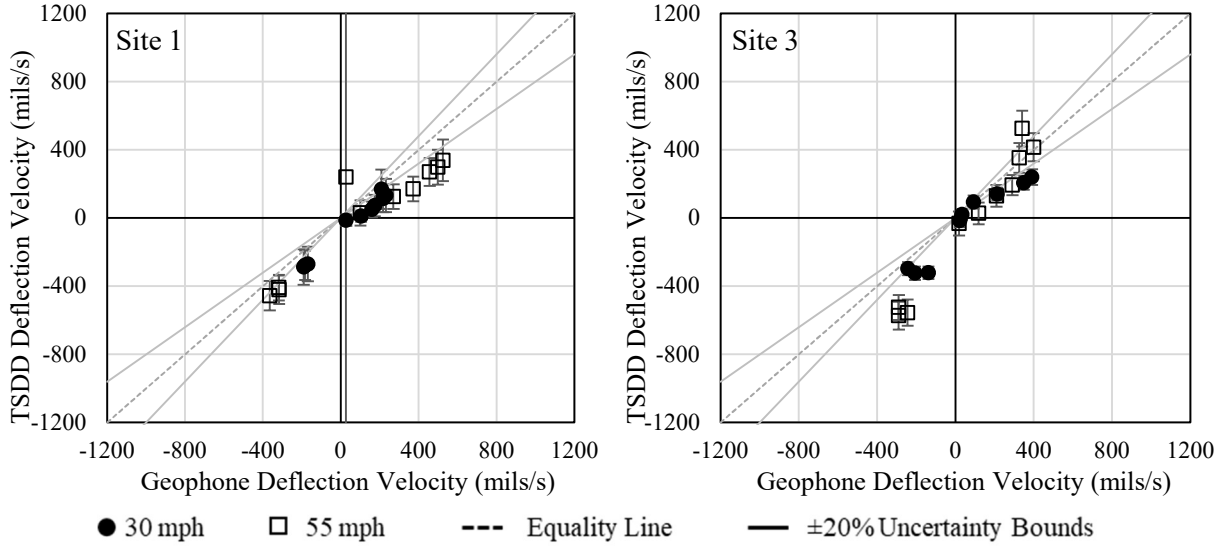

Figure 30. Average TSDD versus geophone deflection velocities for Virginia test sections.

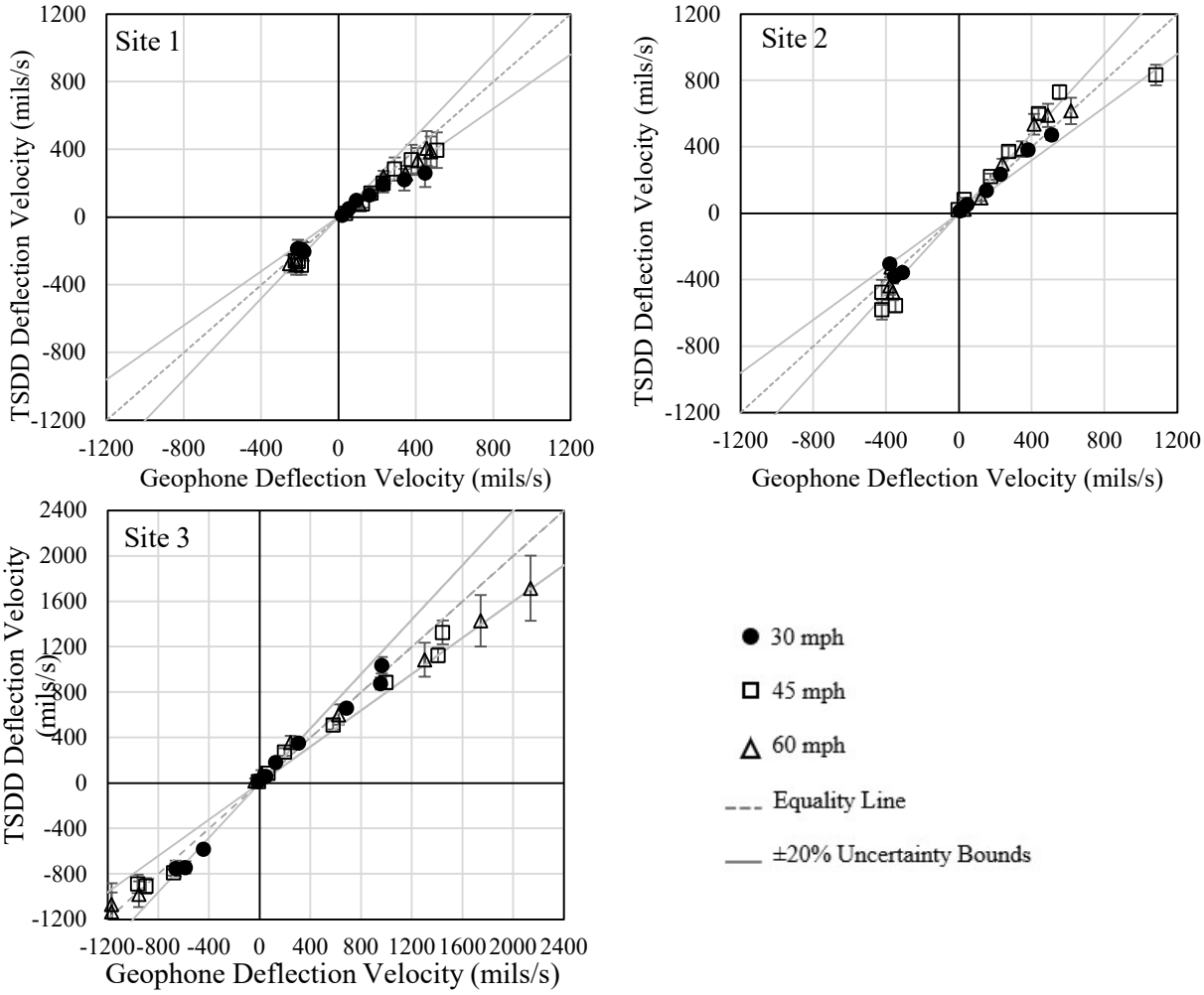

Figure 31. Average TSDD versus geophone deflection velocities for Texas test sections.

To improve the ANN estimates, calibration factors were introduced to make the ANN estimated deflection velocities closer to the experimental values. For each test section, the ANN models were used to estimate the TSDD deflection velocities corresponding to the FWD data and layer thicknesses of the test sections; since the temperatures measured by the two devices at each test section were close, temperature adjustments were not deemed necessary. The results were then averaged along the test section for each sensor for comparison with the average experimental TSDD values.

The average estimated and measured values for each MnROAD LVR test cell are compared in Figure 32. A linear regression model was used to find the relationship between the two sets for each sensor, and the slope of the best-fit line was used as the calibration factor. The MnROAD ML datasets were not included in Figure 32 nor used for the calibration factors because they comprise TSDD measurements with significant variability.

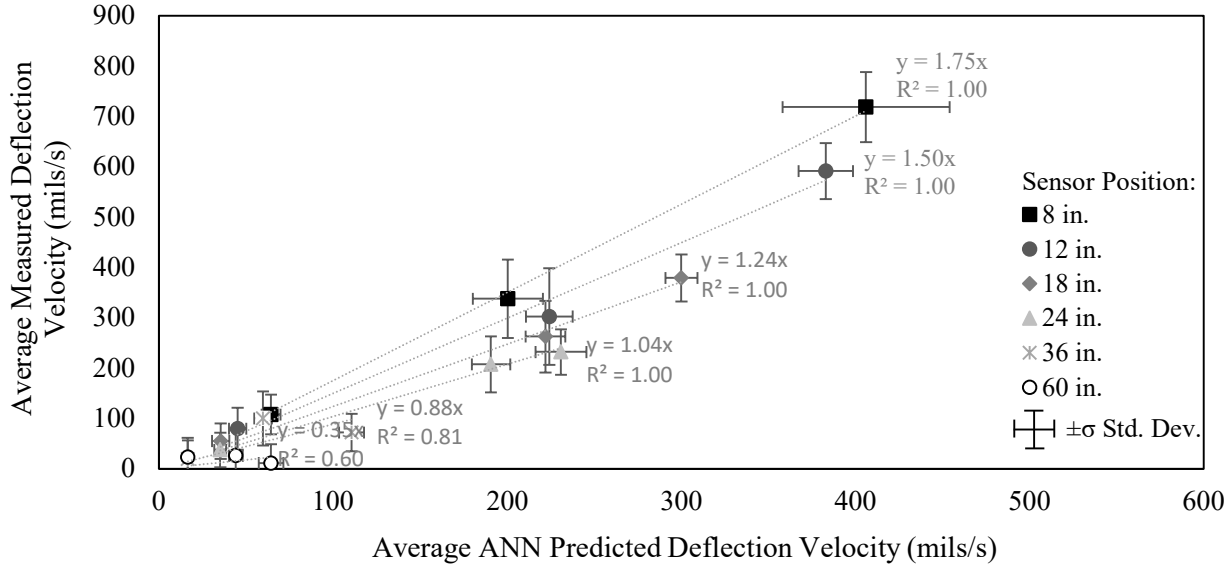

Figure 32. Comparison of measured and estimated ANN deflection velocities.

The final cross plots of the calibrated ANN-predicted parameters and field TSDD parameters for 30 mph (48 kph) are shown for the MnROAD LVR cells and Texas sites in Figure 33. The standard deviation of each averaged parameter is presented as an error bar. The MnROAD ML and Virginia datasets were not included because they comprise TSDD measurements with significant variability. For the MnROAD LVR and Texas sites, the adjusted ANN-based values predicted the TSDD deflection velocities within ±20% uncertainty bounds for most sensor locations and seem to work well in the estimation of the TSDD data.

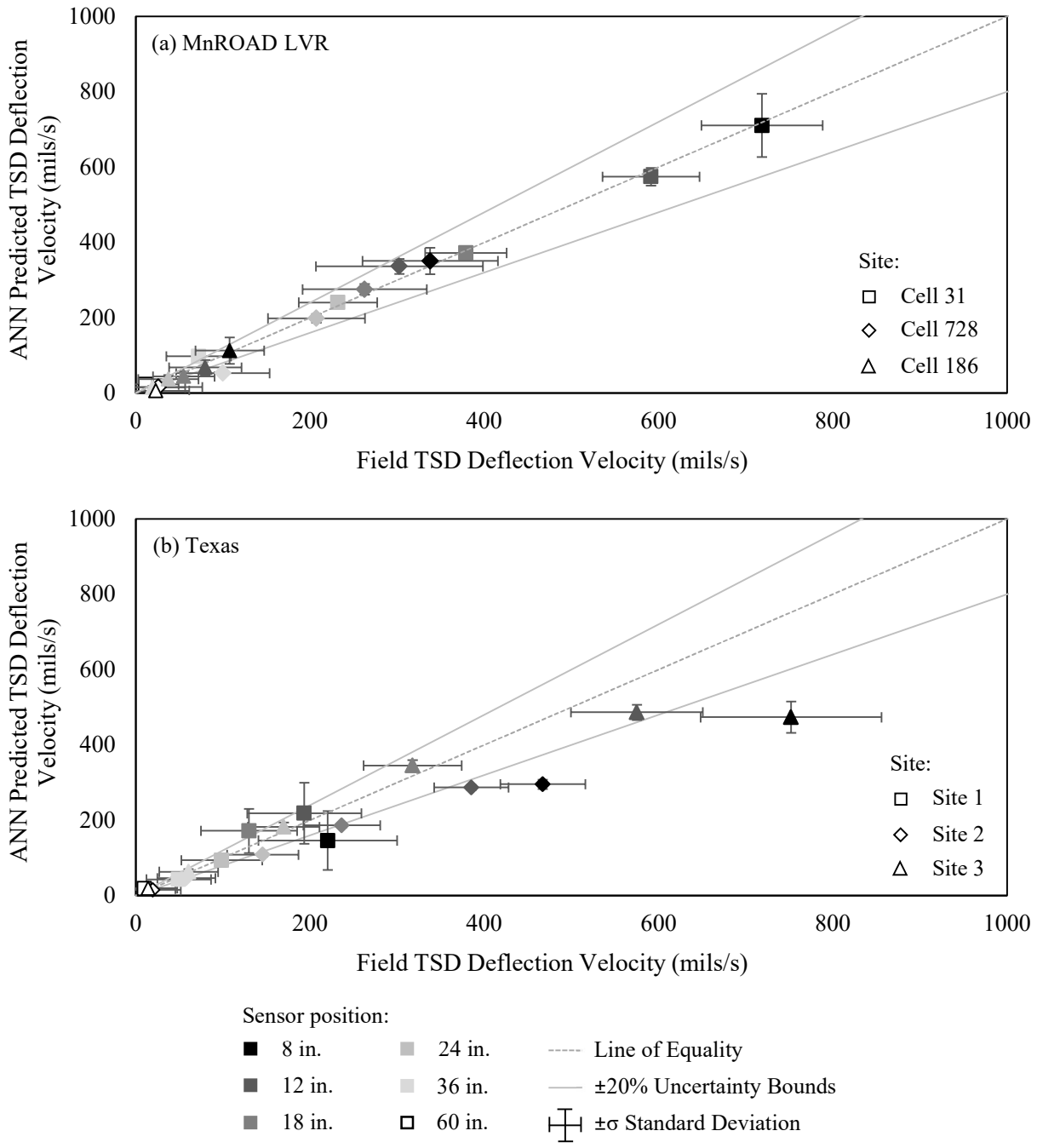

Figure 33. ANN-predicted vs field-measured deflection velocities for LVR and Texas sites.

CHAPTER 6. PREPARATION OF PROPOSED PRACTICE

This chapter summarizes the development of the proposed practice for verification of TSDD measurements on highway pavements, as reflected in Attachment A. In this proposed practice, FWD measurements along with ANN models are used as the reference values against which TSDD measurements are compared to assess their accuracy and precision. The preparation of the draft of the proposed practice was largely driven by the outcomes from the MnROAD LVR field experiments. It was then validated and revised based on outcomes from the field testing carried out in Texas. Because these outcomes are based on measurements performed by one device, the proposed practice may not apply to other devices.

Use of the proposed practice is limited to asphalt-surfaced pavements to help attain a less than 20% level of uncertainty. Limiting the type of pavement to consider and quantifying a 20% uncertainty stem from the limitations of the TSDD sensors, and from the uncertainty of the measurements explained in Chapter 4. This indirect approach to setting limits was necessary because the detectability limit of the mounted lasers (not the laser sensor as reported by manufacturer, but the laser system as mounted on a gyroscope) was not available.

The actual operational aspects of the proposed practice begin by addressing the following elements:

- General requirements, including safety and traffic control, environmental testing conditions, longitudinal grade and horizontal radius of curvature, and surface characteristics.
- Test section requirements, including the need for three 100-ft (30-m) test sections with a safe operational speed of at least 30 mph (48 kph) and FWD maximum deflections of 5 to 10 mils (125 to 250 μm), 10 to 20 mils (250 to 500 μm), and greater than 20 mils (500 μm), respectively.
- FWD test method, including AASHTO and ASTM standard specifications, FWD sensor locations (to match TSDD Doppler laser locations), FWD testing (three repeat drops at 11 FWD test locations using a nominal load of 9,000 lbs [40 kN]), and FWD data collection (peak loads, peak deflections, air temperature, and surface temperature).

The proposed practice then addresses the determination of the accuracy and precision of the TSDD measurements. These determinations require that the TSDD data be summarized at 3.3-ft (1-m) intervals. Once done, the proposed practice requires conducting the following analyses:

- Repeatability between two synchronized runs and overall repeatability (average of repeatability of all pairs of runs);
- Bias between synchronized runs and overall bias (average of bias of all pairs of runs);
- Variance (precision) between repeated runs and overall variance (average of precision of all pairs of runs);
- COV from the overall variance and average of the repeated measurements from the three valid runs.

Lastly, the proposed practice addresses the verification of the TSDD measurements using the FWD measurements. The verification starts by converting the FWD deflections to estimated TSDD deflection velocities using the ANN models developed under this project. At each pavement test section, the FWD estimated deflection velocities are then compared to the measured TSD deflection velocities, and the percentage difference between the two measurements is determined. If the percentage difference is less than the minimum acceptable difference, then the TSDD is validated. If not, two possible actions are suggested: (1) perform another three sets of TSDD measurements and repeat the validation procedure and (2) check for any possible miscalibration in the TSDD or the FWD.

For the TSDD used in this project, the minimum acceptable percentage difference was defined as less than 20% for deflection velocities higher than 5 mm/s (200 mils/s), or less than 30% for deflection velocities between 2.5 and 5 mm/s (100 and 200 mils/s). Verification of the TSDD for deflection velocities less than 2.5 mm/s (100 mils/s) is not recommended because the COV for those low measurements is high.

In general, the TSDD verification approach detailed in the draft of the proposed practice remained the same after the Virginia and Texas field validations, but important improvements were made, including:

- Number of FWD test point locations (for comparison with TSDD measurements) was increased from 10 to 11 points at 3.3-ft (1-m) intervals, which defines a length of 33 ft (10 m). Together with the 33-ft (10-m) approach and leave sides, the total test section length is 100 ft (30 m).
- Preliminary use of FWD testing was recommended to identify test sections that meet the target stiffness requirements as well as to confirm the uniformity of the test sections, in terms of deflections, and help locate the center of the test sections.
- GPR testing or coring was recommended to establish the pavement layer thicknesses and material types for the verification test sections, which are required by the ANN models to converted FWD deflections into estimated TSD deflection velocities.

It is also worth noting that the use of pavement-embedded instrumentation is preferred over the use of FWD measurements as it provides a direct comparison. The proposed practice resulting from this project is of convenience to those highway agencies wishing to avoid the complication of instrumentation.

CHAPTER 7. SUMMARY, CONCLUSIONS AND RECOMMENDATIONS

The objective of this project was to develop a proposed practice for verification of the measurements obtained by TSDDs on highway pavements. To achieve the objective, the project started with a literature review to gather information related to TSDD measurements, with a focus on available technologies, deflection measurement characteristics, and device verification. Despite the availability of different TSDDs throughout the world, only one device was available in the United States. Consequently, the findings of this research are based on measurements by one device and may not apply to other devices; however, the general approach should be applicable in verifying other TSDDs.

The literature review identified the factors affecting the TSDD measurements; pavement factors, environmental factors, and operating conditions. To better understand the effects of these factors, field experiments were conducted at the MnROAD facility. Information collected during the experiments included TSDD, FWD, geophones, and environmental data. Using these data, the macro-variability of the TSDD was calculated. It was determined that the COV varied as a function of deflection velocity for a given testing speed. COVs were high for low-amplitude measurements, but dropped rapidly and leveled out, which had implications in terms of the acceptable range of TSDD measurements.

Because the macro-variability was considered too general for development of the TSDD verification procedure, the measurement uncertainty (i.e., micro-variability) needed to be understood and considered. FWD measurements exhibited maximum COVs of 25% for the concrete and semi-rigid pavements and of 10% for the asphalt pavements. For the TSDD deflection velocities, the COVs varied significantly for different sensor locations and test cells; it increased the most for sensors farther from the load and for stiffer the pavements. In addition, the COVs significantly decreased when the measurements were averaged over longer intervals. An inverse relationship was also observed between deflection velocities and COVs, which seemed to increase with vehicle speed. COVs of less than 20% corresponded to deflection velocities greater than about 200 mils/s (5 mm/s).

To evaluate accuracy, the TSDD deflection velocities were compared with the corresponding geophone measurements. Plots of deflection velocities for the two devices were used, and despite complications aligning the laser sensors directly on top of the geophones, the TSDD deflection velocities matched those measured by the geophones well.

Having established accuracy and precision, the next step was to review the TSDD-generated data to validate that the device was producing reasonable results. The reference data for the validation were the FWD deflection measurements. Because the measurements of the two devices cannot be compared directly, FWD-TSDD relationships were developed to estimate the TSDD deflection velocities from FWD measurements. To do this, a database of numerical pavement response simulation for different pavement structures subjected to FWD and TSDD loadings was developed.

To assess the reliability of the resulting relationships, the numerical responses were validated with data from the field experiments. Data from the three LVR test cells were used as inputs into the models to obtain FWD deflections and TSDD deflection velocities at each sensor location. The numerical and experimental responses agreed with an uncertainty of about ±10% for all cells and sensor locations, indicating that models were able to capture responses adequately. However,

the large uncertainty level of the TSDD-measured values had to be considered. Using the numerical simulations database, ANN models were trained and validated to convert FWD deflections to the corresponding TSDD deflection velocities. Validation of the models showed that they could estimate TSDD deflection velocities well based on pavement layer thicknesses and FWD deflections. More specifically, it was determined that the average TSDD deflection velocity can be predicted using the ANN models within a level of uncertainty less than 20% for most TSDD sensors.

The resulting ANN models were then validated at test sections in Virginia and Texas. As with the field experiments, the deflection velocities varied for different sensor locations and test sections. For the Virginia test sections, most of the sensors exhibited COVs greater than 100%, while the COVs for the Texas TSDD measurements were notably lower, which was attributed to the uniformity and stiffnesses of the selected test sections. Spatial averaging of the deflection velocities resulted in COV decreases. Again, as with the field experiments, an inverse relationship was observed between deflection velocities and COVs of the deflection velocities. Although in many cases COVs less than 20% corresponded to deflection velocities greater than about 200 mils/s (5 mm/s), some COVs were higher than that limit. For deflection velocities greater than about 600 mils/s (15 mm/s), the COV was always less than 20%.

To evaluate the accuracy of the TSDD measurements, the deflection velocities for each test section were compared with the measurements recorded by the two geophones installed at each test section. For the Virginia test sections, the TSDD results were outside the ±20% uncertainty bounds at some of the TSDD sensors. The Texas test sections exhibited less deviation of the TSDD measurements from the geophones as most TSDD sensors' deflection velocities fell within the ±20% uncertainty bounds.

Finally, to calibrate the ANN models, calibration factors were needed to make the ANN estimated deflection velocity values closer to the experimental values. For each test site, the ANN models were used to estimate the TSDD results corresponding to the FWD data and layer thicknesses of the test sections. The results were then averaged along the test section for each sensor to be compared with the average experimental TSD-collected values. It was determined that the TSDD deflection velocities can be predicted using the calibrated ANN models within a level of uncertainty of less than 20% for TSDD sensors that yielded reasonably low uncertainty (COV of less than 50%). Ultimately, the calibrated ANN models were used to develop the proposed practice contained in Attachment A. The resulting proposed practice is considered ready for implementation, but it is again noted that the findings of this research are based on measurements by one device and may not apply to other devices. Also, the proposed practice would benefit from further calibration for conditions different from those encountered in the MnROAD field experiments and Virginia and Texas field validations.

In addition to the proposed practice and this report, the project database and ANN software application developed as part of the project are provided under separate cover as part of the final project deliverables. The database contains the TSDD, FWD and geophone measurements collected during the project, while the software application contains the ANN models developed for use with the proposed practice. Finally, it is recommended that consideration be given to developing a convenient field instrumentation system, which would decrease the uncertainty of the measurements and provide both verification and validation of TSDDs.

REFERENCES

Andersen, S., Levenberg, E., & Andersen, M. B. (2017). Inferring Pavement Layer Properties from a Moving Measurement Platform. In 10th International Conference on the Bearing Capacity of Roads, Railways and Airfields (pp. 675-682). Taylor & Francis.

Andrén, P. (1999, January). High-Speed Rolling Deflectometer Data Evaluation. In Nondestructive Evaluation of Aging Aircraft, Airports, and Aerospace Hardware III (Vol. 3586, pp. 137-147). International Society for Optics and Photonics.

Andrén, P. (2006). Development and Results of the Swedish Road Deflection Tester (Doctoral dissertation, Byggvetenskap).

Andrén, P., & Lenngren, C. A. (2002). Rolling Wheel Deflectometer/FWD Correlation Study. In 6th International Conference on the Bearing Capacity of Roads, Railways and Airfields.

Arora, J., Tandon, V., and Nazarian, S. (2006). Continuous Deflection Testing of Highways at Traffic Speeds, Report No. FHWA/TX-06/0-4380, Texas Department of Transportation, Austin, TX.

Athanasiadis, N. & Zoulis, P. (2019). Viscoelastic Pavement Modeling for Use with the Dynatest Raptor. (Master's Thesis). Technical University of Denmark

Brezina, I; Stryk, J. (2015): Vysokorýchlostný deflektometer TSD – Možnosti Jeho Využitia pri Hodnotení Únosnosti Vozoviek na Úrovni Cestnej Siete na Slovensku. Rozborová úloha. Centrum dopravního výzkumu.

Briggs, R. C., Johnson, R. F., Stubstad, R. N., & Pierce, L. (2000). A Comparison of the Rolling Weight Deflectometer with the Falling Weight Deflectometer. In Nondestructive Testing of Pavements and Backcalculation of Moduli: Third Volume. ASTM International.

Bryce, J., Katicha, S., Flintsch, G. W., & Ferne, B. (2012). Analyzing Repeatability of Continuous Deflectometer Mmeasurements, Transportation Research Board Meeting (paper No. 12-1732).

Chai, G., Manoharan, S., Golding, A., Kelly, G., & Chowdhury, S. (2016). Evaluation of the Traffic Speed Deflectometer data using simplified deflection model. Transportation Research Procedia, 14, 3031-3039.

Chatti, K., Kutay, M. E., Lajnef, N., Zaabar, I., Varma, S., & Lee, H. S. (2017). Enhanced Analysis of Falling Weight Deflectometer Data for Use with Mechanistic-Empirical Flexible Pavement Design and Analysis and Recommendations for Improvements to Falling Weight Deflectometers (No. FHWA-HRT-15-063). Turner-Fairbank Highway Research Center.

Deep, P., Andersen, M. B., Thom, N., & Lo Presti, D. (2020). Toward the Development of Load Transfer Efficiency Evaluation of Rigid Pavements by a Rolling Wheel Deflectometer. Infrastructures, 5(1), 7.

Dickerson, R. S., & Mace, D. G. (1976). A High Speed Profilometer-Preliminary Description. *TRRL Supplementary Report*, *182*.

Elbagalati, O., Mousa, M., Elseifi, M. A., Gaspard, K., & Zhang, Z. (2018). Development of a Methodology to Backcalculate Pavement Layer Moduli Using the Traffic Speed Deflectometer. Canadian Journal of Civil Engineering, 45(5), 377-385.

Elseifi, M., Abdel-Khalek, A. M., & Dasari, K. (2012). Implementation of Rolling Wheel Deflectometer (RWD) in PMS and Pavement Preservation (No. FHWA/11.492). Louisiana Transportation Research Center.

Elseifi, M. A., & Elbagalati, O. (2017). Assessment of Continuous Deflection Measurement Devices in Louisiana-Rolling Wheel Deflectometer: final report 581 (No. FHWA/LA. 17/581). Louisiana Transportation Research Center.

Elseifi, M. A., Zihan, Z. U., & Icenogle, P. (2019). A Mechanistic Approach to Utilize Traffic Speed Deflectometer (TSD) Measurements into Backcalculation Analysis (No. FHWA/LA. 17/612).

Elseifi, M. A., & Zihan, Z. U. (2018). Assessment of the Traffic Speed Deflectometer in Louisiana for Pavement Structural Evaluation (No. FHWA/LA. 18/590). Louisiana Transportation Research Center.

Elseifi, M. A., Abdel-Khalek, A., Gaspard, K., Zhang, Z. D., & Ismail, S. (2011). Evaluation of the Rolling Wheel Deflectometer as a Structural Pavement Assessment Tool in Louisiana. In Transportation and Development Institute Congress 2011: Integrated Transportation and Development for a Better Tomorrow (pp. 628-637).

Fan, J., & Yao, Q. (1998). Efficient Estimation of Conditional Variance Functions in Stochastic Regression. *Biometrika*, *85*(3), 645-660.

Fausett, L.V. (1994), "Fundamentals of Neural Networks: Architectures, Algorithms, and Applications," Pearson Education, 416 p.

Ferne, B. W., Langdale, P., Round, N., and Fairclough, R. (2009). Development of a Calibration Procedure for the UK Highways Agency Traffic-Speed Deflectometer. Transportation Research Record, 2093(1), 111-117.

Ferne, B. W., Drusin, S., Baltzer, S., Langdale, P., & Meitei, B. UK Trial to Compare 1st and 2nd Generation Traffic Speed Deflectometers. International Symposium Non-Destructive Testing in Civil Engineering (NDT-CE), September 15-17, Berlin, Germany.

Ferne, B. W., Langdale, P., Wright, M. A., Fairclough, R., & Sinhal, R. (2013). Developing and Implementing Traffic-Speed Network Level Structural Condition Pavement Surveys. In *Proceedings of the international conferences on the bearing capacity of roads, railways and airfields* (pp. 181-190).

Flintsch, G., & McGhee, K. (2009). Managing the Quality of Pavement Data Collection. *Transportation Research Board of the National Academies, Washington, DC*.

Flintsch, G., Katicha, S., Bryce, J., Ferne, B., Nell, S., & Diefenderfer, B. (2013). Assessment of Continuous Pavement Deflection Measuring Technologies (No. SHRP 2 Report S2-R06F-RW-1).

Flintsch, G. W., Ferne, B., Diefenderfer, B., Katicha, S., Bryce, J., & Nell, S. (2012). Evaluation of Traffic-Speed Deflectometers. Transportation research record, 2304(1), 37-46.

Flora, W. F. (2009). *Development of a Structural Index for Pavement Management: An Exploratory Analysis*. Purdue University.

Gedafa, D. S., Hossain, M., Miller, R. W., & Steele, D. (2008). Network Level Pavement Structural Evaluation Using Rolling Wheel Deflectometer (No. 08-2648).

GeoSolve Ltd. (2016). The Application of TSD Data in New Zealand for Asset Management and Design. Report 150003, GeoSolve Limited, New Zealand Transportation Agency (NZTA).

Saremi, S. (2018). Practical models for Interpreting Traffic Speed Deflectometer Data. M.S. Thesis. The University of Texas at El Paso, El Paso, TX.

Greenwood Engineering (2020, September 15) More than 500,000 Measured Kilometers. Greenwood Engineering. https://greenwood.dk/road/tsd/references/

Harr, M. E., & Ng-A-Qui, N. T. (1977). *Noncontact Nondestructive Determination of Pavement Deflection under Moving Loads*. PURDUE RESEARCH FOUNDATION LAFAYETTE IN.

Hastie, T.; Tibshirani, R.; Friedman, J. The Elements of Statistical Learning: Data Mining, Inference, and Prediction. Springer Science & Business Media: New York, NY, USA, 2009. https://doi.org/10.1007/978-0-387-84858-7.

Hildebrand, G; Rasmussen, S. (2002): Development of a High Speed Deflectograph. (Report 177) Danish Road Institute.

Hildebrand, G; Rasmussen, S.& Andrés, R. (1999): Development of a Laser-Based High Speed Deflectograph. (Report 97). Danish Road Institute.

Ilonen, J.; Kamarainen, J.K.; Lampinen, J. Differential Evolution Training Algorithm for Feed-forward Neural Networks. *Neural Process. Lett.* 2003, *17*, 93–105. https://doi.org/10.1023/A:1022995128597.

Irwin L.H., Orr D.P., and Atkins D. (2011) Falling Weight Deflectometer Calibration Center and Operational Improvements: Redevelopment of the Calibration Protocol and Equipment, Report FHWA-HRT-07-040, Cornell University, 268 p.

International Organization for Standardization (ISO) "Systems and Software Engineering - Vocabulary," ISO/IEC/IEEE std 24765:2010(E), 2010. | verification 5. ...product, service, or system complies with a regulation, requirement, specification, or imposed condition.

International Organization for Standardization (ISO) ISO 5725-1: "Accuracy (trueness and precision) of measurement methods and results - Part 1: General principles and definitions.", p.1 (1994)

Jansen, D. (2017). TSD evaluation in Germany. In Proceedings of the International Symposium Non-Destructive Testing in Civil Engineering (pp. 700-708).

Kannemeyer, L., Lategan, W., and McKellar, A. (2014). Verification of Traffic Speed Deflectometer Measurements using Instrumented Pavements in South Africa. Pavement Evaluation 2014, Blacksburg, VA.

Katicha, S.W., Flintsch, G.W., and Ferne, B. (2012). Estimation of Pavement TSD Slope Measurements Repeatability from a Single Measurement Series, 91st Meeting of the Transportation Research Board, Washington, DC.

Katicha, S. W., Flintsch, G. W., & Ferne, B. (2013). Optimal Averaging and Localized Weak Spot Identification of Traffic Speed Deflectometer Measurements. *Transportation research record*, *2367*(1), 43-52.

Katicha, S. W., & Flintsch, G. W. (2015). Field Demonstration of the Traffic Speed Deflectometer in New York, Transportation Research Board Meeting, (paper No. 15-4630).

Katicha, S. W., Ercisli, S., Flintsch, G. W., Bryce, J. M., & Diefenderfer, B. K. (2016). *Development of Enhanced Pavement Deterioration Curves* (No. VTRC 17-R7). Virginia Transportation Research Council.

Katicha, S., Flintsch, G., Shrestha, S., and Thyagarajan, S. (2017). Demonstration of Network Level Structural Evaluation with Traffic Speed Deflectometer: Final Report. FHWA.

Katicha, S. W., Shrestha, S., Flintsch, G. W., & Diefenderfer, B. K. (2020). *Network Level Pavement Structural Testing With the Traffic Speed Deflectometer* (No. VTRC 21-R4).

Lee, J., Duschlbauer, D. and Chai, G. (2019). Ground Instrumentation for Traffic Speed Deflectometer (TSD). ARRB Report PRP17037-02, Australian Road Research Board (ARRB), Main Road Western Australia (MRWA).

Madsen, S. S., & Pedersen, N. L. (2019). Backcalculation of Raptor (RWD) Measurements and Forward Prediction of FWD Deflections Compared with FWD Measurements. In Airfield and Highway Pavements 2019: Design, Construction, Condition Evaluation, and Management of Pavements (pp. 382-391). Reston, VA: American Society of Civil Engineers.

Malquori, I. (2019) An example of How to Use Deflection Measurements Collected with the Dynatest RAPTOR® to Plan Road Maintenance Activities. Presented at ERPUG

Muller, W. B. (2015). A comparison of TSD, FWD and GPR Field Measurements. In Proceedings of the International Symposium Non-Destructive Testing in Civil Engineering (pp. 713-722).

Muller, W. B., & Roberts, J. (2013). Revised Approach to Assessing Traffic Speed Deflectometer Data and Field Validation of Deflection Bowl Predictions. International journal of pavement engineering, 14(4), 388-402.

Muller, W., and Wix, R. (2014). Preliminary Field Validation of the Updated Traffic Speed Deflectometer (TSD) device. In ARRB Conference, 26th October 2014, Sydney, New South Wales, Australia (No. 4.2).

Nillson, R. (2019) News about Swedish Trials with the TSD and Raptor. Presented at ERPUG

Peekna, A. (2002). Data Reduction Procedures and Effects of Propagation of Errors for the Rolling Deflectometer. Rev. Ing. Constr, 18(2), 79-85.

Perera, R. W. (2018). Inertial Profiler Certification for Evaluation of International Roughness Index (No. Project 20-05, Topic 48-12).

Rada, G.R. and Nazarian, S. (2011). The State-of-the-Technology of Moving Pavement Deflection Testing, Report No. FHWA-HIF-11-013, Federal Highway Administration (FHWA), Washington, DC.

Rada, G. R., Nazarian, S., Visintine, B. A., Siddharthan, R., & Thyagarajan, S. (2016). Pavement Structural Evaluation at the Network Level: final report. Washington, DC: US Federal Highway Administration Report FHWA-HRT-15–074.

Rocha, S., Tandon, V., & Nazarian, S. (2001). Reproducibility of Texas Department of Transportation Falling Weight Deflectometer Fleet (No. RR-1784-1). University of Texas.

Rocha, S., Nazarian, S., & Tandon, V. (2003). A Comprehensive Calibration Strategy for Texas Department of Transportation Falling Weight Deflectometer Fleet.

Rocha S., Tandon V. and & Nazarian S. (2004) Falling Weight Deflectometer Fleet, Road Materials and Pavement Design, 5:2, 215-238, DOI: 10.1080/14680629.2004.9689970

Ruppert, David, et al. "Local Polynomial Variance-Function Estimation." *Technometrics* 39.3 (1997): 262-273.

Shrestha, S., Katicha, S. W., Flintsch, G. W., & Thyagarajan, S. (2018). Application of Traffic Speed Deflectometer for Network-Level Pavement Management. Transportation research record, 2672(40), 348-359.

Siddharthan, R., Krishnamenon, N., & Sebaaly P. (2000). Finite-Layer Approach to Pavement Response Evaluation. Transportation Research Board: Journal of the Transportation Research Board, 1709, 43-49.

Skar, A., Levenberg, E., Andersen, S., & Andersen, M. B. (2020). Analysis of a Moving Measurement Platform based on Line Profile Sensors for Project-Level Pavement Evaluation. Road Materials and Pavement Design, 1-17.

Steele, D. A., Beckemeyer, C. A., & Van, T. P. (2015, June). Optimizing Highway Funds by Integrating RWD Data into Pavement Management Decision Making. In 9th International Conference on Managing Pavement Assets.

Steele, D. A., Lee, H., & Beckemeyer, C. A. (2020). Development of the Rolling Wheel Deflectometer (RWD) (No. FHWA-DTFH-61-14-H00019). United States. Federal Highway Administration.

Steele, D., Hall, J., Stubstad, R., Peekna, A., & Walker, R. (2002). Development of a High-Speed Rolling Wheel Deflectometer. In Pavement Evaluation Conference, 2002, Roanoke, Virginia, USA.

Stokoe II, K. H., Lee, J. S., Nam, B. H., Lewis, M., Hayes, R., Scullion, T., & Liu, W. (2012). *Developing a Testing Device for Total Pavements Acceptance: Third-Year Report* (No. FHWA/TX-11/0-6005-4).

Stonecliffe-Jones, M. (2017) Introduction to the Dynatest RAPTOR Rolling Wheel Deflectometer. Presented at RPUG

Strategic Highway Research Program. (1994). SHRP/LTPP FWD Calibration Protocol, Transportation Research Board, Washington, DC.

Wahba, G. (1990). *Spline Models for Observational Data*. Society for industrial and applied mathematics.

Wix, R., Murnane, C., & Moffatt, M. (2016). Experience Gained Investigating, Acquiring and Operating the First Traffic Speed Deflectometer in Australia. *Transportation Research Procedia*, *14*, 3060-3069.

Wilke, P. W. (2014). Rolling Wheel Deflectometer for Pavement Evaluation. In T&DI Congress 2014: Planes, Trains, and Automobiles (pp. 259-268).

Zaghloul, S., He, Z., Vitillo, N., & Brian Kerr, J. (1998). Project Scoping Using Falling Weight Deflectometer Testing: New Jersey experience. *Transportation Research Record*, *1643*(1), 34-43.

Zofka, A., Graczyk, M., & Rafa, J. (2015). Qualitative Evaluation of Stochastic Factors Affecting the Traffic Speed Deflectometer Results. In *Transportation Research Board 94th Annual Meeting Washington DC*.

APPENDIX A: EFFECT OF SPATIAL AVERAGING ON TSDD MEASUREMENTS

Figures 1 and 2 summarize the effects of spatial averaging on the TSDD measurements for the MnROAD LVR and ML test cells, respectively. The TSDD measurements were averaged at 3.3-ft (1-m) intervals for each sensor. Both figures show that the COVs of the deflection velocities decrease significantly for the averaged data when compared to the 2 in. (50 mm) data. The decreases in the COVs of the sensors with larger deflection velocities are more pronounced. However, the variability of the data of the ML test cells for many sensors is still significant, as the COVs still exceed 50%.

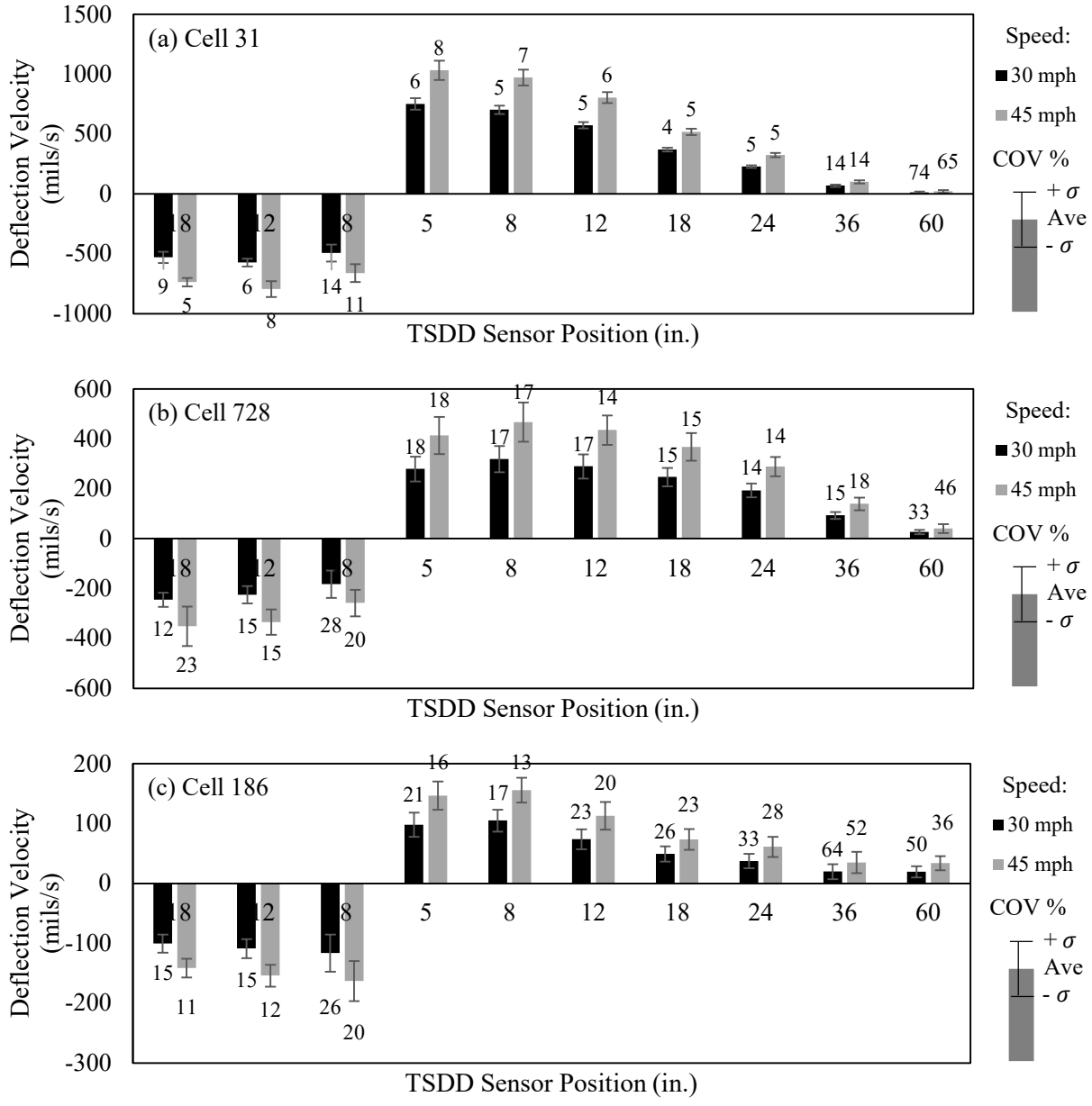

σ = standard deviation, Ave = average

Figure 1. Variability of TSDD deflection measurements in LVR test cells – 3.3 ft interval.

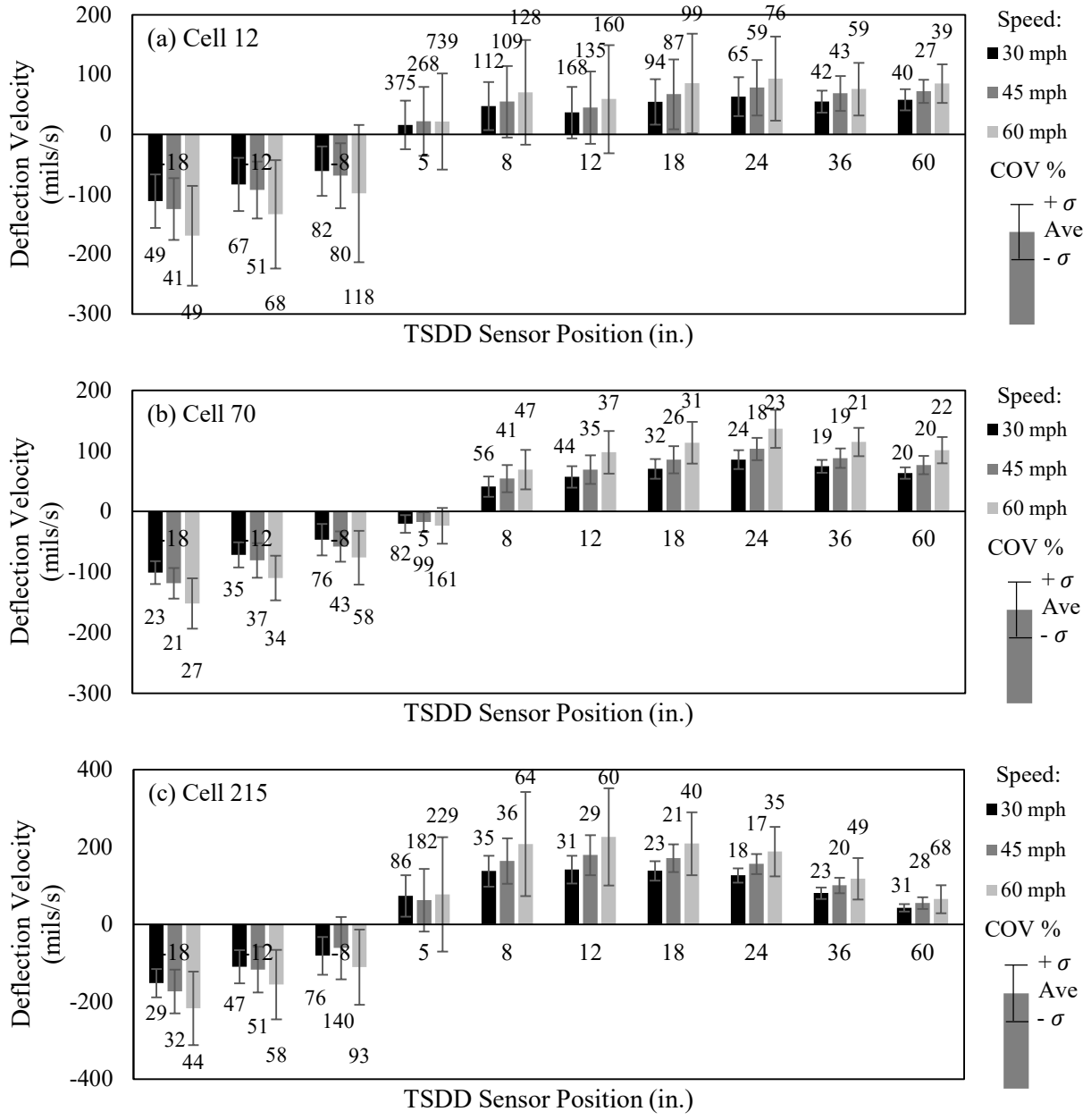

σ = standard deviation, Ave = average

Figure 2. Variability of TSDD deflection measurements in ML test cells – 3.3 ft interval.

APPENDIX B: EVALUATION OF 3D-MOVE MODELS

Figure 1 compares the predicted FWD deflections using the backcalculated layer moduli against the measured FWD deflections for Cells 31, 728, and 186 of the LVR. Based on the FWD data, the backcalculation process was carried out properly, as the differences between the modeled and measured deflections are typically within the ±10% uncertainty lines for all three cells.

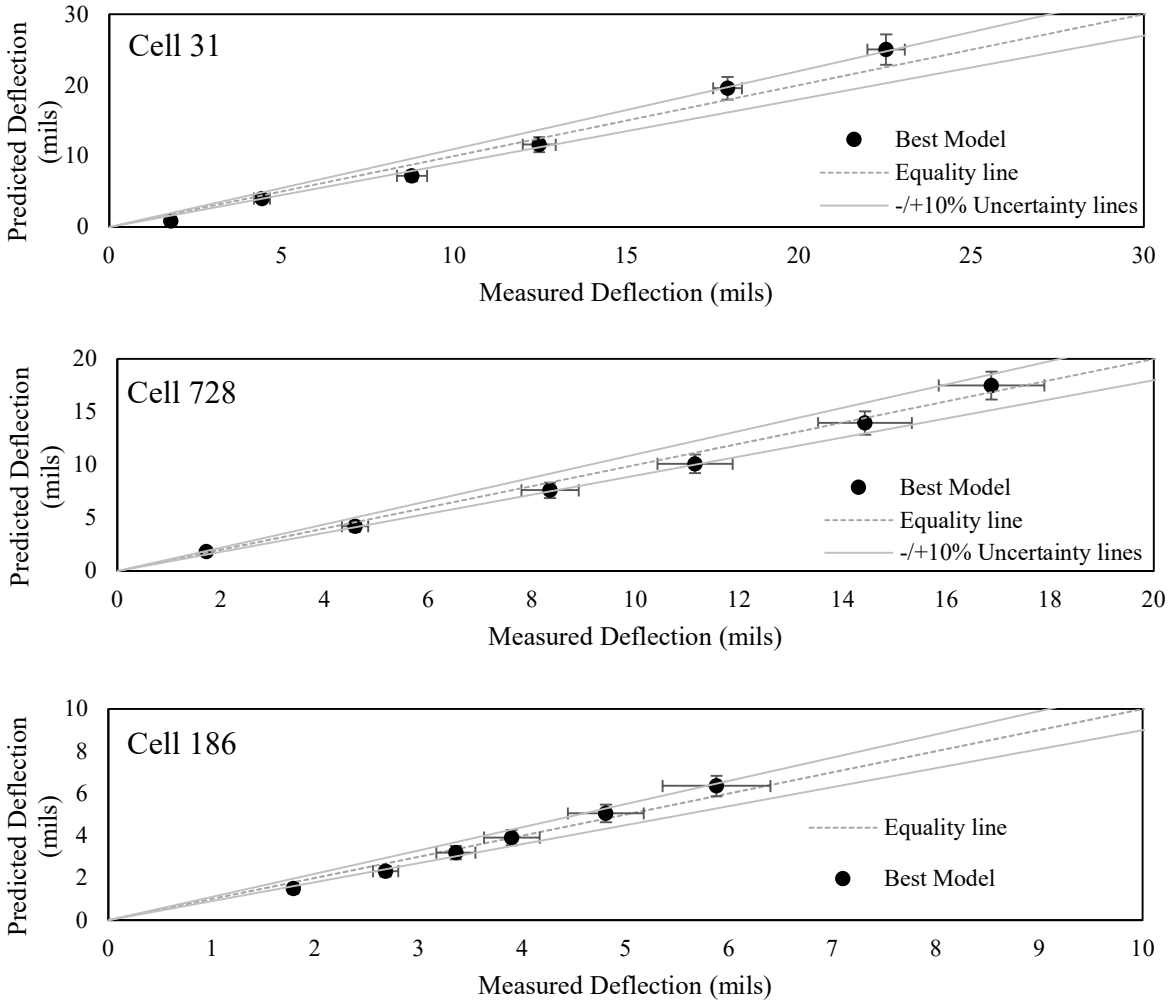

Figure 1. Comparison of 3D-Move simulated and FWD measured deflections – LVR cells.

The TSDD-predicted against measured deflection velocity plots for the three LVR cells are shown in Figure 2. The 3D-Move models executed using the FWD backcalculated moduli on average predict the results from the field experiment with an uncertainty of about 10%. However, the error bars that represent one standard deviation are large and become larger as the cell becomes stiffer.

The information provided in Figure 2 is reproduced in Figure 3 but using TSDD data averaged over 3.3 ft (1 m) instead of the 2 in. (50 mm) data. The standard deviation error bars are significantly shorter in this case.

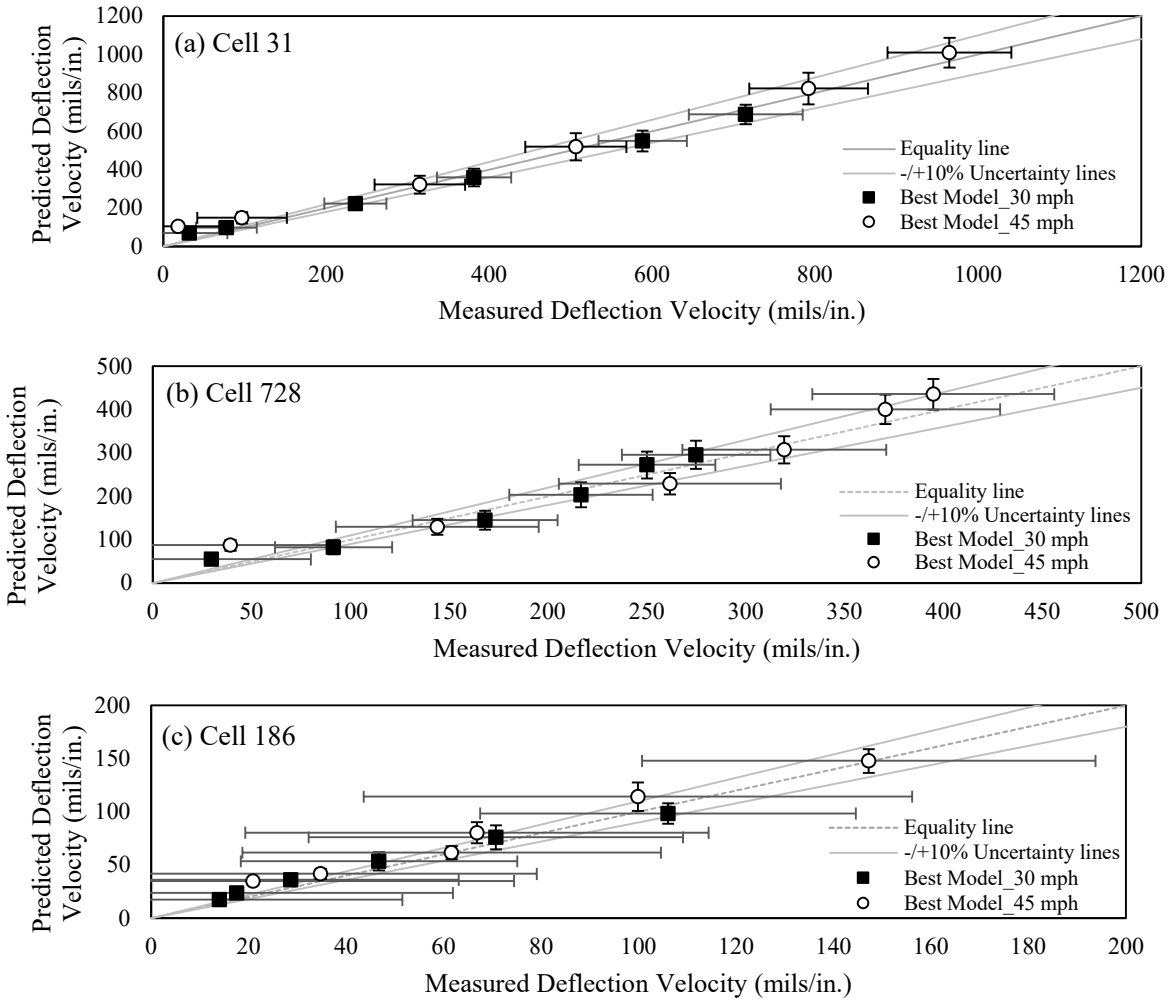

Figure 2. Comparison of 3D-Move simulated and TSDD measured deflection velocities – LVR cells and 2 in data.

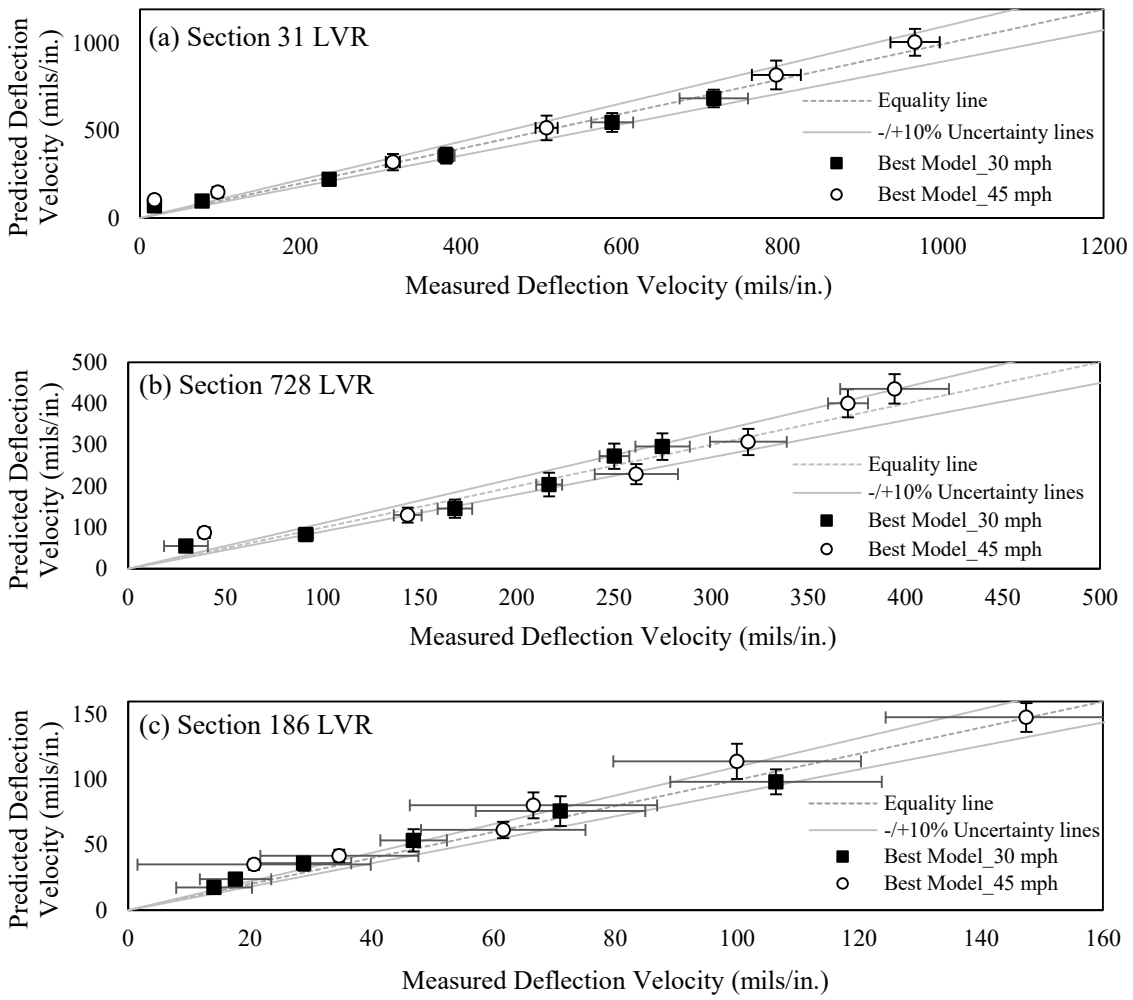

Figure 3. Comparison of 3D-Move simulated and TSDD measured deflection velocities – LVR cells and 3.3 ft data.

APPENDIX C: EVALUATION OF ANN MODELS

Before evaluation of the ANN models using field data, the performance of these models was evaluated following established industry protocols (e.g., Fausett, 1994). Using these protocols, the database was divided into three components – 70% of the data for training, 15% for testing, and another 15% for evaluation. This appendix contains the results of the evaluation of the ANN models with 15% of the data never seen by the ANN models before. As shown in Figure 1, the ANN-based models predict the TSDD deflection velocity at three different speeds for HMA pavements with an UGB layer well. The ANN predicted surface deflection velocities for speeds of 30, 45, and 60 mph (48, 72, and 96 km/h) with coefficients of determination close to unity, and standard errors of estimate SEEs of less than 0.2 mils/s (8 mm/s).

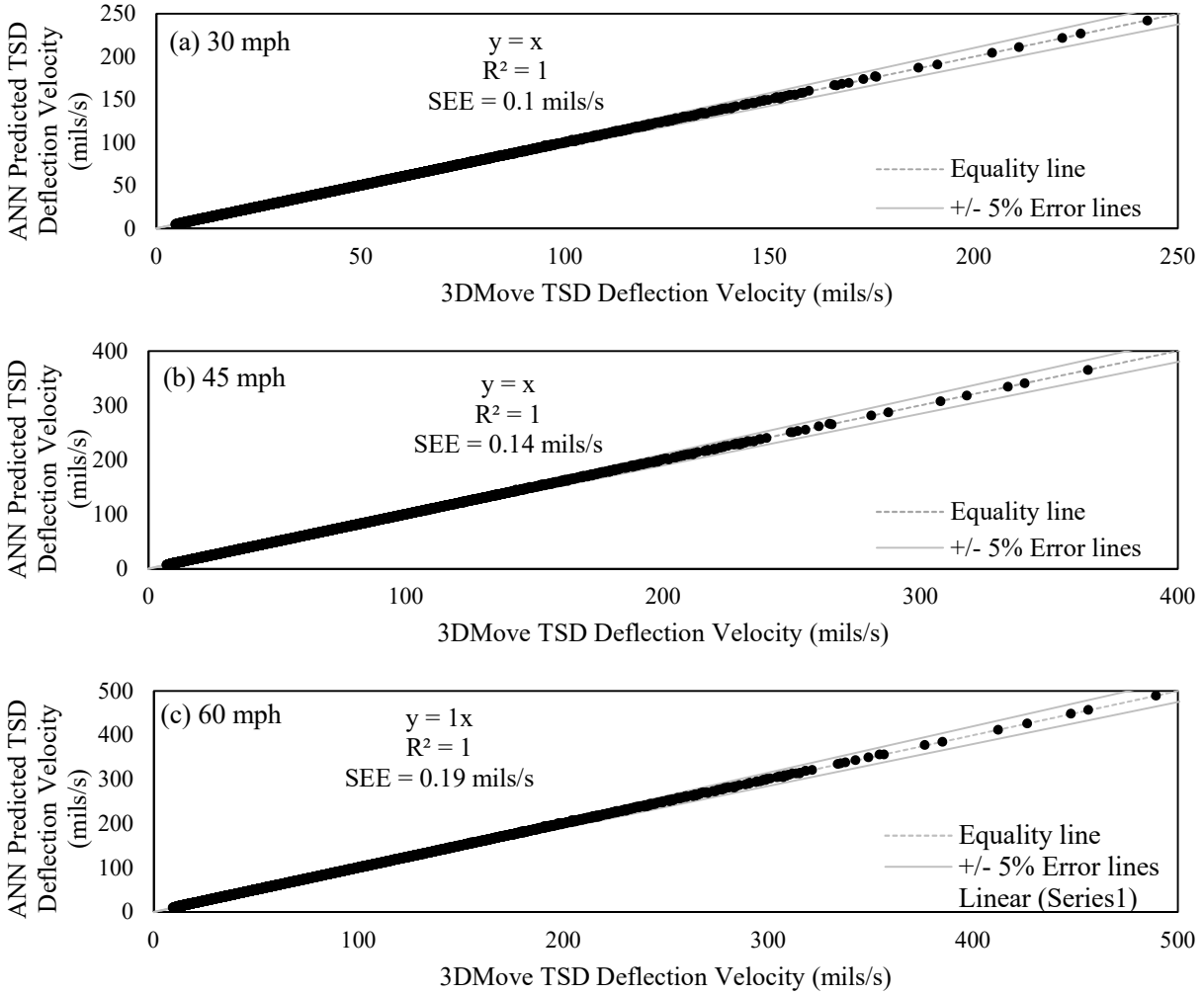

Figure 1. Comparison of ANN-predicted versus 3D-Move simulated deflection velocities – AC on UGB pavements.

Likewise, Figures 2 and 3 compare the TSDD deflection velocities under different speeds predicted by the ANN-based models and determined using 3D-Move for the HMA pavements with a stabilized base layer and rigid pavements, respectively. Based on these plots, the ANN-based models predict the TSDD deflection velocity for both pavement types well with standard error of estimates (SEEs) of less than 0.5 and 1 mils/s (20 and 39 mm/s).

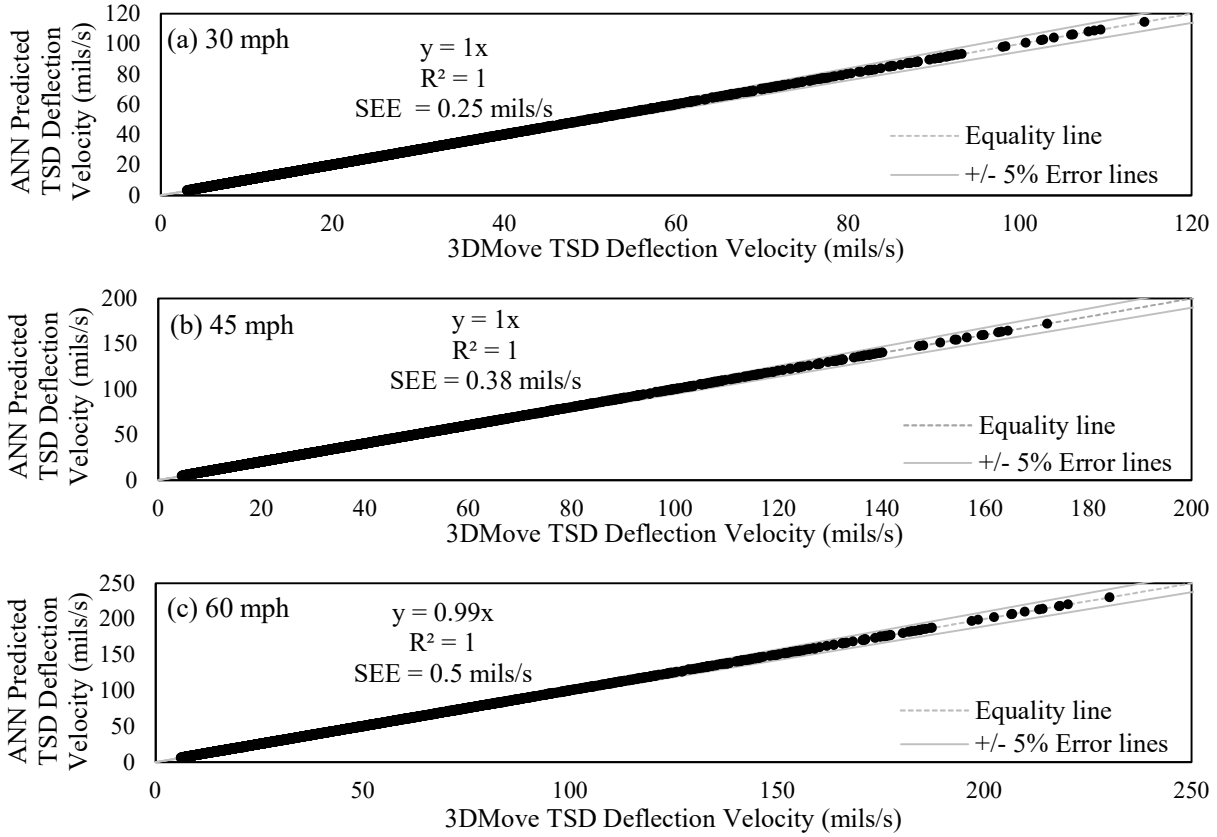

Figure 2. Comparison of ANN-predicted versus 3D-Move simulated deflection velocities – AC on stabilized base pavements.

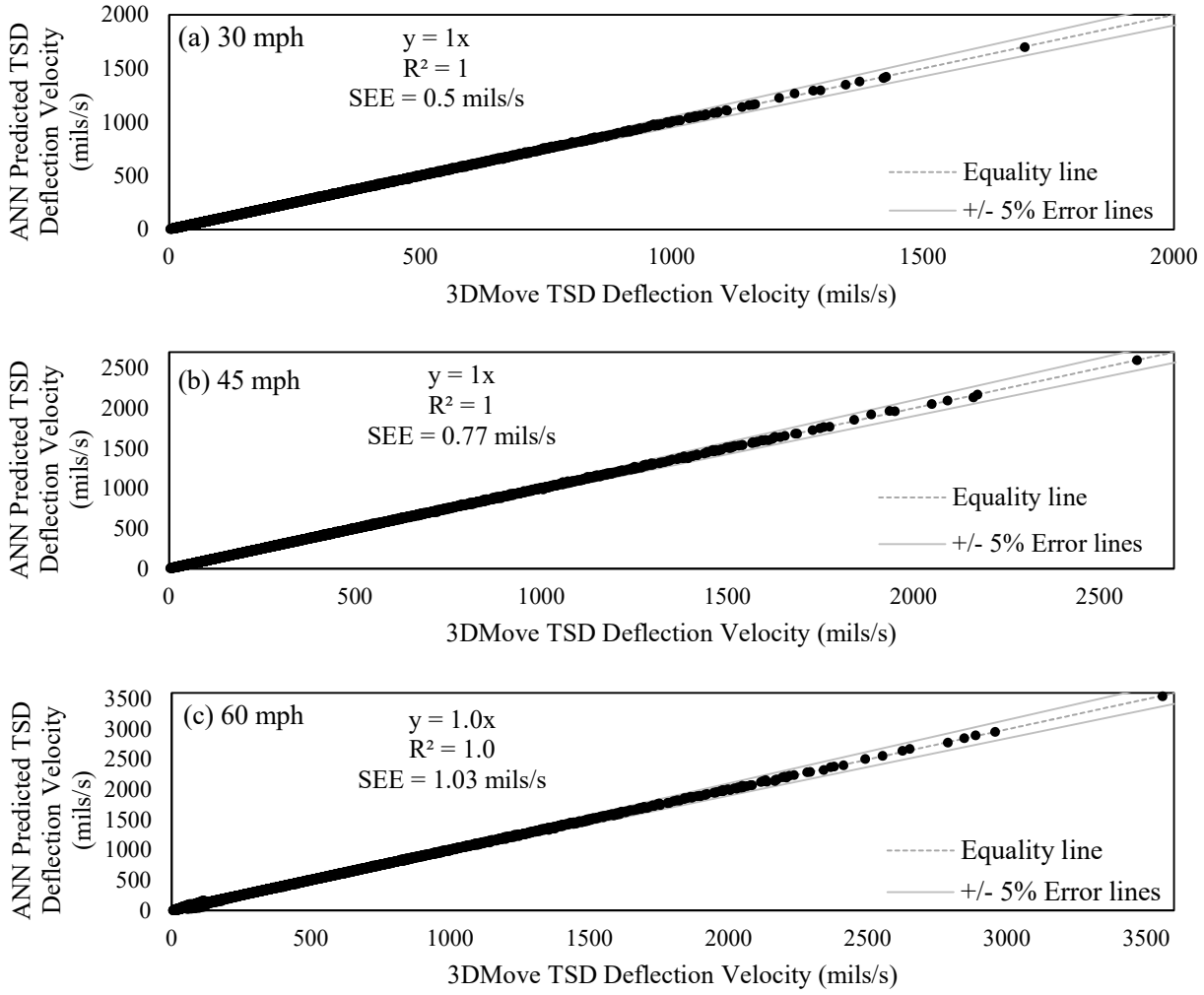

Figure 3. Comparison of ANN-predicted versus 3D-Move simulated deflection velocities – PCC pavements.

ATTACHMENT A: PROPOSED PRACTICE

Proposed Practice for Verification of Traffic Speed Deflection Device (TSDD) Measurements with the Falling Weight Deflectometer

Disclaimer: This proposed practice for "Verification of Traffic Speed Deflection Device (TSDD) Measurements with the Falling Weight Deflectometer" is the recommendation of the NCHRP Project 10-105 staff at WSP USA Environment & Infrastructure Inc. The findings that led to this standard practice are based on measurements by one TSDD device and may not apply to other TSDD devices This standard practice has not been approved by NCHRP or any AASHTO committee nor formally accepted for the AASHTO specifications.

1. SCOPE

1.1. This practice describes a procedure for verifying traffic speed deflection device (TSDD) measurements using falling weight deflectometer (FWD) measurements. The TSDD measurements are obtained while the device travels along three pavement test sections. FWD measurements are collected on the same three pavement test sections according to the procedures described in AASHTO T 256-01 (2011). This standard practice describes the procedures for TSDD and FWD measurements, provides the general information that shall be obtained, and explains the analysis method that shall be undertaken to perform the verification.

1.2. This practice is applicable to TSDD measurements performed on asphalt concrete (AC) or semi-rigid (AC on stabilized base). Portland Cement Concrete (PCC) pavements are not recommended for the verification of TSDD measurements.

1.3. The values stated in SI units are to be regarded as standard. The values in the U.S. Customary units given in parentheses are for information purposes only.

1.4. *This practice does not purport to address the safety concerns, if any, associated with its use. It is the responsibility of the user of this practice to establish appropriate safety and health practices and determine the applicability of regulatory limitations related to and prior to its use*.

2. REFERENCED DOCUMENTS

2.1 AASHTO Standards:

- R 32, Calibrating the Load Cell and Deflection Sensors for a Falling Weight Deflectometer.
- T 256-01, Pavement Deflection Measurements.

2.2 ASTM Standards:

- D4694, Standard Test Method for Deflections with a Falling-Weight-Type Impulse Load Device.
- D4695, Standard Guide for General Pavement Deflection Measurements.

3. TERMINOLOGY

3.1. *Definition of terms specific to this standard practice.*

3.1.1. *Laser Sensors*: laser-based sensors mounted on the TSDD to measure the pavement response as the device travels along each of the three (3) pavement test sections.

3.1.2. *Strain Gauge(s)*: sensor(s) mounted on the TSDD rear axle to measure the strain that is caused by the load applied to the axle. The measured strains are used to estimate the dynamic load applied to the axle during testing.

3.1.3. *Load Cell*: FWD load cell that is capable of accurately measuring the load applied perpendicular to its loading plate.

3.1.4. *Deflection Basin*: the deformed pavement surface due to the FWD stationary impact load or the TSDD rolling wheel load.

3.1.5. *TSDD Deflection Response*: the pavement surface response that is caused by the movement of the TSDD and that is measured by the laser sensors.

3.1.6. *Testing Speed*: the speed at which the TSDD is moving on the three pavement test sections.

3.1.7. *Test Location*: the point at which the center of the load plate is placed for FWD testing. There are eleven (11) FWD test locations at each pavement test section, which also define the path the TSDD laser-sensors shall follow.

3.1.8. *Accuracy*: the ability of a measuring device to collect measurements with an expected value that is close to a selected reference value. For this standard practice, the measuring device is the TSDD, and the reference device is the FWD. Accuracy can be quantified with the statistical measure of bias, with zero bias corresponding to perfect accuracy.

3.1.9. *Precision*: the ability of a measuring device to collect measurements at the same location that are closely bunched together. Precision can be quantified with the statistical measure of variance, with zero variance corresponding to perfect precision.

3.1.10. *Repeatability*: the square root of the mean square of the difference among two or more repeated measurements at the same location. Repeatability is closely related to precision.

3.1.11. Reproducibility: the square root of the mean square difference of the measurements of two (2) different measuring devices.

4. SIGNIFICANCE AND USE

4.1. This-practice consists of methods for measuring the pavement response to a TSDD and verifying these measurements with FWD deflection measurements. Each device is operated according to the standard operating procedure applicable to that device.

4.2. This practice pertains to tests performed on AC and semi-rigid pavement sections. This practice does not apply to PCC pavements.

4.3. Standards for collection of general information, such as test setup, ambient temperature, pavement temperature, number of tests, and test locations, pertain to all devices.

5. EQUIPMENT

5.1. The equipment used in this practice shall be a TSDD as described in Section 5.2 and the FWD device (see ASTM D4694).

5.2. *Traffic Speed Deflection Device*: a TSDD is an articulated truck with a rear-axle load ranging between 60 kN and 130 kN (13 kips and 22 kips) and measures the pavement response while traveling at speeds typically ranging between 50 km/h and 100 km/h (30 mph and 60 mph). A TSDD has several lasers, mounted on a beam, that measure the pavement response of the device as it travels along the road. For purposes of this standard practice, lasers shall be located at 200, 300, 450, 600, 900, and 1,500 mm (8, 12, 18, 24, 36, and 60 in) from the tire load. Additional laser sensors at locations other than the six specified will not be used in the verification process.

6. EQUIPMENT CALIBRATION

6.1 The TSDD shall be calibrated according to the manufacturer's recommended procedure to ensure readings are within the manufacturer’s specified limits.

6.2 *TSDD Lasers Calibration*: lasers measuring the pavement response shall be calibrated following the manufacturer's recommended procedure.

6.3 *TSDD Strain Gauges Calibration*: strain gauges shall be calibrated prior to the start of the Section 7 field testing activities using portable scales.

6.4 *TSDD Distance Measuring Instrument (DMI) Calibration*: perform DMI calibration as recommended by the manufacturer.

6.5 *TSDD Tire Pressure Check*: tire pressure shall be checked prior to the start of the Section 7 field testing activities, adjusted as needed, and recorded.

6.6 FWD Calibration: the FWD used to perform the verification of the TSDD device shall be calibrated according to AASHTO R 32. The calibration shall be performed less than six (6) months before verification of the TSDD.

7. FIELD FWD AND TSDD TESTING

7.1 *General Testing Parameters and Conditions.*

7.1.1 *Environmental Testing Conditions*: TSDD and FWD testing shall be performed on the same day, under similar environmental conditions. Testing shall be performed when the air ambient temperature is within the equipment manufacturer recommended range and on a dry pavement surface. A surface is considered dry if the laser measurements incur 25% or less dropout (i.e., no signal is detected). The wind speed during testing shall be less than 30 km/h (20 mph) to limit the effect of crosswind loading on the TSDD trailer.

7.1.2 *Geometry of the Loading Area*: for proper application of the verification procedure, the pavement test sections shall be free of cracks or other forms of distress. A visual inspection of the pavement test sections shall be performed, and distresses shall be avoided. The longitudinal grade shall be less than 3% and horizontal radius of curvature shall be more than 600 m (2,000 ft).

7.1.3 *Surface Characteristic of Loading Area*: the loaded area shall be selected so that the collected data incur less than 25% dropout. Pavements with binder-rich surfaces (does not imply all new AC pavements) less than 6 months old are not appropriate for verification testing as they may cause faulty operation of the TSDD laser sensors.

7.1.4 *Load*: record the TSDD loads measured by the strain gauge(s) during testing, and the peak loads measured by the FWD load cell.

7.1.5 *Time of Test*: record the date and time the TSDD and FWD measurements are obtained.

7.1.6 *Stationing or Chainage*: record the station number or location of the 11 FWD test points at each pavement test section.

7.1.7 *Repeated Measurements*: record the TSDD and FWD test repeat numbers.

7.1.8 *Air and Pavement Temperatures*: record the ambient air temperature and pavement surface temperature at the beginning and the end of testing.

7.2 *Test Sections*: three (3) pavement test sections with a safe operational speed of at least 70 km/h (45 mph) shall be selected. The test sections shall cover a range of stiffnesses as determined based on FWD measurements obtained directly under

the center of the load plate. The recommended ranges of FWD deflections are 127 to 254 μm (5 to 10 mils), 254 to 508 μm (10 to 20 mils), and greater than 508 μm (20 mils). Ground penetrating radar (GPR) or coring to confirm the pavement layer thicknesses and material types is recommended.

7.2.1 *Length of Test Sections*: test sections shall have a minimum length of 30 m (100 ft). Preliminary FWD testing shall be performed at the three pavement test section locations, at 3-m (10-ft) intervals, to confirm that the desired stiffnesses have been achieved and the pavement test section produce uniform deflections, and to locate the center of the test sections.

7.2.2 *Test Locations*: mark on each pavement test section the location of the 11 FWD test points spaced at 1-m (3.3-ft) intervals along the wheel path[1], roughly in the longitudinal middle of the test section as shown in Figure 1. Record the locations of the FWD test points using a Global Positioning System (GPS) tracking device. Mark the wheel path at the beginning of the test section. In addition, reflective tape shall be used at the start and end of the test section, as illustrated in Figure 1.

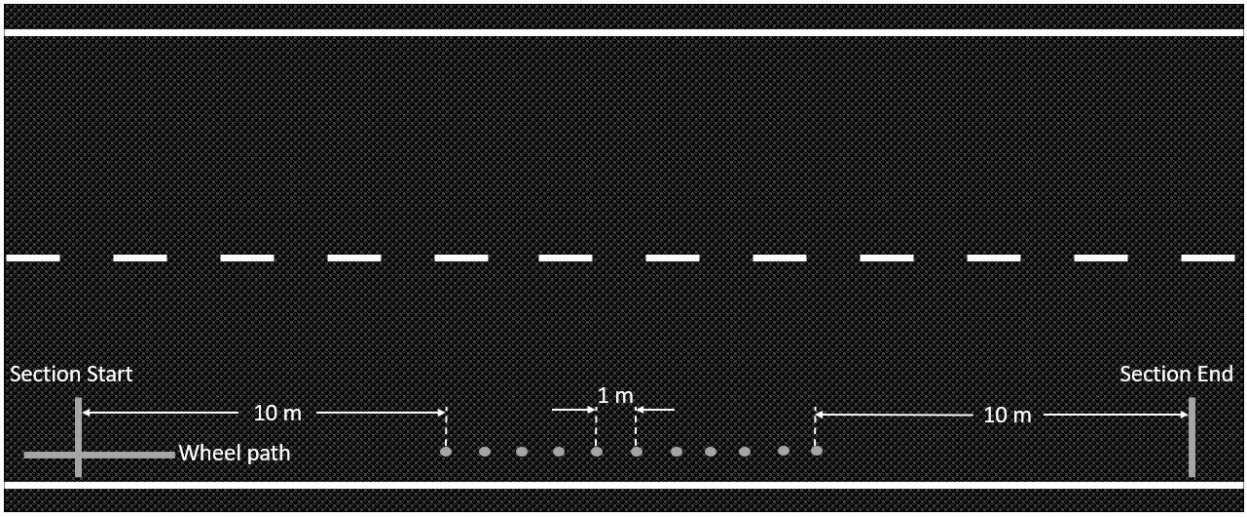

Figure*1.* Schematic of a test section

7.3 *TSDD Tests*: perform TSDD tests as discussed in this section.

7.3.1 *General*: operate the TSDD following the manufacturer's recommendations.

7.3.2 *Calibration*: all calibrations pertaining to the TSDD shall be performed as described in Section 6.

7.3.3 *TSDD Sensor Locations*: the TSDD lasers sensors shall be located at 200, 300, 450, 600, 900, and 1,500 mm (8, 12, 18, 24, 36, and 60 in) from the load center. As detailed in Section 7.4, FWD sensors will also be located at these six (6)

[1] The wheel path is the area that is between 0.3 m and 1 m (1 and 3 ft) from the shoulder edge.

locations. Additional TSDD or FWD sensors will not be used in the verification procedure.

7.3.4 *TSDD Testing*: perform at least three (3) valid repeat runs[2] (as defined in Section 7.3.5) for each of the three (3) test sections at two (2) different testing speeds. These testing speeds can be selected depending on the site characteristics. The testing speeds shall be chosen so that the highest testing speed is at least 25 km/h (15 mph) higher than the lowest testing speed. The lowest testing speed shall be at least 50 km/h (30 mph).

7.3.5 *Valid Test Run*: a run shall be considered valid if the eleven (11) FWD test locations fall within the TSDD dual tire loading area during the run (see Figure 2). This shall be determined using a TSDD-mounted camera.

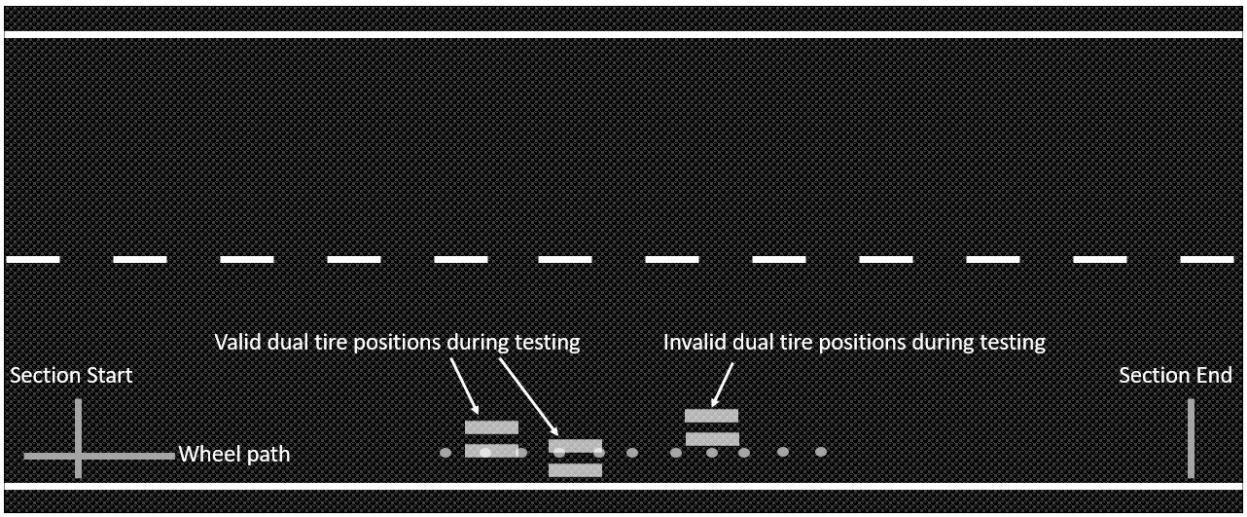

Figure *2.* Schematic showing valid and invalid tire positions.

7.3.6 *TSDD Data Collection*: collect TSDD data on each pavement test section over at least 30 m (100 ft) – 10 m (33 ft) before the first marked FWD test location, and 10 m after the last marked FWD test location. Data collected shall consist of the laser measurements, vehicle speed, strain gauge load measurements, air temperature, asphalt pavement surface temperature, and video of the TSDD dual ties as they pass over the eleven (11) FWD test locations.

7.4 *FWD Tests*: perform FWD tests following the process described below.

7.4.1 *General*: FWD testing shall be performed according to standard specifications for the device such as described in AASHTO T256-01, ASTM D4694, and ASTM D4695. The surface of the pavement shall be free of loose aggregate and other materials before conducting the tests.

[2] It is recommended that more than three (3) runs be performed so that at least three (3) of the total number of runs are valid runs.

7.4.2 *FWD Sensors Locations*: FWD deflection measuring sensors shall be configured to match the location of the TSDD lasers that are in front of the loading wheel (with respect to the center of the wheel load). The FWD sensors shall be located at distances of 200, 300, 450, 600, 900, and 1,500 mm (8, 12, 18, 24, 36, and 60 in) from the load plate center. FWD sensors other than the six (6) specified will not be used in the verification process.

7.4.3 *FWD Testing*: perform three (3) repeat drops (in addition to a seating drop) on each of the 11 marked FWD test locations in each of the three (3) pavement test sections by maneuvering the FWD so that the marked location is the center of the loading plate. Testing shall be performed while the device is positioned in the direction of the testing performed by the TSD. The FWD testing stress shall be within 10% of the TSDD static stress measured during the calibration of the strain gauges.

7.4.4 *FWD Data Collection*: record the peak load, peak deflections, air temperature, and surface temperature during testing.

7.5 *TSD and FWD data normalization*: the collected TSDD and FWD data shall be normalized to a reference load of 40 kN (9,000 lb).

8. TSDD ACCURACY AND PRECISION

8.1. *General Statistical Analyses*: the TSDD data shall be summarized at 1-m (3.3-ft) intervals for the statistical analyses.

8.1.1. *Matching sets of measurements*: use the method of cross-correlation described in Appendix X1 to match the valid test runs determined in 7.3.5.

8.1.2. *Repeatability*: calculate the repeatability between two synchronized TSDD runs using measurements collected over the 30-m (100-ft) length of the three pavement test sections. For a given pavement test sections, the repeatability between two matched runs is calculated as follows.

$$Repeatability = \sqrt{\frac{1}{n}\sum_{i=1}^{n}\big(f(i) - g(i)\big)^2}$$

where *f* is the first run and *g* is the second run. The overall repeatability is then calculated as the average of the repeatability of all pairs of runs (three pairs in the case of three runs).

8.1.3. *Bias between repeated runs*: calculate the bias between two (2) synchronized runs using the measurements collected over the 30 m (100 ft) length of the three pavement test sections. The bias between two matched runs is calculated as follows:

$$Bias = \frac{1}{n}\sum_{i=1}^{n}|f(i) - g(i)|$$

The overall bias is then calculated as the average bias of all pairs of runs (three [3] pairs in the case of three valid runs).

8.1.4. *Variance (precision) between repeated runs*: calculate the variance between two synchronized runs using measurements collected over 30 m. The variance between two runs is calculated from the following:

$$Variance = Repeatability^2$$

The overall variance is then calculated as the average variance of all pairs of runs (three [3] pairs in the case of three valid runs).

8.1.5. *Coefficient of Variation (COV)*: calculate the COV from the variance as follows:

$$COV = \frac{\sqrt{Variance/2}}{Average}$$

where Average is the average of the repeated measurements for the three (3) valid runs.

9. TSDD VERIFICATION

9.1. Convert FWD deflection measurements to TSDD measurements. This shall be done using the artificial neural network (ANN) software application developed for this standard practice. The input to this software application includes the TSDD and FWD measurements for sensors located at 200, 300, 450, 600, 900 and 1,500 mm (8, 12, 18, 24, 36 and 60 in) from the load, the peak FWD load, and the thicknesses of the asphalt concrete surface and base layers.

Note 1 – This practice is based on measurements by one device and consequently may not apply to other devices.

9.2. For each TSDD and FWD sensor (located at 200, 300, 450, 600, 900, and 1,500 mm [8, 12, 18, 24, 36, and 60 in] from the load), average the measurements obtained from the three repeats at the eleven (11) FWD test locations (see Figure 1). This step shall be repeated for each of the three (3) pavement test sections. The outcome will be one (1) measurement per sensor per device per pavement test section.

9.3. For each pavement test section, determine the percentage differences between the TSDD measurements, R_{TSDD}, and the FWD measurements converted to equivalent TSDD measurement, R_{FWD}, for each TSDD sensor location as follows:

$$\%Difference = \left|\frac{R_{FWD} - R_{TSDD}}{R_{TSDD}}\right|$$

This will yield six (6) percent differences per test section, each corresponding to one of the six (6) sensors. If the percent differences for all sensors and pavement

test sections are less than the minimum acceptable difference, then the TSDD is validated.

Note 2 – For this practice, the minimum acceptable difference is defined as less than 20% for deflection velocities higher than 5 mm/s (200 mils/s), or less than 30% for deflection velocities between 2.5 and 5 mm/s (100 and 200 mils/s). Verification of the TSDD for velocities less than 2.5 mm/s (100 mils/s) is not recommended because the COV for those low measurements is high.

If the TSDD fails the verification, then the following three possible actions can be taken:

- Perform another three (3) sets of TSDD measurements and repeat the validation procedure.
- Check for any possible miscalibration in the TSDD or the FWD.

9.4. *Test Results*: The results of the validation tests shall be documented by the testing agency. Results of the validation shall include the following information:

9.4.1. Identification of the tested TSDD and the FWD device used for validation.

9.4.2. Date of test.

9.4.3. Operator of the TSDD.

9.4.4. Name of the individual from the testing agency who conducted the test.

9.4.5. Overall determination from the test: Pass or Fail.

9.4.6. Results of *Repeatability*, *Bias*, *COV*, and %*Difference*.

APPENDIX

(Nonmandatory Information)

X1. CROSS-CORRELATION

X1.1 Cross-correlate any pair of valid TSDD measurements using the following steps.

X1.1.1. *Step 1*: For the three valid TSDD measurements on each pavement test section and at each testing speed, select all measurements from 5 m (16.5 ft) before the start of the test section to 5 m after the end of the test section.

X1.1.2. *Step 2*: Select a reference set of valid TSDD measurements for each test section and test speed. It will also be considered the location reference. The measurements will have a recording interval Δx of 1 m (3.3 ft).

X1.1.3. *Step 3*: Offset the valid TSDD measurements to have a mean of zero.

X1.1.4. Step 4: Calculate the cross-correlation between the reference set of measurements and the remaining two sets of measurements g as follows.

$$c(m) = \sum_{i=0}^{n} \left[f(i) - \bar{f} \right] [g(i+m) - \bar{g}]$$

where *f* represents the reference set of measurements, *g* represents any of the remaining two sets of measurements, $\bar{f}$ is the average of the reference set of measurements, $\bar{g}$ is the average of the second set of measurements, *n* is the total number of measurements, in this case 40, and *m*, with $-39 \leq m \leq 39$ is the amount of shifting.

X1.1.5. *Step 5*: Determine the optimal amount of shifting m_{opt} as the value of *m* that maximizes $c(m)$.